Application of foodomics towards identification and characterization of bioactive lipids in dietary grains and herbs (食用穀物およびハーブに含まれる生理活性脂質の同定と特性解析に向けたフードミクスの応用)

北海道大学大学院 国際食資源学院

国際食資源専攻 博士後期課程

Hokkaido University Graduate School of Global Food Resources

Division of Global Food Resources Doctoral Course

Lipsa Rani Nath

Dedication

I dedicate this dissertation to my father, Pramoda Chandra Nath; my mother, Radhamani Devi; my uncle, Pravat Kumar Nath; my aunt, Rashmita Panda; and my brothers, Abinash Kumar Nath, Pritish Kumar Nath. Their support, love, and encouragement have helped me throughout this journey. Without them, this work would not have been possible.

Acknowledgments

First and foremost, I would like to express my heartfelt gratitude to my supervisor, Associate Professor Siddabasave Gowda B. Gowda of Hokkaido University, for his invaluable guidance, encouragement, and unwavering support throughout these three years. His mentorship and the opportunities he provided, from attending conferences to gaining advanced technical knowledge, have greatly enriched both my academic and personal growth.

I am sincerely thankful to Assistant Professor Divyavani Gowda, Assistant Professor Perumalasamy Parasuraman, and Assistant Professor Quin Win of the Faculty of Health Sciences, Hokkaido University, for their experimental guidance, advice, and motivation. I also extend my sincere appreciation to Professor Shu-Ping Hui and Professor Hitoshi Chiba for their kind support and for providing essential research facilities.

I wish to acknowledge Associate Professor Ganesh Pandian Namshivayam of Kyoto University, whose valuable guidance and encouragement during my internship significantly contributed to my academic experience.

My sincere thanks go to all the members of the Laboratory of Advanced Lipid Analysis (LALA) for their continuous cooperation and camaraderie. I am especially grateful to my colleague Jayashankar Jayaprakash, whose positive spirit and constant support made my time in the lab memorable and motivating.

In addition, I would like to thank my well-wisher, Dr. Soumyaranjan Ratha, for his continuous encouragement and thoughtful guidance throughout my academic journey.

Finally, I gratefully acknowledge the DX Fellowship from Hokkaido University for providing financial support, which made this research possible.

Table of contents

Abbreviations

LIPID MAPS	LIPID MAPS
FAs	Fatty Acyls
GPs	Glycerophospholipids
GLs	Glycerolipids
SPs	Sphingolipids
STs	Sterol Lipids
PRs	Prenol Lipids
SAs	Saccharolipids
PKs	Polyketides
LC- HRMS	Liquid Chromatography- High-Resolution Mass Spectrometry
CVD	Cardiovascular Diseases
PAF	Platelet-Activating Factor
PUFAs	Polyunsaturated Fatty Acids
SFAs	Saturated Fatty Acids
MUFAs	Mono-Unsaturated Fatty Acids
SCFAs	Short-chain Fatty Acids
MCFAs	Medium-chain Fatty Acids
LCFAs	Long-chain Fatty Acids
MAGs	Monoacylglycerols
DAGs	Diacylglycerols
TAGs	Triacylglycerols
PC	Phosphatidylcholine
PE	Phosphatidylethanolamine

PI	Phosphatidylinositol
FAHFAs	Fatty Acid esters of Hydroxy Fatty Acids
MRM	Multiple Reaction Monitoring
LC-MS	Liquid Chromatography- Mass Spectrometry
Q-TOF	Quadrupole Time-of-Flight
QqQ	Triple Quadrupole
LTQ	Linear Ion Trap
MS-DIAL	Mass Spectrum Data Independent Acquisition-based Identification and quantification of Metabolites and Lipidomes
MS	Mass Spectrometry
LC	Liquid Chromatography
ESI	Electrospray Ionization
m/z	Mass to charge ratios
PCA	Principal Component Analysis
SIMCA	Soft Independent Modelling of Class Analogy
HSV-1	Herpes Simplex Virus
HIV	Human Immunodeficiency Virus
HeLa	Henrietta Lacks
UPLC	Ultra Performance Liquid Chromatography
HPLC	High Pressure Liquid Chromatography
SE	Standard Error
ANOVA	One-way Analysis of Variance
PC 1/2	First/Second Principal Component
HexCer	Hexosylceramides

AHexCer	Acylhexosylceramides
Cer	Ceramides
MGDG	Monogalactosyldiacylglycerol
DGDG	Digalactosyldiacylglycerol
SQDG	Sulfoquinovosyldiacylglycerol
ASG	Acylated Sterol Glucosides
PA	Phosphatidic Acids
CL	Cardiolipins
P:S	Polyunsaturated to Saturated fatty acids ratio
Nrf2	Nuclear factor erythroid factor 2-like 2
SFAHFAs	Short chain Fatty Acid esters of Hydroxy Fatty Acids
PNA	9-Phenyl nonanoic acid
EIC	Extracted Ion Chromatograms
RT	Retention Times
AAHPNA	Acetic acid esters of Hydroxy Phenyl Nonanoic Acid
PAHPNA	Propanoic Acid esters of Hydroxy Phenyl Nonanoic Acid
BAHPNA	Butyric Acid esters of Hydroxy Phenyl Nonanoic Acid
VAHPNA	Valeric Acid esters of Hydroxy Phenyl Nonanoic Acid
HFA	Hydroxy Fatty Acid
FAOSTAT	Food and Agriculture Organization Corporate Statistical Database
USDA- FAS	United States Department of Agriculture (USDA)- Foreign Agricultural Service
GC	Gas Chromatography

T2D	Type 2 Diabetes
MR	Mitch-Rated
DMED	N, N-dimethylethylenediamine
CMPI	2-Chloro-1-Methylpyridinium Iodide
TEA	Triethylamine
ACN	Acetonitrile
OAHOA	Oleic Acid esters of Hydroxy Oleic Acid
sPLSDA	sparse Partial Least Squares-Discriminant Analysis
FW	Fresh Weight
DW	Dry Weight
KEGG	Kyoto Encyclopedia of Genes and Genomes
FFA	Free Fatty Acids
G3P	Glycerol-3-Phosphate
LPA	Lysophosphatidic Acid
TNF-α	Tumor Necrosis Factor-alpha
IL-1β	Interleukin-1β
LPC	Lysophosphatidylcholine
PAHLA	Palmitic Acid Ester of Hydroxy-Linoleic Acid
CRC	Colorectal Cancer
LAHOA	Linoleic Acid Ester of Hydroxy-Oleic Acid
LAHLA	Linoleic Acid Ester of Hydroxy-Linoleic Acid
PAHOA	Palmitic Acid Ester of Hydroxy-Oleic Acid
SLs	Strach Lipids
NSLs	Non-Strach Lipids

GI	Glycemic Index
TS	Total Starch
RS	Resistant Starch
Cv.	Cultivar
OAHNA	Oleic Acid Esters of Hydroxy Nonanoic Acid
GOPOD	Glucose Oxidase Peroxidase
SKU	Stock Keeping Unit
AMG	Amyloglucosidase
HNA	Hydroxy Nonanoic Acid
HR-ESI-MS	High-Resolution Electrospray Ionization Mass Spectrometry
^{1}H NMR	proton Nuclear Magnetic Resonance
^{13}C NMR	carbon-13 Nuclear Magnetic Resonance
eGI	estimated Glycemic Index
RDS	Rapidly Digestible Starch
SDS	Slowly Digestible Starch
AUC	Area Under Curve
HI	Hydrolysis Index
OPLSDA	Orthogonal Partial Least-Squares Discriminant Analysis
VIP	Variable Importance in Projection
AWD	Alternate Wetting and Drying
AWMD	Alternate Wetting and Moderate Drying
HPI	Health Promotion Index
AI	Atherogenicity Index
HH	Hypo/Hypercholesterolemic ratio

PL	Phospholipids
LNAPE	N-acyl-Lysophosphatidylethanolamines
NAPE	N-acyl-Phosphatidylethanolamines
OAHCA	Oleic Acid esters of Hydroxy Caprylic Acid
HCA	Hydroxy Caprylic Acid
POHOA	Palmitoleic Acid esters of Hydroxy Oleic Acid
SH	Starch Hydrolysis

Thesis abstract

Lipids are fundamental components of food that serve not only as a source of energy but also as essential molecules involved in cellular structure, signaling, and regulation of metabolic processes. In recent years, the nutritional importance of specific lipid classes, such as polyunsaturated fatty acids (PUFAs), sterol lipids (STs), and bioactive lipid derivatives, has gained increasing attention for their roles in promoting health and preventing lifestyle-related diseases, including obesity, diabetes, and cardiovascular disorders. Despite this growing interest, much of the existing lipidomic research has focused on animal and clinical systems, while the diversity and function of plant-derived lipids, particularly those found in traditional herbs and whole grains, remain underexplored. This study addresses the gap by applying untargeted lipidomics to identify and characterize novel lipid species in Japanese herbs, sorghum, and rice cultivars. It asks how lipid profiles vary across plant types, what new bioactive lipids can be uncovered, and how these relate to nutritional function and potential agricultural applications. Using high-resolution liquid chromatography-mass-spectrometry, the study identified hundreds of lipid molecules and discovered several novel species such as fatty acid esters of hydroxy fatty acids (FAHFAs) and N-acyl-lysophosphatidylethanolamines (LNAPEs). Functional assays, including glycemic index prediction, confocal imaging, and gene expression studies, linked lipid profiles to health-related traits and plant physiological responses. The findings highlight the value of lipidomics in food science, uncovering unique plant lipids with potential nutritional and agronomic significance. Chapter one presents an overview of dietary lipids, their classifications, occurrence in food, and the emerging role of foodomics in comprehensively analyzing these compounds. The chapter addresses the limitations in current lipidomics methodologies, particularly the lack of standardized protocols for food lipid analysis. It highlights future trends integrating lipidomics with other omics technologies for precision nutrition.

In Chapter two, a non-targeted lipidomic study was performed on four traditional Japanese herbal teas. Using high-resolution LC-Orbitrap-MS analysis, a total of 344 lipid molecular species were identified across various lipid classes, including fatty acyls (FAs), glycerophospholipids (GPs), glycerolipids (GLs), sphingolipids (SPs), and STs. Importantly, four novel short-chain fatty acid esters of hydroxy fatty acids (SFAHFAs) were discovered for the first time in these herbal teas. Multivariate statistical analysis revealed distinct lipidomic profiles between tea species, demonstrating both compositional diversity and potential health-promoting lipid content in herbal beverages.

Chapter three extends lipidomic profiling to six commercial sorghum cultivars grown under controlled field conditions in Australia. A total of 194 lipid molecular species

were annotated, highlighting significant differences among cultivars in total lipid content and fatty acid composition. Cultivars such as MR43 and Bazley displayed higher levels of PUFAs and fatty acid esters of hydroxy fatty acids (FAHFAs), offering promising dietary and health benefits. The study also identified five novel FAHFAs in sorghum grain for the first time. It also utilized derivatization techniques to confirm hydroxyl positions in these molecules. This chapter establishes the unique lipidomic signatures of sorghum cultivars, emphasizing their nutritional potential and functional application in health-oriented grain products.

Chapter four presents an integrated analysis of lipidomics and glycemic response in 56 pigmented *japonica* rice cultivars. A total of 198 lipid species across five categories were profiled, leading to the identification of novel bioactive lipids, including FAHFAs and LNAPEs. Among the selected cultivars, black and green rice varieties exhibited healthier lipid profiles, with higher polyunsaturated to saturated fatty acid ratios, increased health promotion indices, and lower estimated glycemic index (eGI) values. Multivariate analysis further revealed that fatty acyls and glycerophospholipids were key markers distinguishing farming practices. These findings offer valuable molecular insights into the nutritional quality of pigmented rice and support the development of low-eGI rice cultivars for better metabolic health.

Chapter five explored the agricultural application of hijiki-derived carbon nanodots (CND-H) on rice seedling growth. The study confirmed the successful uptake of CND-H in germinating rice grains using confocal microscopy and emission spectral matching. Seed germination studies demonstrated enhanced shoot and root elongation in CND-H-treated seedlings compared to controls. Furthermore, gene expression analysis revealed a significant upregulation of *OsDGAT1*, a key enzyme in triacylglycerol biosynthesis, indicating a possible lipid accumulation-promoting effect of CND-H treatment in rice seedlings. While no significant change was observed in *OsACBP4* expression, these preliminary results suggest a beneficial role of nanomaterials in promoting seed vigor and lipid metabolism.

Collectively, this thesis advances the understanding of plant lipid diversity, reports several novel lipid molecular species for the first time, and demonstrates the potential of lipidomics combined with functional studies in both nutritional science and agriculture. The findings emphasize the importance of untargeted lipidomics in identifying health-relevant lipids in food crops and herbal products and propose innovative strategies, including nanotechnology, for improving crop performance and lipid quality.

Chapter 1

General Introduction

1.1 Overview and classification of dietary lipids

Lipids are chemically defined as hydrophobic or amphipathic molecules that are insoluble in water but soluble in non-polar organic solvents[1]. Biologically, they are vital components of food and living systems, serving as a dense source of energy, essential fatty acids, and fat-soluble vitamins[2]. Lipids are present across a wide range of food items, such as oils and fats, and are also found in varying levels in animal products, grains, vegetables, and herbs[3].

Certain lipids, such as specific fatty acids (e.g., linoleic and alpha-linolenic acid) and fat-soluble vitamins (A, D, E, and K), are classified as essential nutrients due to the human body's inability to synthesize them endogenously[3]. Beyond their nutritional importance, dietary lipids exert diverse biological functions, including modulation of inflammation, cellular signaling, and regulation of metabolic health. Their functional significance underscores their role as integral components of a balanced and health-promoting diet[4]. According to the widely adopted classification system proposed by the Lipid Metabolites and Pathways Strategy (LIPID MAPS) project, lipids are organized into eight main categories based on structural and biosynthetic criteria: fatty acyls (FA), glycerolipids (GL), glycerophospholipids (GP), sphingolipids (SP), sterol lipids (ST), prenol lipids (PR), saccharolipids (SL), and polyketides (PK) (**Figure 1**). As of 2025, more than 49,000 lipid species have been identified under this classification, highlighting the immense structural diversity within the lipidome. This complexity presents significant analytical challenges, necessitating the use of high-resolution analytical platforms such as liquid chromatography coupled with high-resolution mass spectrometry (LC-HRMS)[5].

Biologically, lipids serve a wide array of functions beyond energy storage. They are integral components of cellular membranes, contributing to membrane structure,

fluidity, communication, and intracellular transport. Lipids also play critical roles in maintaining homeostasis and act as signaling molecules involved in various physiological and pathological pathways, including metabolic disorders, cardiovascular disease (CVD), cancer, and neurodegeneration[4,6] (**Figure 2**).

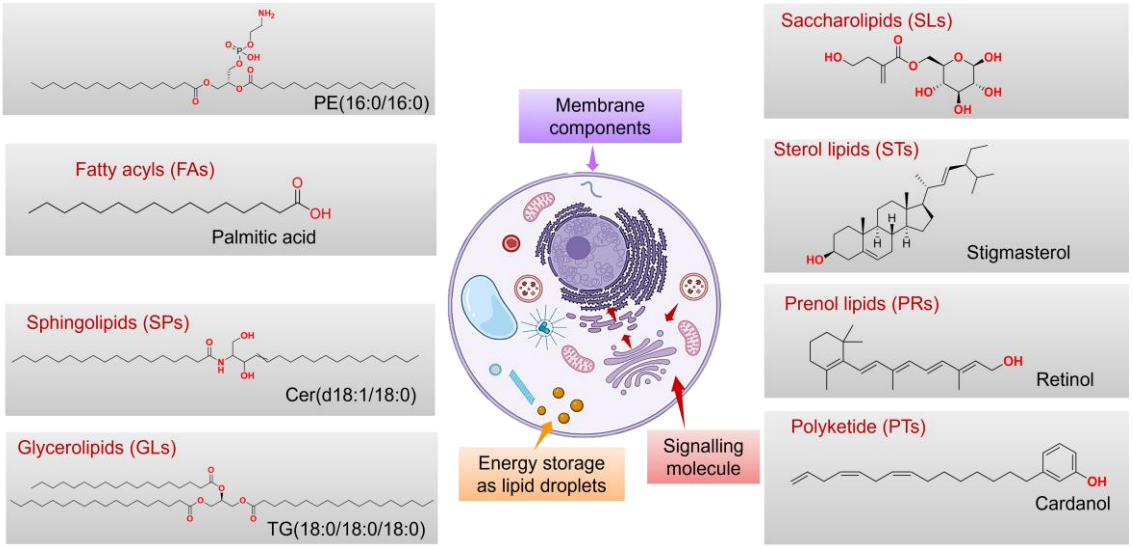

Figure 1: The common structures and functions of eight major lipid classes.

Historically, lipids were primarily regarded as energy sources and membrane constituents. However, important discoveries, such as the identification of platelet-activating factor (PAF) in 1979, have since revealed the dynamic roles of lipids in cellular signaling and disease modulation. These discoveries gave rise to the concept of bioactive lipids, which are specific lipid molecules that influence biological functions beyond basic nutrition[7]. Bioactive lipids such as polyunsaturated fatty acids (PUFAs), phytosterols, fat-soluble vitamins, and carotenoids have gained increasing attention for their potential to promote health and reduce disease risk. They are naturally present in diverse food matrices, including oilseeds, grains, nuts, dairy, eggs, and herbs. Additionally, bioactive lipids can be incorporated into functional foods and nutraceutical formulations to enhance their

health-promoting properties[6]. Building on this foundational understanding of lipids, the following sections delve into their occurrence in food systems and their functional roles.

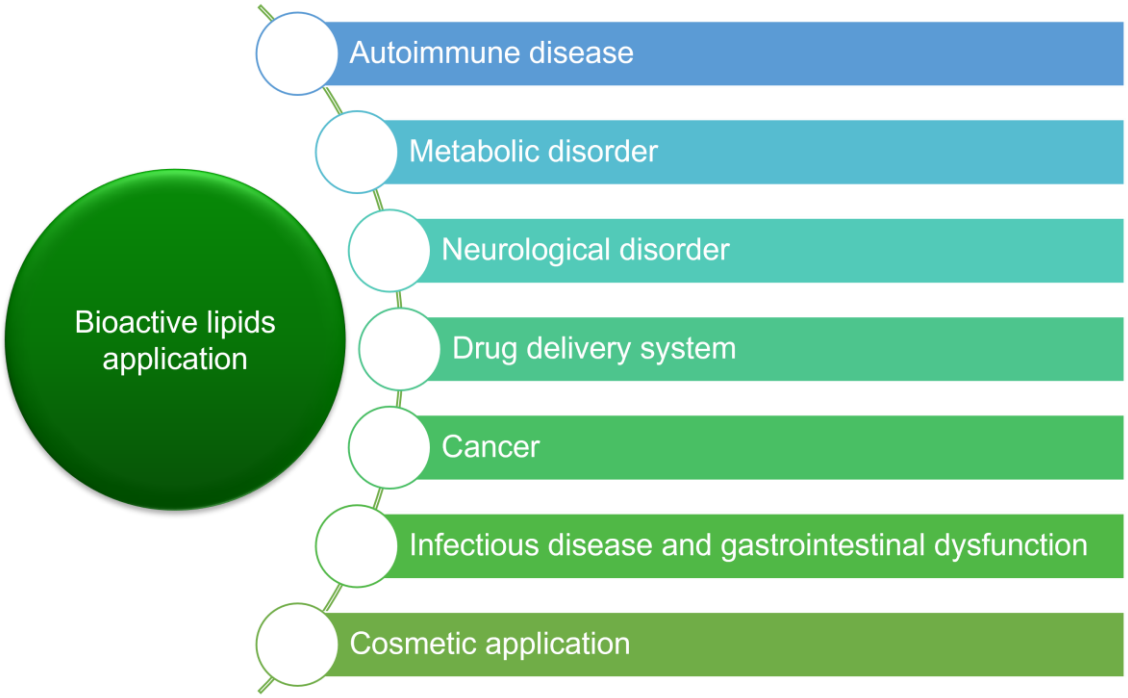

Figure 2: Applications of bioactive lipids in human health.

1.2 Lipids in food

1.2.1 Fatty Acyls

FAs include a wide range of fatty acids, which may be saturated (SFAs), monounsaturated (MUFAs), or PUFA, as well as their oxidized and conjugated derivatives[8]. They are essential components of edible fats and oils and play significant roles in flavor, texture, and nutritional quality[3]. Short-chain fatty acids (SCFAs), medium-chain fatty acids (MCFAs), and long-chain fatty acids (LCFAs) are present in dairy, coconut oil, and animal fats, respectively[3,9,10]. PUFAs such as linoleic acid (C18:2) and α-linolenic acid (C18:3) are essential nutrients found in plant oils, while longer-chain ω-3 PUFAs like DHA

(C22:6) and EPA (C20:5) are predominantly found in marine foods[3]. Oxidation products such as eicosanoids also fall into this category, contributing to both health effects and flavor compounds[11].

1.2.2 Glycerolipids

GLs are esters of glycerol and fatty acids, including mono-, di-, and triacylglycerols (MAGs, DAGs, and TAGs). TAGs are the main storage form of energy in many foods and constitute the bulk of lipids in plant and animal fats and oils. In addition, glycolipids and betaine lipids also belong to this class, with roles in membrane structure and functionality, particularly in microbial and plant systems[3].

1.2.3 Glycerophospholipids

GPs are composed of glycerol, two fatty acids, and a phosphate-containing headgroup. Key examples include phosphatidylcholine (PC), phosphatidylethanolamine (PE), and phosphatidylinositol (PI). These lipids are fundamental components of cell membranes and are also found in significant quantities in foods such as egg yolk, meat, and milk[3]. They influence food texture, emulsification properties, and have nutraceutical value, particularly in brain and cardiovascular health[13].

1.2.4 Sphingolipids

SPs are composed of a sphingoid base backbone, often with a fatty acid and a polar head group. Ceramides, sphingomyelins, and glycosphingolipids such as glucosylceramides are important subtypes[14]. These are prominent in animal-derived foods like meat and milk and have bioactive properties related to skin integrity, inflammation modulation, and cell signaling[15].

1.2.5 Sterol Lipids

STs include cholesterol and plant sterols (phytosterols), along with secosteroids like vitamin D[3]. Cholesterol is abundant in animal-derived foods, while phytosterols are present in nuts, seeds, and vegetable oils[16,17]. These compounds are critical for hormone synthesis, membrane fluidity and are associated with cardiovascular health when used as dietary cholesterol-lowering agents[3].

1.2.6 Prenol Lipids

Prenol lipids are derived from isoprene units and encompass important subgroups such as carotenoids, retinoids (vitamin A), and quinones (including vitamins K, E, and coenzyme Q10). These compounds are richly present in fruits, vegetables, and marine foods, contributing to color, antioxidant activity, and vitamin functionality[3]. For instance, β-carotene in carrots and astaxanthin in seafood are key representatives[18,19].

1.2.7 Saccharolipids

SLs are a unique class where fatty acids are directly linked to sugar backbones. They are less common in typical foods but are integral components of bacterial membranes, including those found in fermented foods. Their structural diversity contributes to the functionality and integrity of microbial cell envelopes, with implications for food microbiota and fermentation[3].

1.2.8 Polyketides

Polyketides are secondary metabolites synthesized by repeated condensation of acetyl-CoA or propionyl-CoA units[20]. While not traditionally abundant in major food lipids, they are found in food-derived fungi and bacteria and include important bioactive compounds such as antibiotics, pigments, and mycotoxins. Some also serve as nutraceuticals and are

under exploration for functional food applications[3].

1.3 Foodomics: A modern approach to lipid research

In recent years, food research has undergone a paradigm shift through the integration of advanced analytical technologies and systems biology, giving rise to a field known as foodomics. First introduced by Cifuentes in 2009, foodomics refers to the application of omics technologies, such as genomics, transcriptomics, proteomics, metabolomics, and lipidomics, to study food and nutrition in a comprehensive and holistic manner[21]. It is used to evaluate food safety, quality, traceability, and functionality, and to better understand how food components interact with biological systems[22]. Within this framework, lipidomics, a branch of metabolomics, is emerging as a critical tool for understanding the role of lipids in food and health. The lipidome refers to the complete set of lipid species in a biological system. Lipidomics involves the systematic identification and quantification of lipids and their associated metabolic pathways, enabling researchers to detect changes in lipid composition resulting from processing, storage, cultivar differences, or physiological conditions.

Lipidomics can be broadly classified into untargeted and targeted approaches[23]. Untargeted lipidomics aims to detect as many lipid species as possible in a given sample without prior knowledge, making it ideal for discovering novel compounds such as fatty acid esters of hydroxy fatty acids (FAHFAs). In contrast, targeted lipidomics focuses on quantifying specific known lipids, typically using internal standards and predefined multiple reaction monitoring (MRM) methods.

Technological advancements, particularly in liquid chromatography-mass spectrometry (LC-MS), have been central to the development of lipidomics. High-

resolution mass spectrometers such as Orbitrap, quadrupole time-of-flight (Q-TOF), and triple quadrupole (QqQ) systems offer enhanced sensitivity, resolution, and mass accuracy. These systems allow for comprehensive profiling of a wide range of lipids, including fatty acids, glycerolipids, phospholipids, sterols, and oxidized lipid species. Among them, the linear ion trap quadrupole (LTQ-Orbitrap) platform has been widely applied in untargeted lipidomics due to its superior performance in detecting unknown lipid species[22].

In food research, untargeted lipidomics is particularly valuable for uncovering novel lipid structures and understanding the impact of agricultural practices, genetic variation, and processing methods on food lipid profiles[22]. For example, studies have shown that roasting flaxseeds significantly alters their lipid composition, including oxidation products and changes in polyunsaturated fatty acid content[24]. Similarly, metabolomics-based sensory studies, such as those on stored tea leaves, have helped correlate changes in metabolite profiles with flavor and quality deterioration[25]. Despite its power, lipidomics requires robust bioinformatics tools to process large and complex datasets. Software like Mass spectrum data independent acquisition-based identification and quantification of metabolites and lipidomes (MS-DIAL) facilitates peak detection, alignment, and compound identification. However, challenges remain in annotating unknown lipids and integrating lipidomic data across multiple platforms.

1.4 Scope, significance, and objectives of the present study

Food lipidomics is a rapidly evolving discipline that aims to systematically identify and quantify the diverse lipid species present in food matrices, using advanced mass spectrometry (MS)-based techniques. Lipids play essential roles in determining the

nutritional quality, functional properties, and potential health benefits of food, yet their comprehensive characterization in plant-based foods remains limited. This study focuses on the application of a non-targeted lipidomics approach to profile the lipid composition of staple food crops such as rice and sorghum, along with selected herbal materials. By employing liquid chromatography coupled with LTQ-Orbitrap, this research seeks to capture a broad spectrum of lipid species, including both abundant and minor bioactive components, across different cultivars and food types.

The significance of this study lies in its potential to expand the existing knowledge of lipid diversity in food systems, particularly in traditionally important but under-characterized crops. While metabolomics research has made considerable progress in recent years, lipidomics in food science is still in its developmental stages, especially regarding the identification of health-promoting lipid molecules such as ω-3 and ω-6 fatty acids, as well as novel compounds like FAHFAs. These bioactive lipids are increasingly recognized for their functional roles in modulating metabolic processes, glycemic response, and inflammatory pathways. By elucidating the lipidomic profiles of diverse food sources, this study aims to contribute valuable insights into the nutritional and functional attributes of these crops, which may support future applications in health-oriented food development, nutraceutical research, and crop improvement initiatives.

The central objective of this research is to develop and implement a comprehensive, MS-based lipidomics workflow for the analysis of plant-based food materials. This includes optimizing extraction protocols, conducting high-resolution lipidomic analysis, and applying advanced multivariate data analysis and visualization tools to interpret the resulting data. Through this approach, the study aims to characterize lipid composition differences across cultivars, identify potential bioactive lipids, and

explore their possible implications for food quality and human health. Ultimately, this research seeks to advance the field of food lipidomics by providing a detailed, cultivar-specific understanding of lipid diversity, while also establishing a methodological framework that can be applied in future food chemistry and nutritional studies.

1.4.1 MS-based lipidomics workflow

Lipidomics is an advanced field of metabolomics focused on the comprehensive analysis of lipids within biological systems. MS-based lipidomics has emerged as a powerful technique for characterizing lipid compositions, profiles, and metabolic alterations in plant-based food matrices such as rice, sorghum, and herbal plants. This study employed an untargeted MS-based lipidomics approach, which includes pre-treatment, MS analysis, and data processing, as summarized in **Figure 3**.

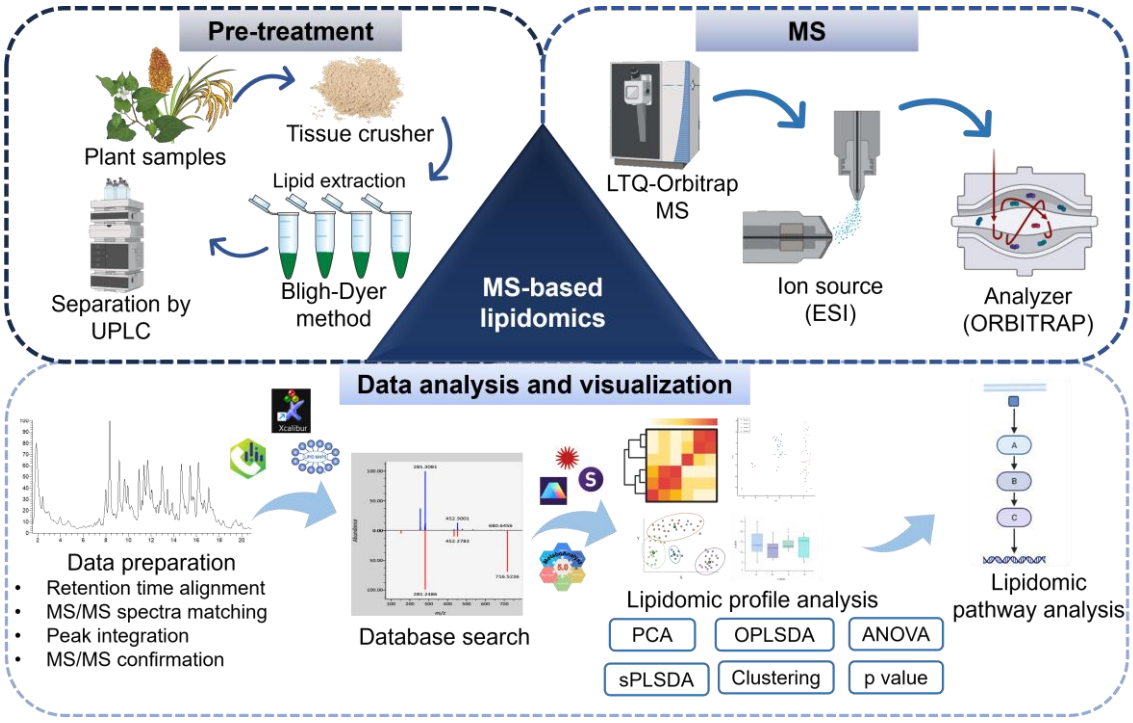

Figure 3: The role of MS-based lipidomics in food research. Lipidomics, as a core part of foodomics, enables the discovery of novel lipid species and elucidates their roles in

food quality, nutrition, and functionality. This study focuses on the untargeted lipidomics of Japanese herbal tea, sorghum, and rice.

Plant samples, including rice grains, sorghum grains, and herbal leaves, were first ground into a fine powder. Lipids were then extracted using a solvent-based extraction method, typically involving mixtures of methanol, chloroform, and water, as described by Bligh and Dyer[26]. Following extraction, the lipid-rich layers were separated and transferred into microcentrifuge tubes for subsequent analysis.

Lipid extracts were analyzed using a high-resolution LC-MS system. The LC system was used for lipid separation, while the mass spectrometer, equipped with an electrospray ionization (ESI) source, detected the ions in both positive and negative modes. Full-scan and MS^n data were acquired, allowing for the identification and quantification of various lipid classes based on their mass-to-charge ratios (*m/z*) and fragmentation patterns.

Raw MS data were processed using software such as MS-DIAL, Xcalibur (Thermo Fisher Scientific), and LipidSearch (Thermo Fisher Scientific) for peak detection, lipid identification, and quantification. Further data normalization and multivariate analyses, including principal component analysis (PCA) and hierarchical clustering, were performed using MetaboAnalyst, soft independent modelling of class analogy (SIMCA), and other statistical tools. Results were visualized through heatmaps, box plots, and clustering diagrams to highlight lipid profile variations across different cultivars and sample types.

1.5 Reference:

1. Park, J., Choi, J., Kim, D. D., Lee, S., Lee, B., Lee, Y., Kim, S., Kwon, S., Noh, M., Lee, M. O., Le Q. V., & Oh, Y. K. (2021). Bioactive lipids and their derivatives in biomedical applications. Biomolecules & Therapeutics, 29(5), 465.
2. Zheng, L., Fleith, M., Giuffrida, F., O'Neill, B. V., & Schneider, N. (2019). Dietary polar lipids and cognitive development: A narrative review. Advances in nutrition, 10(6), 1163-1176.
3. Tietel, Z., Hammann, S., Meckelmann, S. W., Ziv, C., Pauling, J. K., Wölk, M., ... & Domingues, M. R. (2023). An overview of food lipids toward food lipidomics. Comprehensive reviews in food science and food safety, 22(6), 4302-4354.
4. Levental, K. R., Malmberg, E., Symons, J. L., Fan, Y. Y., Chapkin, R. S., Ernst, R., & Levental, I. (2020). Lipidomic and biophysical homeostasis of mammalian membranes counteracts dietary lipid perturbations to maintain cellular fitness. Nature communications, 11(1), 1339.
5. Wang, D., Xiao, H., Lyu, X., Chen, H., & Wei, F. (2023). Lipid oxidation in food science and nutritional health: A comprehensive review. Oil Crop Science, 8(1), 35-44.
6. Duhan, N., Barak, S., & Mudgil, D. (2020). Bioactive lipids: Chemistry & health benefits. Biointerface Res. Appl. Chem, 10(6), 6676-6687.
7. Vázquez, L., Corzo-Martínez, M., Arranz-Martínez, P., Barroso, E., Reglero, G., & Torres, C. (2019). Bioactive lipids. *Bioactive Molecules in Food; Mérillon, J.-M., Ramawat, KG, Eds*, 467-527.
8. McClements, D. J., & Decker, E. A. (2008). Lipids. In S. Damodaran, K. L. Parkin, & O. R. Fennema (Eds.), *Fennema's food chemistry* (4th ed.). Taylor & Francis Group.

pp 155–216.

9. Rauf, A., Khalil, A. A., Rahman, U.-U., Khalid, A., Naz, S., Shariati, M. A., Rebezov, M., Urtecho, E. Z., Albuquerque, R. D. D. G. D., & Anwar, S. (2021). Recent advances in the therapeutic application of short-chain fatty acids (SCFAs): An updated review. *Critical Reviews in Food Science and Nutrition*, **62**(22), 1–21
10. Deen, A., Visvanathan, R., Wickramarachchi, D., Marikkar, N., Nammi, S., Jayawardana, B. C., & Liyanage, R. (2021). Chemical composition and health benefits of coconut oil: An overview. *Journal of the Science of Food and Agriculture*, **101**(6), 2182–2193.
11. Shahidi, F., & Hossain, A. (2022). Role of lipids in food flavor generation. *Molecules (Basel, Switzerland)*, **27**(15), 5014.
12. Wang, K., Xu, L., Wang, X., Chen, A., & Xu, Z. (2021). Discrimination of beef from different origins based on lipidomics: A comparison study of DART-QTOF and LC-ESI-QTOF. *LWT—Food Science and Technology*, **149**, 111838.
13. Lordan, R., Redfern, S., Tsoupras, A., & Zabetakis, I. (2020). Inflammation and cardiovascular disease: Are marine phospholipids the answer? *Food & Function*, **11**(4), 2861–2885.
14. Mamode Cassim, A., Grison, M., Ito, Y., Simon-Plas, F., Mongrand, S., & Boutté, Y. (2020). Sphingolipids in plants: A guidebook on their function in membrane architecture, cellular processes, and environmental or developmental responses. *FEBS Letters*, **594**(22), 3719–3738.
15. Ali, A. H., Wei, W., & Wang, X. (2022). A review of milk gangliosides: Occurrence, biosynthesis, identification, and nutritional and functional significance. *International Journal of Dairy Technology*, **75**(1), 21–45.

16. Duong, S., Strobel, N., Buddhadasa, S., Auldist, M. J., Wales, W. J., Moate, P. J., Cox, G., Orbell, J. D., & Cran, M. J. (2019). Modification of the sterol profile in milk through feeding. *Journal of Dairy Science*, **102**(7), 5933–5944.
17. Zuorro, A., Lavecchia, R., Medici, F., & Piga, L. (2013). Enzyme-assisted production of tomato seed oil enriched with lycopene from tomato pomace. *Food and Bioprocess Technology*, **6**(12), 3499–3509.
18. Britton, G., & Khachik, F. (2009). Carotenoids in food. In *Carotenoids* (pp. 45–66). Springer.
19. Arunkumar, R., Gorusupudi, A., & Bernstein, P. S. (2020). The macular carotenoids: A biochemical overview. *Biochimica Et Biophysica Acta (BBA)—Molecular and Cell Biology of Lipids*, **1865**(11), 158617.
20. Shukla, S., & Dubey, K. K. (2018). CoQ10 a super-vitamin: Review on application and biosynthesis. *3 Biotech*, **8**(5), 249.
21. Subramanian, I., Verma, S., Kumar, S., Jere, A., & Anamika, K. (2020). Multi-omics data integration, interpretation, and its application. Bioinformatics and biology insights, 14, 1177932219899051.
22. Muguruma, Y., Nunome, M., & Inoue, K. (2022). A review on the foodomics based on liquid chromatography mass spectrometry. Chemical and Pharmaceutical Bulletin, 70(1), 12-18.
23. Creydt, M., & Fischer, M. (2020). Food phenotyping: recording and processing of non-targeted liquid chromatography mass spectrometry data for verifying food authenticity. Molecules, 25(17), 3972.
24. Zhang, D., Li, X., Duan, X., Sun, H., & Cao, Y. (2021). Lipidomics reveals the changes in lipid profile of flaxseed oil affected by roasting. Food Chemistry, 364,

130431.

25. Fan, F. Y., Huang, C. S., Tong, Y. L., Guo, H. W., Zhou, S. J., Ye, J. H., & Gong, S. Y. (2021). Widely targeted metabolomics analysis of white peony teas with different storage time and association with sensory attributes. Food Chemistry, 362, 130257.
26. Bligh, E. G., & Dyer, W. J. (1959). A rapid method of total lipid extraction and purification. Canadian journal of biochemistry and physiology, 37(8), 911-917.

Chapter 2

Comprehensive Lipid Profiling of Herbal Tea Using Untargeted LC-MS

2.1 Introduction

Tea, one of the most widely consumed non-alcoholic beverages globally, has a rich history dating back over 2000 years to its origins in China[1]. As noted by the Japanese author Okakura Kakuzo in The Book of Tea, "Tea started as a medication and developed into a beverage." Broadly, teas can be classified into two categories: those derived from the leaves, buds, and internodes of *Camellia sinensis*, and herbal teas, which are prepared from a diverse range of plant species other than *C. sinensis*[2]. Herbal teas, also known as tisanes, are infusions made from a mixture of dried leaves, grasses, seeds, fruits, bark, flowers, or other plant parts, each contributing to their distinctive flavors and potential health benefits[3]. Herbal teas are valued not only for their sensory qualities but also for their various biological activities. Numerous studies have reported their antioxidant, anti-inflammatory, antibacterial, antiviral, anti-carcinogenic, anti-thrombotic, vasodilatory, antimutagenic, anti-aging, and antiglycation effects. Among the wide range of herbal teas traditionally consumed in Japan, several are particularly notable for their therapeutic properties[4].

Houttuynia cordata (Heart leaf), known as dokudami from the Saururaceae family, has been used in traditional medicine for its virucidal effects against herpes simplex virus (HSV-1), Human immunodeficiency virus (HIV), and influenza viruses, alongside its antioxidative, antibacterial, anti-obesity, and immunomodulatory activities[5-7]. *Sasa veitchii* (Japanese bamboo grass), referred to as kumazasa from the Gramineae family, exhibits anti-cancer, anti-ulcer, antiviral, antioxidant, and anti-inflammatory properties, and its extract has been shown to reduce obesity-induced insulin resistance[8,9]. *Equisetum arvense* (Horsetail), or sugina from the Equisetaceae family, has long been employed for its medicinal effects in treating hemorrhage, urethritis, jaundice, and hepatitis, and is

recognized for its antioxidant, antimicrobial, anticancer, anti-inflammatory, and antidiabetic properties[10-12]. Lastly, *Artemisia princeps* (First wormwood), known as yomogi from the Asteraceae family, possesses well-documented anti-cancer, anti-inflammatory, and antioxidant activities[13].

When consumed as tea, the bioactive components of these plants retain many of their therapeutic properties. For instance, eupafolin, a flavonoid found in *A. princeps*, induces apoptosis in human cervical adenocarcinoma-derived Henrietta Lacks (HeLa) cells through a caspase-dependent mechanism[14]. A metabolomic study on four South African herbal tea varieties has revealed the presence of various bioactive compounds such as flavonoids, phenolics, lignans, and megastigmane glycosides, reinforcing the potential of herbal teas as health-promoting beverages[15]. While several studies have explored the metabolomic profiles of herbal teas, research specifically focusing on their lipid compositions remains limited.

Lipids are essential components of plants, functioning both as structural constituents of cell membranes and as bioactive compounds involved in signaling processes[16]. Bioactive lipids, including PUFAs, carotenoids, phytosterols, polyphenols, and fat-soluble vitamins, are of particular interest due to their potential roles in the prevention and management of various diseases, such as CVD, hypertension, cancer, and diabetes[17,18]. Our laboratory has previously identified several bioactive lipids in various food sources, including salmon, shellfish, seaweed, and adzuki beans[19-22].

In the context of tea, lipidomics studies have primarily been conducted on green tea. For example, research demonstrated that lipid-soluble chlorophylls and carotenoids contribute to the color of green tea, while unsaturated fatty acids influence its aroma[23,24]. Additionally, it has been observed that significant lipid loss occurs during black tea

processing[25]. Recent investigations using advanced ultra-performance liquid chromatography (UPLC) Q-TOF-based metabolomics and lipidomics approaches identified 26 lipids and 45 metabolites that distinguish early and late spring green teas[26]. Another comprehensive study utilizing ultrahigh performance liquid chromatography coupled to an ESI-quadrupole Orbitrap mass spectrometer successfully profiled 283 lipid molecular species across 22 lipid subclasses during green tea manufacturing[27].

Despite these advancements, studies focusing on herbal tea lipidomics remain scarce. This knowledge gap is particularly significant given the rich variety of plant species used in herbal teas and their well-established health benefits. Recognizing this, the present study aims to apply an untargeted high-pressure liquid chromatography (HPLC)/LTQ-Orbitrap-MS lipidomics approach to comprehensively profile the lipid compositions of four different varieties of traditional Japanese herbal teas: *H. cordata*, *S. veitchii*, *E. arvense*, and *A. princeps*. Furthermore, the study seeks to identify and characterize previously unreported lipid molecules within these teas using MS^n spectral analysis. By clarifying the lipid composition of these herbal teas, this research intends to provide new insights into the potential roles of bioactive lipids in herbal teas as functional, health-promoting beverages.

2.2 Materials and methods

2.2.1 Sample collection

Four different herbal tea varieties were locally sourced from Takayama, Japan (36.1461°N, 137.2522°E). These included dried leaves from *Houttuynia cordata* (Heart leaf, locally known as dokudami), *Sasa veitchii* (Japanese bamboo, kumazasa), *Equisetum arvense* (Horsetail, sugina), and *Artemisia princeps* (First wormwood, yomogi).

Approximately 500 grams of each plant species were harvested during the summer month of August. The dried leaves and twigs were finely ground into a uniform powder and stored in airtight glass containers at -80°C until further lipid extraction and analysis.

2.2.2 Materials

All solvents used for LC-MS analysis, including isopropanol, chloroform, and methanol, were of analytical grade and purchased from Wako Pure Chemical Industries, Ltd. (Osaka, Japan). A 1 M aqueous solution of ammonium acetate, used as an LC-MS eluent additive, was obtained from Sigma-Aldrich (St. Louis, USA). The internal standards, EquiSPLASH LIPIDOMIX quantitative standard and deuterium-labeled oleic acid-d9, were supplied by Avanti Polar Lipids, Inc. (Alabaster, USA).

2.2.3 Lipid Extraction

Lipids were extracted from herbal tea samples using a modified version of the Bligh and Dyer method[28]. Briefly, 20 mg of powdered herbal tea (n=5) was weighed into a 2 mL Eppendorf tube. To this, 300 µL of methanol and 300 µL of a mixture of internal standards (EquiSPLASH Lipidomix, 1 µg/mL, and oleic acid-d9, 10 µg/mL) were added. The mixture was vortexed gently for 10 seconds, followed by the addition of 200 µL chloroform and 40 µL Milli-Q water. The resulting solution was vortexed at 3500 rpm for 5 minutes and left at room temperature for 2 hours, with an additional brief vortexing after 1 hour. Following incubation, the samples were centrifuged at 15,000 rpm for 10 minutes, and the lipid-containing lower phase was transferred to a fresh 2 mL Eppendorf tube. To the remaining residue, 1 mL of methanol-chloroform (2:1 v/v) was added, vortexed for 5 minutes, and centrifuged again. The resulting extracts were combined, filtered using animal charcoal, and evaporated using a centrifugal concentrator at 4°C for

5–6 hours. The dried lipid extracts were reconstituted in 100 µL of methanol, centrifuged at maximum speed for 10 minutes, and transferred to LC-MS vials for analysis.

2.2.4 LC-MS Analysis

Lipid separation was performed using an Atlantis T3 C18 column (2.1 × 150 mm, 3 µm, Waters, USA) installed in a Prominence HPLC system (Shimadzu, Kyoto, Japan). The chromatographic separation was conducted at a constant flow rate of 200 µL/min and a column oven temperature of 40°C. The mobile phase consisted of 10 mM aqueous ammonium acetate (solvent A), isopropanol (solvent B), and methanol (solvent C). A programmed gradient elution was applied as follows: 0-1 min, 30% B and 35% C; 1-9 min, 75% B and 15% C; 9-21 min, 82.5% B and 15% C; 21-25 min, 95% B and 5% C; 25-26 min, returning to 30% B and 35% C, with a total run time of 30 minutes. The injection volume for each sample was set at 10 µL.

Mass spectrometric analysis was performed using an LTQ Orbitrap mass spectrometer (Thermo-Fisher Scientific Inc., San Jose, USA), operating in both positive and negative ESI modes. The ESI parameters were optimized as follows: the capillary temperature was maintained at 330 °C, with sheath gas flow set to 50 units. The auxiliary gas flow was adjusted to 20 units for positive mode and 30 units for negative mode. In negative ionization mode, the source and capillary voltages were set to 3 kV and 10 V, respectively, while in positive mode, they were set to 4 kV and 25 V. For mass spectrometric detection, MS^1 scans were acquired in Fourier transform mode at a resolution of 60,000, over an m/z range of 160–1900 for negative mode and 100–1750 for positive mode. High-resolution mass spectra were collected with a collision energy of 35 V. Additionally, low-resolution MS/MS spectra were obtained in the ion-trap mode using a collision energy of 40 V.

The raw mass spectrometry data were processed using MS-DIAL software (version 4.9) for peak alignment, extraction, identification, and integration of peak areas. The parameters applied during this process included a minimum peak height threshold of 1000 amplitude, a mass slice width of 0.1 Da, and a smoothing level of 3 with a minimum peak width of 5 scans. The sigma window value was set to 0.5, with a signal intensity threshold set at five times greater than the blank signal. The tolerances for retention time (RT) and MS^1 were set to 0.5 minutes and 0.015 Da, respectively. Lipid molecular species were identified based on their corresponding MS/MS spectra. Extracted ion chromatograms (EIC) and mass spectra were generated using Xcalibur software (version 2.2, Thermo Fisher Scientific, Waltham, USA). For relative quantification, the study followed the Lipidomics Standards Initiative recommendations for level 2 and level 3 identification. Quantification was conducted using labeled internal standards representative of the same lipid subclass or major lipid class. The relative abundance of each lipid species was determined by calculating the ratio of the analyte's peak area to that of the internal standard and multiplying it by the known concentration of the internal standard.

2.2.5 Statistical Analysis

The annotated lipid data acquired in both positive and negative ion modes were compiled for statistical analysis. The results were expressed as mean values ± standard error (SE). One-way analysis of variance (ANOVA) followed by Tukey's multiple comparison test was applied to determine significant differences, using a significance threshold of $p < 0.05$. Data visualization, including bar charts and error plots, was performed using Microsoft Excel 2021. Multivariate statistical analyses, such as cluster analysis, were conducted using MetaboAnalyst version 5.0, while PCA was performed using SIMCA

software version 17.0.2 (Sartorius Stedim Biotech Umetrics AB, Umeå, Sweden) to assess the overall variation and sample grouping patterns.

2.3 Results and discussion

2.3.1 Lipid profiling of herbal tea samples

An untargeted lipidomics analysis was conducted on four herbal tea varieties using LC-MS, and lipid molecular species were annotated based on accurate mass measurements. This comprehensive analysis successfully identified 344 distinct lipid molecular species across the samples. The relative quantification of these annotated lipids was performed using an internal standard-based method to ensure consistency and comparability. A summary of the statistical distribution of these lipid species is presented in **Figure 1A**, which highlights the significance levels of the identified lipids. Out of the total, 286 lipid species exhibited statistically significant variations ($p < 0.05$) among the four herbal tea types and are indicated in blue, while the remaining non-significant lipids are represented in grey. This indicates a considerable degree of diversity and specificity in the lipid composition across different herbal teas.

The identified lipids were classified into five major lipid categories, consistent with the LIPID MAPS classification: FAs, GLs, GPs, SPs, and STs. These categories reflect the broad structural diversity of plant lipids and their varied functional roles in biological systems. The distribution of lipid species based on their *m/z* values and RT is illustrated in **Figure 1B**. As expected, FA eluted first, followed by GLs and GPs, while STs was the last to elute. This elution order aligns with the polarity and structural properties of these lipid classes. Among these categories, GPs were the most abundant lipid class detected in all four herbal tea samples. This finding is consistent with previous

studies on plant-based lipidomics, where GPs often dominate due to their critical roles in cellular membranes and signaling pathways. For comparison, a recent lipidomics study on green tea reported higher levels of GPs and acylglycerolipids in early spring harvests, highlighting the influence of environmental and seasonal factors on lipid profiles[26]. However, comprehensive lipidomic datasets for the specific herbal tea species analyzed in this study remain scarce in the existing literature, further emphasizing the novelty and importance of this research.

The lipidomic profile established in this study contributes valuable new data to the field of plant-based lipidomics, providing a deeper understanding of the lipid diversity in traditional Japanese herbal teas. It offers a foundation for further investigation into the potential health-promoting properties of these bioactive lipid compounds and their functional significance in herbal beverages.

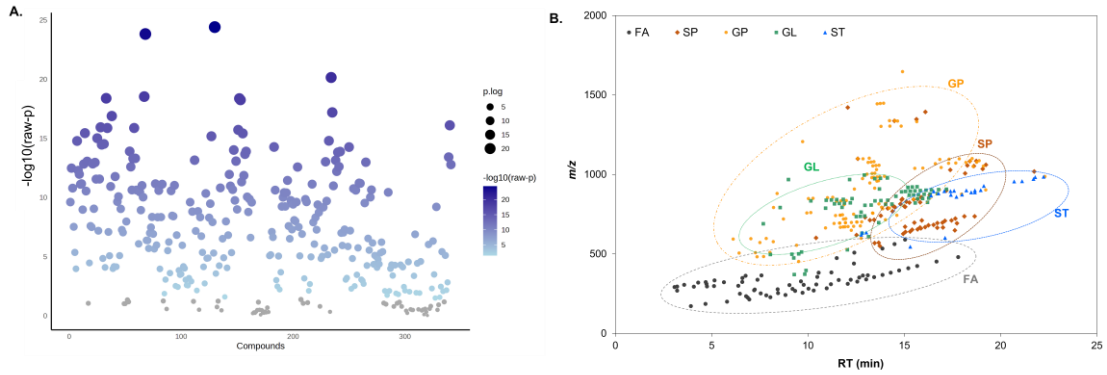

Figure 1: (A) One-way ANOVA displaying the statistical significance of the 344 identified lipid molecular species across four herbal tea varieties. Blue points represent statistically significant lipids ($p < 0.05$), while grey points indicate non-significant lipids. (B) Scatter plot representing the distribution of all identified lipid molecular species based on their *m/z* values and RT. The five major lipid categories (FAs, GLs, GPs, SPs, STs) are visualized according to their elution pattern, with FAs eluting earliest and sterol lipids

STs latest.

2.3.2 Multivariate statistical analysis of herbal tea lipidome

To investigate the overall variation and relationships within the herbal tea lipidome dataset, multivariate statistical analysis was performed using PCA. The dataset consisted of 20 lipidomic profiles (n = 5 for each of the four herbal tea species). The resulting PCA model revealed that the first principal component (PC1) accounted for 33.0% of the total variance, while the second principal component (PC2) explained 20.6%. Together, these two components captured a significant proportion of the total variability within the data. The PCA score plot, shown in **Figure 2A**, exhibited four distinct clusters corresponding to the four herbal tea varieties, indicating clear separation based on their lipidomic profiles. Notably, all sample points were positioned within Hotelling's T2 confidence ellipse, suggesting that the data fell within the acceptable range of natural biological variability.

A detailed examination of the score plot indicated that dokudami and sugina displayed pronounced differences in their lipidomic signatures, as reflected by their separation along the principal components. In contrast, kumazasa and yomogi demonstrated a closer similarity in lipid composition, as evidenced by their proximity and grouping within the same cluster. This suggests that these two herbal tea varieties may share comparable lipid molecular profiles. The PCA loading plot, presented in **Figure 2B**, provides insight into the lipid species responsible for the observed separations among the tea varieties. The loading plot illustrates the relationships among the 344 annotated lipid molecular species, identifying key lipid classes contributing to the differentiation seen in the score plot. The analysis revealed that the FAs, STs, and SPs showed positive correlations with one another, indicating that variations in these lipid classes significantly

influenced the overall separation of the herbal tea samples in the multivariate space.

Additionally, the relative abundance of PUFA-rich GPs and GLs appeared to play a critical role in distinguishing the herbal tea species. These findings are consistent with earlier observations from our laboratory, particularly in seaweed lipidomics studies, where PUFA-enriched GPs and GLs contributed to the separation of sea mustard and kombu species. These seaweeds, similar to herbal teas, are valued for their antioxidant properties and health benefits attributed to their high levels of PUFA-rich lipid species[21].

Overall, this multivariate analysis offers valuable insights into the lipid class-specific contributions to the distinct lipidomic profiles of the four herbal tea varieties. The differentiation patterns observed, particularly about FAs, STs, SPs, and PUFA-rich GPs and GLs, highlight the biochemical diversity of these traditional Japanese herbal teas and suggest potential functional implications related to their lipid composition.

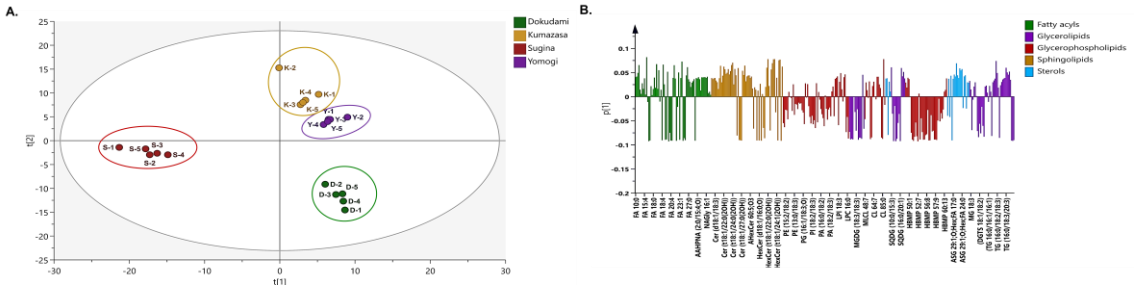

Figure 2: (A) Principal component analysis (PCA) score plot of lipidomic profiles in four herbal tea samples (n=5 per group). The plot illustrates clear clustering of the four tea varieties, with PC1 and PC2 explaining 33.0% and 20.6% of the total variance, respectively. (2) Loading plot of the PCA model, showing the contribution of individual lipid molecular species to the variance observed among the herbal tea varieties. Lipid classes such as FAs, STs, and SPs display positive correlations, indicating their significance in differentiating the herbal teas.

2.3.3 Hierarchical cluster analysis of the herbal tea lipidome

To further investigate the distribution and abundance of lipid molecular species in the four herbal tea varieties, hierarchical clustering analysis was performed, and the results were visualized through heatmaps. These heatmaps provide a comparative visualization of lipid concentrations, with intense red indicating higher abundance and intense blue indicating lower abundance across the samples. The clustering patterns highlighted clear differences in the concentration of major lipid classes among the four herbal teas. The heatmap of SPs molecular species is shown in **Figure 3A**. In plants, SPs represent a significant proportion of total lipids and are known for their structural and functional roles in higher plants[29]. Among the sphingolipids detected, hexosylceramides (HexCer), acylhexosylceramides (AHexCer), and ceramides (Cer) showed distinct clustering patterns across the herbal teas. Notably, AHexCer species were most abundant in yomogi, as reflected by the intense red coloration in the heatmap. This is a novel finding, as although a prior study by Li et al. identified 22 SPs, including seven Cer, in green tea, to our knowledge, this is the first report describing these specific sphingolipid classes in the selected Japanese herbal teas[27].

The hierarchical clustering of GLs is presented in **Figure 3B**. Among the GL classes, monogalactosyldiacylglycerol (MGDG), digalactosyldiacylglycerol (DGDG), and sulfoquinovosyldiacylglycerol (SQDG) were predominantly higher in sugina compared to the other species. These GLs are recognized as the most abundant chloroplast membrane lipids in higher plants and are essential for photosynthetic membranes, cellular energy storage, and signaling functions in eukaryotic cells[30,31]. Similar lipid profiles have been reported in other plant species, including green tea, seaweeds, and purple-leaf teas[21,27,32]. Additionally, it is known that these glycerolipids undergo degradation during

tea manufacturing processes, leading to notable changes in their profiles[27]. However, comprehensive molecular-level profiling of GLs in herbal teas remains limited, making this analysis one of the first of its kind for these species. The sterol lipid content distribution among the herbal teas is depicted in **Figure 3C**. The concentration of acylated (esterified) sterol glucosides (ASGs) was lowest in kumazasa, followed by sugina, yomogi, and highest in dokudami. In plant systems, sterol esters are predominantly localized within cytosolic oil bodies and are important for regulating membrane fluidity and stability. These phytosterols have been reported to inhibit intestinal cholesterol absorption in humans, thereby potentially contributing to cholesterol-lowering effects[33].

Further, **Figures 3D** and **3E** display the heatmap and hierarchical clustering of GPs identified in the herbal teas, respectively. The heatmap reveals that lipid classes such as PC, PI, and phosphatidic acids (PA) were present at higher concentrations in yomogi and lower in kumazasa. In contrast, hemibismonoacylglycerophosphate and cardiolipin (CL) levels were elevated in sugina relative to the other samples. This finding aligns partially with previous work by Chen et al., who identified similar phospholipid classes in different tea types, noting their roles in flavor formation and bioactivity[32]. Notably, this current study represents the first report of these GPs in these traditional Japanese herbs, contributing novel insights into their lipidomic composition. The comprehensive lipidomic profiling conducted in this study not only reveals significant differences in the distribution of individual lipid classes but also provides a foundation for understanding their potential functional and nutritional implications. One key nutritional parameter is the P:S ratio (polyunsaturated to saturated fatty acids), a widely recognized index for assessing dietary lipid quality and its potential impact on cardiovascular health[34].

The distribution of SFAs, MUFAs, and PUFAs in the four herbal teas is

summarized in **Table 1**. The results indicate that PUFAs levels were highest in kumazasa, followed by dokudami, sugina, and yomogi. These findings suggest that certain herbal teas, particularly kumazasa, may serve as health-promoting beverages rich in beneficial PUFAs. These results are consistent with our previous studies on seaweeds and fish, which emphasized the nutritional importance of the P:S ratio in evaluating the health benefits of dietary lipids[21,22]. Altogether, these hierarchical clustering analyses and lipid distribution patterns offer a comprehensive overview of the lipidomic diversity among the herbal tea species examined in this study. They also support the potential of these traditional herbs as sources of bioactive, health-promoting lipid compounds.

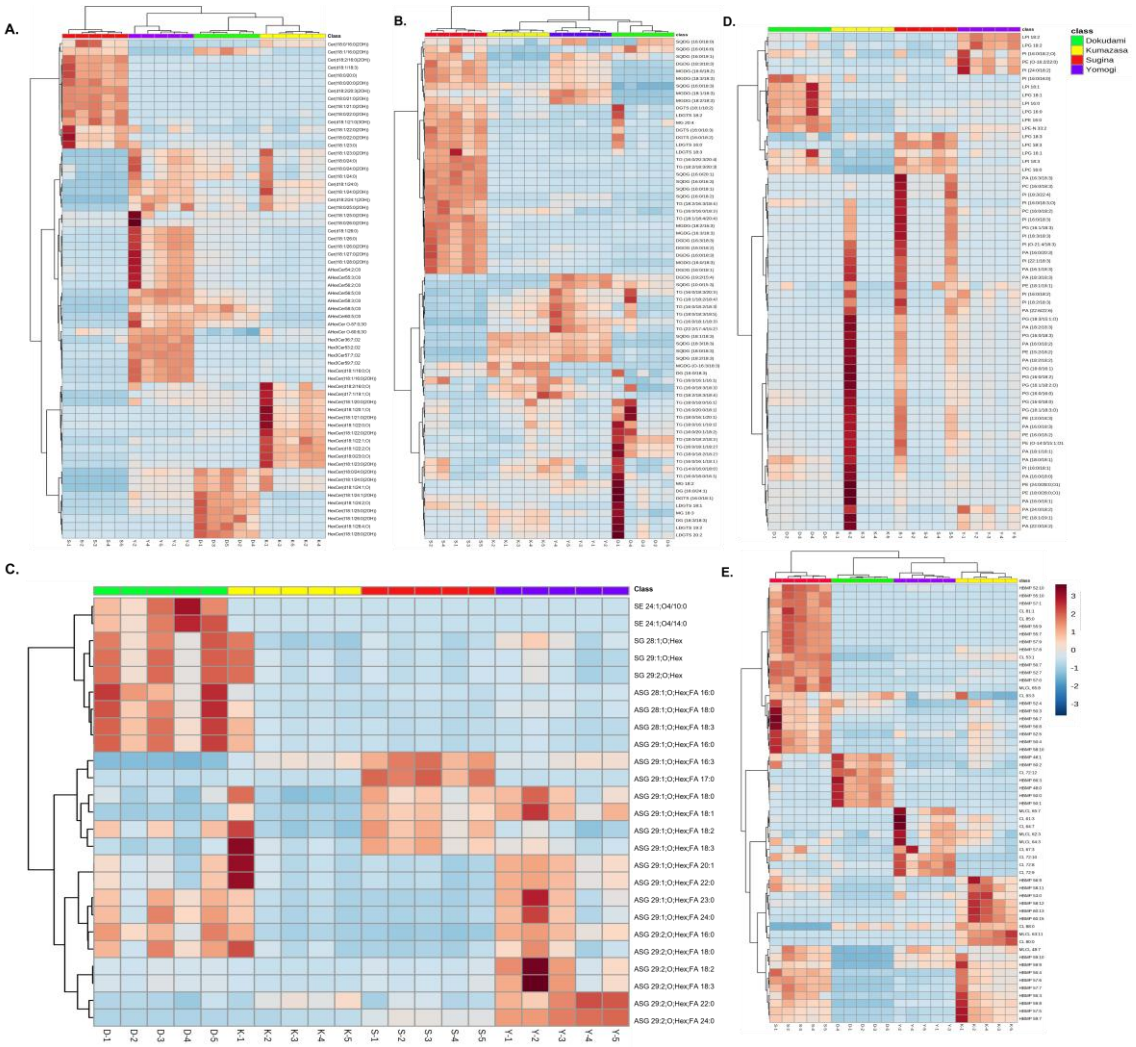

Figure 3: (A) Hierarchical clustering dendrogram of SPs molecular species concentrations in four herbal teas. Intense red and blue colors indicate higher and lower concentrations, respectively. (B) Hierarchical clustering dendrogram of GL molecular species concentrations in four herbal teas. (C) Heatmap of STs molecular species concentrations in four herbal teas. (D) Heatmap of GPs classes identified in four herbal teas. (E) Hierarchical clustering dendrogram of GPs molecular species in four herbal teas, showing relationships and clustering patterns based on lipid abundance similarities.

Table 1. Concentration (Mean ± SE, in mg/g of herbal tea powder) of FA class characterized in four types of herbal tea. (SFA-saturated fatty acids, MUFA-monounsaturated fatty acids, PUFA-polyunsaturated fatty acids).

Fatty acyls (FA)	Dokudami	Kumazasa	Sugina	Yomogi
SFA	0.75 ± 0.05	0.95 ± 0.03	0.51 ± 0.00	0.63 ± 0.01
MUFA	1.13 ± 0.09	1.23 ± 0.00	0.68 ± 0.00	0.23 ± 0.00
PUFA	6.85 ± 1.4	11.06 ± 0.8	5.98 ± 0.28	2.84 ± 0.59

2.3.4 Identification of short-chain fatty acid esters of hydroxy fatty acids in herbal teas

FAHFAs represent a unique class of endogenous bioactive lipids known for their anti-diabetic, anti-inflammatory, and antioxidative properties[35]. Among these, PUFA-esterified FAHFAs have demonstrated immunomodulatory effects by attenuating macrophage activation during inflammatory responses[36]. Additionally, recent *in-vitro* investigations have reported the activation of antioxidant-related genes such as nuclear factor erythroid factor 2-like 2 (Nrf2) by eicosapentaenoic acid-esterified 12-hydroxystearic acid, further emphasizing their biological relevance[37]. FAHFAs have been widely detected in various plant-derived foods, including vegetable oils, fruits, grains, cereals, and fermented products, with numerous families and regioisomers characterized to date[38]. For example, Zhu et al. identified 49 FAHFA families and 138 regioisomers in post-fermented and non-fermented tea types such as green, white, oolong, and black teas[39]. Recently, a new subclass of isomeric structures termed short-chain fatty acid esters of hydroxy fatty acids (SFAHFAs) was identified in murine samples, expanding the known FAHFAs family[40]. These novel SFAHFAs have also been implicated in modulating

immune responses during viral infections, including influenza, and are abundant in the gastrointestinal contents of rodents[41,42]. Despite the widespread occurrence of 2- and 3-hydroxy fatty acids in plants, there has been no evidence thus far of SFAHFA derivatives occurring naturally in plants[43]. In the present study, four novel molecular species of SFAHFAs were identified in the herbal tea samples. These compounds were structurally characterized as esters of 9-phenyl nonanoic acid (PNA), a phenyl-terminated fatty acid that has previously been reported in the seeds of aroids belonging to the Araceae family[44]. Interestingly, these PNA derivatives were detected in herbal teas derived from four plant families other than Araceae, marking a novel discovery in plant lipidomics.

The extracted chromatograms (EIC) corresponding to these FAHFAs are illustrated in **Figure 4A**, while **Figure 4B** presents the hierarchical clustering analysis of fatty acid subclasses, highlighting differences in PUFA content across the samples. Among the PUFAs, α-linolenic acid (FA 18:3) was particularly abundant in kumazasa, whereas arachidonic acid (FA 20:4) was more prevalent in sugina. It is noteworthy that arachidonic acid, an ω-6 fatty acid, is typically associated with pro-inflammatory properties, whereas α-linolenic acid, also classified as an ω-3 fatty acid in this study, exhibits anti-inflammatory effects[45].

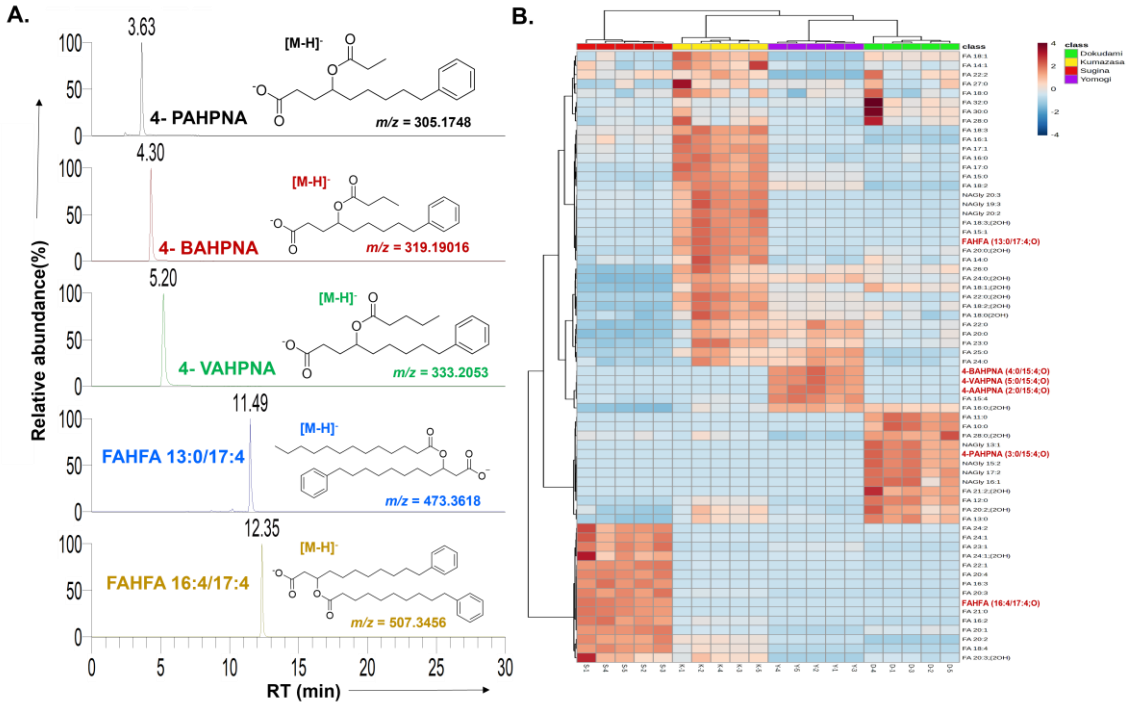

Figure 4: (A) Extracted ion chromatograms (EIC) of four identified SFAHFAs in herbal tea samples. (B) Hierarchical clustering heatmap of fatty acid subclasses in four herbal tea species.

Detailed MS, MS/MS, and MS^3 spectra of the identified FAHFA molecular species are shown in **Figure 5**. All FAHFAs ionize in negative mode, producing characteristic $[M-H]^-$ precursor ions. The high-resolution MS spectrum for 4-propanoic acid esters of hydroxy phenyl nonanoic acid (4-PAHPNA) is presented in **Figure 5A**, showing a precursor ion at *m/z* 305.1748. This ion produced a major fragment ion at *m/z* 249 in the MS/MS spectrum by the loss of CH_3CHCO (56 Da), confirming the esterified short-chain fatty acid as propanoic acid[40]. Further fragmentation of *m/z* 249 resulted in ions at *m/z* 231 and *m/z* 205 by successive losses of H_2O (18 Da) and CO_2 (44 Da), respectively, consistent with a hydroxy phenyl nonanoic acid backbone. A key fragment at *m/z* 175, formed by the neutral loss of CH_3CH_2COOH (74 Da) from *m/z* 249, confirmed the hydroxylation at the 4th position of the PNA chain, consistent with previously

established fragmentation patterns[35]. These results conclusively identified the compound as 4-PAHPNA. Similarly, **Figure 5B** displays the spectra for 4-butyric acid hydroxy phenyl nonanoic acid (4-BAHPNA). This lipid exhibited an $[M-H]^-$ ion at *m/z* 319.1903. In MS/MS mode, this precursor ion produced *m/z* 249 by the loss of CH_3CH_2CHCO (70 Da), indicating the esterification with butyric acid. Further losses of H_2O and CO_2 yielded fragment ions identical to those of 4-PAHPNA, reaffirming the hydroxy phenyl nonanoic acid core and 4-position hydroxylation. **Figure 5C** illustrates the mass spectra for 4-valeric acid hydroxy phenyl nonanoic acid (4-VAHPNA). This lipid species ionized to produce an $[M-H]^-$ ion at *m/z* 333.2054. Subsequent fragmentation generated *m/z* 249 by the loss of $CH_3(CH_2)_2CHCO$ (84 Da), consistent with a valeric acid ester group. As with the other SFAHFAs, the subsequent MS/MS fragment ions at *m/z* 231 and *m/z* 205, suggested the loss of H_2O (18 Da) and CO_2 (44 Da), respectively. The *m/z* 175 due to neutral loss of CH_3CH_2COOH (74Da) confirmed the hydroxylation at the 4^{th} position of PNA.

Similarly, the newly identified FAHFAs characterized in this study, along with their corresponding MS spectra, are presented in **Figures 6D** and **6E**. The fragmentation behavior of these molecular ions was found to be comparable. As depicted in **Figure 6D**, FAHFA (13:0/17:4) exhibited a product ion $[M-H]^-$ at *m/z* 473.3618. In the MS^2 spectra, this precursor ion produced fragment ions at *m/z* 277, corresponding to hydroxy fatty acid (HFA) $[HFA17:4-H]^-$, and *m/z* 213, representing $[FA13:0-H]^-$. The fragment at *m/z* 277 further lost a neutral water molecule (H_2O), yielding a peak at *m/z* 259. Subsequent MS^3 analysis of the *m/z* 277 ion revealed fragments at *m/z* 259, *m/z* 233, and *m/z* 231, which indicate sequential losses of H_2O, CO_2, and HCOOH, respectively. The observation of a neutral HCOOH loss suggests the presence of a hydroxyl group at the second carbon

position of FA 17:4, consistent with earlier findings[37]. Likewise, in **Figure 6E**, FAHFA (16:4/17:4) displayed a $[M-H]^-$ molecular ion at *m/z* 507.3457. This ion fragmented in the MS^2 spectra to generate product ions at *m/z* 277 ($[HFA17:4-H]^-$) and *m/z* 247 ($[FA16:4-H]^-$). The *m/z* 277 again underwent the loss of a water molecule, forming a peak at *m/z* 259. Further fragmentation in the MS^3 spectra of the *m/z* 277 ion produced signals at *m/z* 259, *m/z* 233, and *m/z* 217, indicating successive losses of H_2O, CO_2, and CH_3COOH, respectively. The neutral loss of CH_3COOH points to the likely presence of a hydroxyl group at the third carbon position in FA 17:4.

A summary of all characterized FAHFA species identified in the herbal tea samples is provided in **Table 2**. These findings represent the first report of PNA-derived SFAHFAs in these plant species, expanding the known diversity of FAHFAs in plant-based foods and revealing novel lipid structures with potential biological relevance.

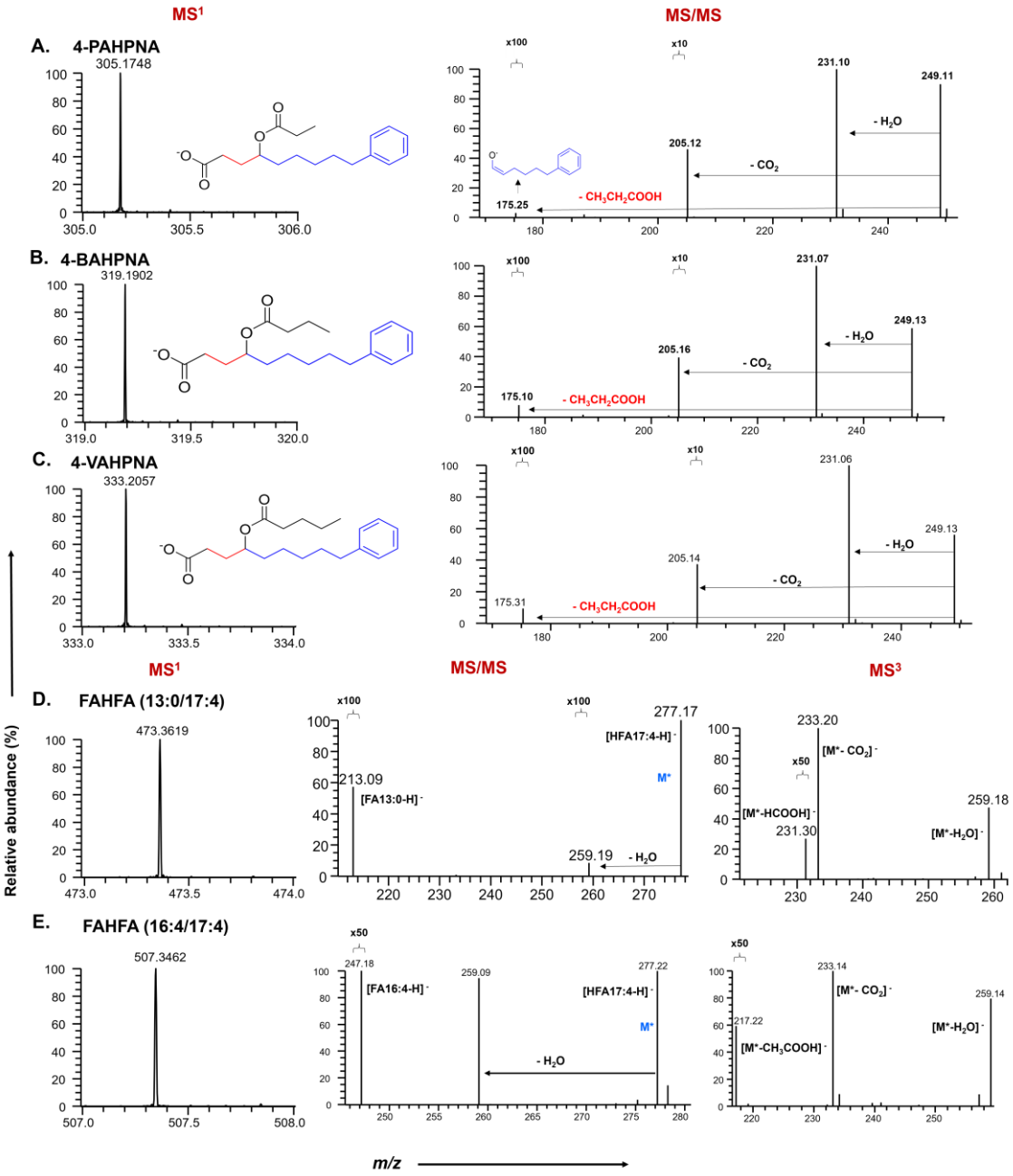

Figure 5: (A) High-resolution MS, MS/MS, and MS³ spectra of 4-propanoic acid hydroxy phenyl nonanoic acid (4-PAHPNA) in negative ion mode. Fragmentation pathways confirm esterified propanoic acid and hydroxylation at the 4th position of PNA. (B) Mass spectral analysis of 4-butyric acid hydroxy phenyl nonanoic acid (4-BAHPNA). Fragment ions support the identification of butyric acid esterification and confirm

structural features identical to 4-PAHPNA. (C) MS, MS/MS, and MS^3 spectra of 4-valeric acid hydroxy phenyl nonanoic acid (4-VAHPNA), showing characteristic fragmentation corresponding to valeric acid esterification and hydroxylation at the 4th position of PNA. (D) FAHFA (13,0/17:4) and (E) FAHFA (16,4/17:4). M* is the precursor ion of hydroxy fatty acid.

Table 2. List of detected FAHFAs in four herbal teas as $[M-H]^-$ ions. 4-AAHPNA: Acetic acid esters of 4-hydroxy -9-phenyl nonanoic acid; 4-PAHPNA: Propanoic acid esters of 4-hydroxy 9-phenyl nonanoic acid; 4-BAHPNA: Butyric acid esters of 4-hydroxy 9-phenyl nonanoic acid; 4-VAHPNA: Valeric acid esters of 4-hydroxy 9-phenyl nonanoic acid; FAHFA: Fatty acid esters of hydroxy fatty acids.

Lipid species	Molecular formula	RT (minutes)	Theoretical mass (*m/z*)	Experimental mass (*m/z*)	Mass error (ppm)
4-AAHPNA	$C_{17}H_{24}O_4$	3.14	291.1602	291.1593	-3.09
4-PAHPNA	$C_{18}H_{26}O_4$	3.63	305.1758	305.1749	-2.94
4-BAHPNA	$C_{19}H_{28}O_4$	4.31	319.1915	319.1903	-3.75
4- VAHPNA	$C_{20}H_{30}O_4$	5.20	333.20713	333.2056	-4.50
FAHFA (16:4/17:4)	$C_{33}H_{48}O_4$	12.35	507.3480	507.3457	-4.53
FAHFA (13:0/17:4)	$C_{30}H_{50}O_4$	13.89	473.3636	473.3619	-3.59

2.4 Limitations

While this study successfully identified and characterized SFAHFAs in herbal teas and provided a comprehensive overview of their lipid composition, several limitations should be acknowledged. Firstly, the concentrations reported for the identified lipids, including SFAHFAs, are semi-quantitative rather than absolute, due to the absence of commercial

standards for these novel lipid species. As a result, lipid identification and confirmation in this study relied heavily on high-resolution MS and MS/MS spectral data. Although MS/MS fragmentation provided important insights into the structural features of these lipids, particularly regarding the presence of hydroxy groups, the exact positional assignments of hydroxylation sites could not be conclusively determined due to the lack of higher-order MS^3 data. In addition, while FAHFAs were successfully detected in the herbal tea samples, the specific positions of double bonds in their unsaturated fatty acid chains remain unconfirmed, leaving aspects of their full structural identity unresolved. Another limitation involves the study's scope, which did not address environmental factors, growth conditions, harvest stages, or post-harvest handling practices, all of which are known to influence lipid composition in plants. Without this contextual information, it is difficult to fully assess the natural variability or stability of lipid profiles in these herbal teas under different cultivation or processing conditions. Future studies should aim to address these gaps by including absolute quantification with synthesized standards, incorporating MS^3 fragmentation analysis for more precise structural elucidation, and examining the influence of environmental and agronomic factors on lipid profiles to strengthen the broader relevance of these findings.

2.5 Conclusion

This study provides a comprehensive lipidomic characterization of four traditional Japanese herbal teas, revealing significant variations in their lipid molecular profiles. Utilizing untargeted LC-MS-based lipidomics and multivariate statistical analyses, a total of over 300 distinct lipid molecular species were identified and annotated. These findings highlight the diverse and complex lipid compositions of the selected herbal teas, with a

particular emphasis on the abundance and distribution of bioactive lipid classes. Among the noteworthy outcomes of this investigation was the first-time identification and structural characterization of SFAHFAs in these plant-based samples. These newly discovered lipids represent the first known PNA-based SFAHFAs reported in plants, expanding the chemical diversity of the FAHFAs family, which has previously been studied primarily in animal systems. The identification of these unique lipid species marks a significant advancement in plant lipidomics, opening up new research opportunities for understanding their potential physiological and nutritional roles. This study also confirmed the presence of health-promoting PUFAs, such as α-linolenic acid, in varying concentrations across the different herbal tea varieties. These bioactive lipids are known for their anti-inflammatory and cardioprotective properties, underscoring the potential health benefits associated with herbal tea consumption.

Collectively, this work offers a qualitative and comparative overview of lipid profiles in herbal teas, contributing valuable baseline data for future functional and nutritional studies. The discovery of novel bioactive lipid species, particularly the PNA-derived SFAHFAs, highlights the untapped chemical diversity within traditional herbal teas and suggests promising implications for human health. Moving forward, further investigations will be undertaken to evaluate the biological significance of these SFAHFAs *in-vitro* and *in vivo*, exploring their potential roles in modulating inflammatory responses, oxidative stress, and metabolic processes. In addition, future research will aim to identify other dietary sources and herbal preparations containing these unique lipid molecules, broadening our understanding of their distribution, health effects, and possible nutraceutical applications. Ultimately, this research paves the way for deeper exploration into the role of lipids in herbal teas, offering new insights into the intersection of plant

lipidomics, functional foods, and human health. By expanding the current knowledge of bioactive lipid components in commonly consumed herbal products, this work contributes to the growing body of evidence supporting the nutritional and therapeutic potential of plant-based diets.

2.6 References

1. Pan, S. Y., Nie, Q., Tai, H. C., Song, X. L., Tong, Y. F., Zhang, L. J. F., Wu, X. W., Lin, Z. H., Zhang, Y. Y., Ye, D. Y., Zhang, Y., Wang, X. Y., Zhu, P.L., Chu, Z. S., Yu, Z. L., & Liang, C. (2022). Tea and tea drinking: China's outstanding contributions to the mankind. Chinese medicine, 17(1), 27.
2. Mandiwana, K. L., Panichev, N., & Panicheva, S. (2011). Determination of chromium (VI) in black, green and herbal teas. Food Chemistry, 129(4), 1839-1843.
3. Liu, Y., Ahmed, S., & Long, C. (2013). Ethnobotanical survey of cooling herbal drinks from southern China. Journal of ethnobiology and ethnomedicine, 9, 1-8.
4. Wargovich, M. J., Woods, C., Hollis, D. M., & Zander, M. E. (2001). Herbals, cancer prevention and health. The Journal of nutrition, 131(11), 3034S-3036S.
5. Hayashi, K., Kamiya, M., & Hayashi, T. (1995). Virucidal effects of the steam distillate from Houttuynia cordata and its components on HSV-1, influenza virus, and HIV. Planta medica, 61(03), 237-241.
6. Lau, K. M., Lee, K. M., Koon, C. M., Cheung, C. S. F., Lau, C. P., Ho, H. M., Lee, M. Y. H., Au S. W. N., Cheng, C. H. k., Lau, C. B. S., Tsui, S. K. W., Wan, D. C. C., Waye, M. M. Y., Wong K. B., Wong, C. K., Lam, C. W. K., Leung, P. C., & Fung, K. P. (2008). Immunomodulatory and anti-SARS activities of Houttuynia cordata. Journal of ethnopharmacology, 118(1), 79-85.
7. Miyata, M., Koyama, T., & Yazawa, K. (2010). Water extract of Houttuynia cordata Thunb. leaves exerts anti-obesity effects by inhibiting fatty acid and glycerol absorption. Journal of nutritional science and vitaminology, 56(2), 150-156.
8. Ichimaru, Y., Kanaeda, N., Tominaga, S., Suzui, M., Maeda, T., Fujii, H., Nakao, M., & Yoshioka, H. (2020). Sasa veitchii extract induces anticancer effects via inhibition

of cyclin D1 expression in MCF-7 cells. Nagoya Journal of Medical Science, 82(3), 509.

9. Yoshioka, H., Mori, M., Fujii, H., & Nonogaki, T. (2017). Sasa veitchii extract reduces obesity-induced insulin resistance and hepatic steatosis in obese mice fed a high-fat diet. Nagoya Journal of Medical Science, 79(3), 279.
10. Asgarpanah, J., & Roohi, E. (2012). Phytochemistry and pharmacological properties of Equisetum arvense L. Journal of Medicinal Plants Research, 6(21), 3689-3693.
11. Četojević-Simin, D. D., Čanadanović-Brunet, J. M., Bogdanović, G. M., Djilas, S. M., Ćetković, G. S., Tumbas, V. T., & Stojiljković, B. T. (2010). Antioxidative and antiproliferative activities of different horsetail (Equisetum arvense L.) extracts. Journal of medicinal food, 13(2), 452-459.
12. Saeed, B. Q., Hassan, H. F., & Arteen, H. I. (2014). Effect of Some Medical Plant Extracts on Metabolism of Leishmania tropica Promastigotes. J Med Microb Diagn, 3(165), 2161-0703.
13. Ding, W., Ji, T., Xiong, W., Li, T., Pu, D., & Liu, R. (2018). Realgar, a traditional Chinese medicine, induces apoptosis of HPV16-positive cervical cells through a HPV16 E7-related pathway. Drug Design, Development and Therapy, 3459-3469.
14. Chung, K. S., Choi, J. H., Back, N. I., Choi, M. S., Kang, E. K., Chung, H. G., ... & Lee, K. T. (2010). Eupafolin, a flavonoid isolated from Artemisia princeps, induced apoptosis in human cervical adenocarcinoma HeLa cells. Molecular nutrition & food research, 54(9), 1318-1328.
15. Malongane, F., McGaw, L. J., Nyoni, H., & Mudau, F. N. (2018). Metabolic profiling of four South African herbal teas using high resolution liquid chromatography-mass spectrometry and nuclear magnetic resonance. Food Chemistry, 257, 90-100.

16. Suh, M. C., Uk Kim, H., & Nakamura, Y. (2022). Plant lipids: trends and beyond. Journal of Experimental Botany, 73(9), 2715-2720.
17. Rodríguez, J., Martín, M. J., Ruiz, M. A., & Clares, B. (2016). Current encapsulation strategies for bioactive oils: From alimentary to pharmaceutical perspectives. Food Research International, 83, 41-59.
18. Sokoła-Wysoczańska, E., Wysoczański, T., Wagner, J., Czyż, K., Bodkowski, R., Lochyński, S., & Patkowska-Sokoła, B. (2018). Polyunsaturated fatty acids and their potential therapeutic role in cardiovascular system disorders—a review. Nutrients, 10(10), 1561.
19. Gangadhara, R. M., Gowda, S. G. B., Gowda, D., Inui, K., & Hui, S. P. (2023). Lipid composition analysis and characterization of acyl sterol glycosides in adzuki and soybean cultivars by non-targeted LC-MS. Foods, 12(14), 2784.
20. Gowda, S. G. B., Minami, Y., Gowda, D., Furuko, D., Chiba, H., & Hui, S. P. (2021). Lipidomic analysis of non-esterified furan fatty acids and fatty acid compositions in dietary shellfish and salmon by UHPLC/LTQ-Orbitrap-MS. Food Research International, 144, 110325.
21. Gowda, S. G. B., Yifan, C., Gowda, D., Tsuboi, Y., Chiba, H., & Hui, S. P. (2022). Analysis of antioxidant lipids in five species of dietary seaweeds by liquid chromatography/mass spectrometry. Antioxidants, 11(8), 1538.
22. Gowda, S. G. B., Minami, Y., Gowda, D., Chiba, H., & Hui, S. P. (2022). Detection and characterization of lipids in eleven species of fish by non-targeted liquid chromatography/mass spectrometry. Food Chemistry, 393, 133402.
23. Yu, X., Hu, S., He, C., Zhou, J., Qu, F., Ai, Z., Chen, Y., & Ni, D. (2019). Chlorophyll metabolism in postharvest tea (Camellia sinensis L.) leaves: variations in color

values, chlorophyll derivatives, and gene expression levels under different withering treatments. Journal of agricultural and food chemistry, 67(38), 10624-10636.

24. Ho, C. T., Zheng, X., & Li, S. (2015). Tea aroma formation. Food science and human wellness, 4(1), 9-27.
25. Ravichandran, R., & Parthiban, R. (2000). Lipid occurrence, distribution and degradation to flavour volatiles during tea processing. Food Chemistry, 68(1), 7-13.
26. Cui, H. N., Gu, H. W., Li, Z. Q., Sun, W., Ding, B., Li, Z., Chen, Y., Long, W., Yin, X. L., & Fu, H. (2023). Integration of lipidomics and metabolomics approaches for the discrimination of harvest time of green tea in spring season by using UPLC-Triple-TOF/MS coupled with chemometrics. Frontiers in Sustainable Food Systems, 7, 1119314.
27. Li, J., Hua, J., Yuan, H., Deng, Y., Zhou, Q., Yang, Y., C., Dong, J., Zeng, & Jiang, Y. (2021). Investigation on green tea lipids and their metabolic variations during manufacturing by nontargeted lipidomics. Food Chemistry, 339, 128114.
28. Bligh, E. G., & Dyer, W. J. (1959). A rapid method of total lipid extraction and purification. Canadian journal of biochemistry and physiology, 37(8), 911-917.
29. Dunn, T. M., Lynch, D. V., Michaelson, L. V., & Napier, J. A. (2004). A post-genomic approach to understanding sphingolipid metabolism in Arabidopsis thaliana. Annals of Botany, 93(5), 483-497.
30. Benning, C., & Ohta, H. (2005). Three enzyme systems for galactoglycerolipid biosynthesis are coordinately regulated in plants. Journal of Biological Chemistry, 280(4), 2397-2400.
31. Voelker, D. R. (2013). Glycerolipid structure, function, and synthesis in eukaryotes.
32. Chen, X., Wang, P., Wei, M., Lin, X., Gu, M., Fang, W., ... & Ye, N. (2022).

Lipidomics analysis unravels changes from flavor precursors in different processing treatments of purple-leaf tea. Journal of the Science of Food and Agriculture, 102(9), 3730-3741.

33. Ostlund Jr, R. E., Racette, S. B., & Stenson, W. F. (2003). Inhibition of cholesterol absorption by phytosterol-replete wheat germ compared with phytosterol-depleted wheat germ. The American journal of clinical nutrition, 77(6), 1385-1389.
34. Kang, M. J., Shin, M. S., Park, J. N., & Lee, S. S. (2005). The effects of polyunsaturated: saturated fatty acids ratios and peroxidisability index values of dietary fats on serum lipid profiles and hepatic enzyme activities in rats. British journal of nutrition, 94(4), 526-532.
35. Yore, M. M., Syed, I., Moraes-Vieira, P. M., Zhang, T., Herman, M. A., Homan, E. A., Ptael, R. T., Lee, J., Chen, S., Peroni, O. D., Dhaneshwar, A. S., Hammarstedt, A., Smith, u., McGraw, T. E., Saghatelian, A., & Kahn, B. B. (2014). Discovery of a class of endogenous mammalian lipids with anti-diabetic and anti-inflammatory effects. Cell, 159(2), 318-332.
36. Kuda, O., Brezinova, M., Rombaldova, M., Slavikova, B., Posta, M., Beier, P., Janovska, p., Veleba, J., Jr, J. K., Kudova, E., Pelikanova, Terezie., & Kopecky, J. (2016). Docosahexaenoic acid–derived fatty acid esters of hydroxy fatty acids (FAHFAs) with anti-inflammatory properties. Diabetes, 65(9), 2580-2590.
37. Gowda, S. G. B., Fuda, H., Tsukui, T., Chiba, H., & Hui, S. P. (2020). Discovery of eicosapentaenoic acid esters of hydroxy fatty acids as potent Nrf2 activators. Antioxidants, 9 (5), 397.
38. Watanabe, A., Balas, L., Saigusa, D., Ogura, J., Durand, T., Mano, N., & Yamaguchi, H. (2022). Analytical evaluation of fatty acid esters of hydroxy fatty acid quantity in

fermented brown rice and rice bran (FRBA). Food Chemistry Advances, 1, 100040.

39. Zhu, Q. F., Ge, Y. H., An, N., Li, N., Xiao, Y., Huang, G. X., Zhang, L. L., Feng, Y. Q., & Wu, J. L. (2022). Profiling of branched fatty acid esters of hydroxy fatty acids in teas and their potential sources in fermented tea. Journal of agricultural and food chemistry, 70(17), 5369-5376.
40. Gowda, S. G. B., Liang, C., Gowda, D., Hou, F., Kawakami, K., Fukiya, S., Yokota, A., Chiba, H., & Hui, S. P. (2020). Identification of short-chain fatty acid esters of hydroxy fatty acids (SFAHFAs) in a murine model by nontargeted analysis using ultra-high-performance liquid chromatography/linear ion trap quadrupole-Orbitrap mass spectrometry. Rapid communications in mass spectrometry, 34(17), e8831.
41. B. Gowda, S. G., Gowda, D., Ohno, M., Liang, C., Chiba, H., & Hui, S. P. (2021). Detection and structural characterization of SFAHFA homologous series in mouse colon contents by LTQ-Orbitrap-MS and their implication in influenza virus infection. Journal of the American Society for Mass Spectrometry, 32(8), 2196-2205.
42. Gowda, S. G. B., Hou, F., Gowda, D., Chiba, H., Kawakami, K., Fukiya, S., Yokota, A., & Hui, S. P. (2024). Synthesis and quantification of short-chain fatty acid esters of hydroxy fatty acids in rat intestinal contents and fecal samples by LC-MS/MS. Analytica Chimica Acta, 1288, 342145.
43. Zhu, Q. F., Yan, J. W., Zhang, T. Y., Xiao, H. M., & Feng, Y. Q. (2018). Comprehensive screening and identification of fatty acid esters of hydroxy fatty acids in plant tissues by chemical isotope labeling-assisted liquid chromatography–mass spectrometry. Analytical Chemistry, 90(16), 10056-10063.
44. Meija, J., & Soukup, V. G. (2004). Phenyl-terminated fatty acids in seeds of various aroids. Phytochemistry, 65(15), 2229-2237.

45. Park, J., Choi, J., Kim, D. D., Lee, S., Lee, B., Lee, Y., Kim, S., Kwon, S., Noh, M., Lee, M. O., Le, Q. V., & Oh, Y. K. (2021). Bioactive lipids and their derivatives in biomedical applications. Biomolecules & Therapeutics, 29(5), 465.

Chapter 3

Cultivar-Dependent Lipidome Diversity and Discovery of Novel Bioactive Lipids in Sorghum Grains Using Untargeted LC-MS

3.1 Introduction:

Sorghum (*Sorghum bicolor* (L.) Moench) is a major cereal crop widely cultivated and consumed in Africa and Asia, where it serves as an essential dietary staple for over 500 million people across more than 30 countries[1,2]. In terms of global cereal production, sorghum ranks fifth after wheat, maize, rice, and barley, both in harvested area and total output (FAOSTAT, 2024). Nigeria stands as the world's leading producer, contributing approximately 12% of global production, followed by Sudan and Mexico, where it is utilized for both human consumption and industrial purposes (USDA FAS, 2024).

Beyond its role as a staple food, sorghum has attracted increasing interest due to its potential health benefits. A growing body of research has highlighted its protective effects against a range of chronic diseases prevalent in modern societies, including inflammation, hypercholesterolemia, cancer, and T2D[3-6]. Additionally, sorghum has been recognized as a naturally gluten-free grain, making it a suitable dietary alternative for individuals with celiac disease, since it lacks the immunogenic gluten peptides found in wheat, rye, and barley[7]. Agronomically, sorghum is valued for its exceptional environmental adaptability, capable of thriving in both drought-prone and waterlogged conditions[8]. Its self-pollinating nature contributes to genetic stability, while its resilience makes it particularly valuable for food security in regions facing harsh climatic and soil conditions[9]. Structurally, sorghum kernels are composed of three main parts: the pericarp (3–6%), endosperm (84–90%), and germ (5–10%)[10]. The grain exhibits diverse pericarp colors including white, yellow, red, brown, and black, reflecting its genetic diversity[11].

Nutritionally, sorghum grain is composed of approximately 75% carbohydrates, 12% protein, 4% lipids, 3% fiber, and 2% ash[11]. Its relatively higher lipid content compared to other cereals like rice and wheat enhances its nutritional value, particularly

through the presence of health-promoting fatty acids such as oleic and linoleic acids[12]. Recent studies have reported that certain sorghum varieties also contain unusual fatty acids, including dicarboxylic acids like octanedioic acid and azelaic acid, in addition to a variety of saturated and unsaturated fatty acids, suggesting their potential as a novel source of high-quality edible oil[13]. Investigations into the fatty acid profiles of sorghum have revealed a lipid composition comprising approximately 14.8% saturated fatty acids, primarily palmitic acid, 38% monounsaturated fatty acids dominated by oleic acid, and about 44% polyunsaturated fatty acids, predominantly linoleic acid[14]. However, most of these earlier studies have been restricted to a narrow focus on fatty acyl classes, largely utilizing gas chromatography (GC) methods, which, while effective for quantifying major fatty acids, are limited by their sensitivity and labor-intensive derivatization requirements[15-17].

Although some research has applied LC-MS techniques to sorghum grain extracts, these efforts have primarily targeted phenolic compounds and anthocyanins, with minimal emphasis on comprehensive lipidomic profiling[18,19]. Consequently, the broader lipidomic landscape of sorghum remains insufficiently explored, particularly about bioactive lipid species that may contribute to health benefits.

In this study, a highly sensitive LC/LTQ-Orbitrap-MS platform was employed to perform an untargeted lipidomic analysis of whole-grain extracts from six commercially cultivated sorghum varieties grown in a single field trial in Australia. This approach enabled the identification of a wide range of lipid molecular species, including bioactive lipids such as FAHFAs, which have gained attention for their anti-inflammatory and metabolic regulatory effects. This research aimed to characterize the lipid composition and variation among sorghum cultivars, providing new insights into their nutritional value

and potential applications in promoting human health.

3.2 Materials and methods

3.2.1 Sample preparation:

Grain samples from six commercially available sorghum (*Sorghum bicolor*) hybrids, Bazley, Buster, Liberty, Cracker, Tiger, and MR43 (mitch-rated), were selected for comprehensive lipidomics analysis. Among these cultivars, Liberty is characterized by a white pericarp, while the remaining five cultivars possess red pericarps. All sorghum plants were cultivated under field trial conditions during the 2017–2018 growing season at the University of Sydney's "Nowley" farm, located in northern New South Wales, Australia (latitude 31°34′31″ S, longitude 150°10′53″ E). Conducting the trial at a single site allowed for direct comparisons between genotypes under uniform environmental conditions, including soil type, light exposure, water availability, temperature, and growing season duration. The experimental design involved planting each cultivar in three to five replicate plots, each measuring 1 × 2 meters, arranged in a randomized block design. Weather and environmental data were collected from the regional meteorological station network to verify normal seasonal conditions during the trial period. The sorghum seeds, commercially treated with protective coatings, were sown in late October 2017 and harvested in March 2018. After harvest, the grains were placed in sealed storage bags and maintained in a climate-controlled grain storage facility at the I. A. Watson Grain Research Centre (Narrabri, NSW) under controlled conditions of 15 °C temperature and regulated relative humidity. Subsequently, the samples were transported to the University of Sydney's main campus and stored at 4 °C in sealed plastic containers. Prior to shipping to Japan for analysis, the grains were coarsely milled, sealed in airtight plastic containers

under a nitrogen atmosphere, and stored at -80 °C to prevent lipid oxidation and degradation.

The solvents, internal standards, and reagents used for lipid extraction and LC-MS analysis in the sorghum grain study were identical to those described in **Chapter 2, Section 2.2.3**. Additional reagents such as N, N-dimethylethylenediamine (DMED) were procured from Sigma-Aldrich (Saint Louis, MO, USA), while 2-chloro-1-methylpyridinium iodide (CMPI) and triethylamine (TEA) of analytical grade were supplied by Tokyo Chemical Industries Co., Ltd. (Tokyo, Japan). These derivatization reagents, including CMPI, TEA, and DMED, were freshly prepared in LC-MS grade acetonitrile (ACN) at a working concentration of 20 mM before use.

The FAHFA standard 12-OAHOA (oleic acid ester of 12-hydroxy oleic acid) used in this study was synthesized in our laboratory following the protocol described by Gowda et al. (2020)[20]. The synthesis was performed before this study and used as a reference standard for lipid identification.

3.2.2 Lipid extraction

Lipid extraction from sorghum grain samples was performed following the modified Bligh-Dyer method described in **Chapter 2, Section 2.2.3**, with one adjustment made to accommodate the sorghum grain matrix. Specifically, 150 mg of finely ground whole-grain sorghum powder (n = 5) was weighed and transferred into 2 mL Eppendorf tubes. The sorghum kernel structure and representative images of the powdered samples are shown in **Figure 1A and 1B**. To each sample, 1.5 mL of methanol was added, and homogenization was carried out using 1.4 mm ceramic beads (catalog no. 15–340-159, Fisherbrand, Fisher Scientific, Pittsburgh, PA, USA) in a Bead Mill 4 homogenizer (Fisherbrand, Tokyo, Japan) for 1 minute (two 30-second cycles). An aliquot of 200 µL

of the homogenate was then transferred into a new 2 mL tube for lipid extraction, following the subsequent steps as described in **Chapter 2, Section 2.2.3**.

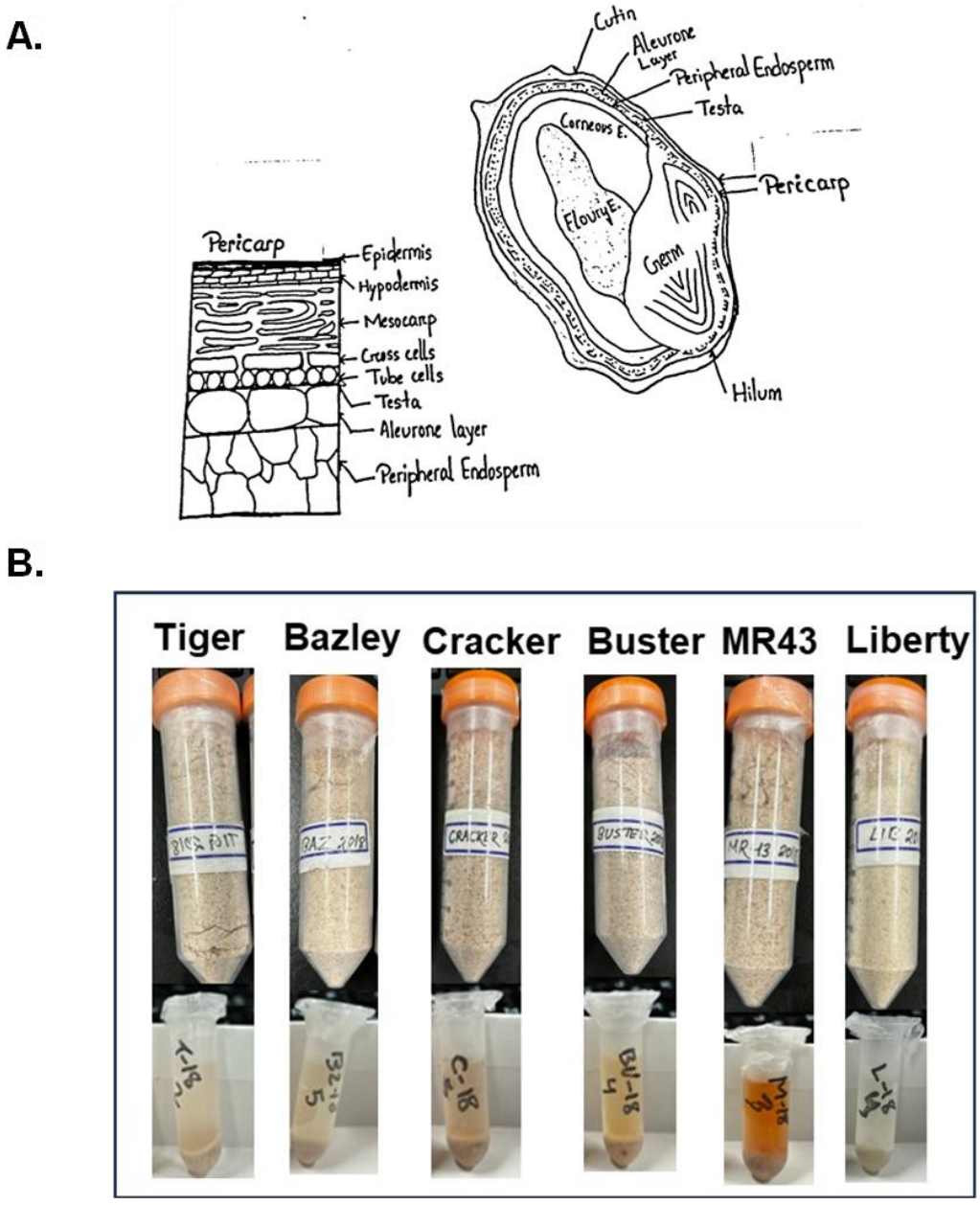

Figure 1: (A) Kernel structure of sorghum grain (B) Images of the powdered sorghum cultivars analyzed in the study.

3.2.3 Total lipid content analysis

The total lipid content of the sorghum grain samples was determined using the Bligh-Dyer method[21]. Briefly, 1 g of whole-grain sorghum flour (n = 3) was weighed into 15 mL Falcon tubes. To each sample, 6 mL of methanol was added, and the mixture was vortexed for 10 seconds. Following this, 3 mL of chloroform and 600 µL of Milli-Q water were added, and the mixture was vortexed at 3,500 rpm for 5 minutes. The mixture was then left to stand at room temperature for 2 hours, with an additional vortexing step at 3,500 rpm for 1 minute after 1 hour. After incubation, the mixture was centrifuged at 15,000 rpm for 10 minutes, and the resulting lipid-containing organic layer was carefully transferred to a new 15 mL Falcon tube. To recover remaining lipids, the residue in the initial tube was treated with a methanol: chloroform mixture (2:1, v/v), vortexed for 5 minutes, and centrifuged for 10 minutes. The organic phases from both extractions were combined in the same tube and dried overnight using a rotary evaporator. The total lipid content was calculated by weighing the final dried lipid extract, with results expressed as milligrams of total lipid per gram of sample.

3.2.4 DMED derivatization of FAHFAs

The DMED derivatization of FAHFAs was performed following the protocol established in our previous study[22]. This derivatization was specifically applied to the lipid extracts from the sorghum cultivar MR43, selected due to its notably higher abundance of FAHFAs (**Table 1**). Before derivatization, the dried lipid extracts were dissolved in 500 µL of ACN. From this solution, 100 µL of lipid extract in ACN was transferred to a reaction tube, to which 25 µL of 12-OAHOA standard solution was added. The mixture was vortexed for 1 minute. Subsequently, 20 µL of TEA and 10 µL of CMPI were added, followed by vortexing for 3 minutes.

Next, 20 μL of DMED was added to the mixture, which was then vortexed for 30 minutes at room temperature. After derivatization, the solvent was evaporated using a centrifugal evaporator at 4 °C. The dried derivatized residue was then redissolved in 100 μL of methanol, centrifuged at maximum speed for 10 minutes, and transferred to LC-MS vials for analysis. An injection volume of 20 μL was used for the subsequent LC-MS measurements.

3.2.5 LC-MS analysis

The LC-MS analysis of sorghum lipid extracts was performed using the same instrumentation, chromatographic conditions, and mass spectrometric parameters described in **Chapter 2, Section 2.2.4**. The DMED derivatized FAHFAs were analysed using the positive mode of ionization.

3.2.6 Statistical analysis

The molecular species of lipids identified in both positive and negative ionization modes were compiled into a comprehensive lipidomics dataset for analysis. The data visualization and summary statistics were performed using Microsoft Excel 2021, with results expressed as mean ± SEM. To investigate patterns of variation and obtain a holistic view of the dataset, multivariate analyses were conducted using MetaboAnalyst (version 5.0). Specifically, a sparse partial least squares-discriminant analysis (sPLS-DA) was performed, along with the generation of hierarchical clustering heatmaps.

3.3 Results and discussion

3.3.1 Total lipid content and multivariate analysis of the sorghum grain lipidome

The total lipid content of the six sorghum cultivars was determined on a fresh weight (FW) basis and is presented as a comparative bar graph in **Figure 2A**. Although the overall differences in total lipid content among cultivars were not statistically significant, Bazley exhibited the highest lipid content at approximately 5.64% FW, while Buster recorded the lowest at around 3.22% FW. These findings are comparable to earlier reports, where the total lipid content of sorghum grain was measured at 3.7% based on dry weight (DW)[23]. Notably, the lipid content observed for Buster in this study aligns closely with these previously reported values[23]. In contrast, the other four cultivars, Cracker, Liberty, MR43, and Tiger, showed higher lipid contents of 4.66%, 5.27%, 4.92%, and 4.96%, respectively. These values exceed previously reported data, reflecting cultivar-specific differences in lipid accumulation when grown under identical field conditions[23]. It is also important to note that all samples in this study were stored at -80°C before extraction, and as a result, the lipid content values reported here are based on fresh weight rather than dry weight, which could explain the higher values obtained.

The total lipid extracts were further classified into five major lipid categories: FA, SPs, GPs, GLs, and STs, according to the LIPID MAPS classification system. The accurate identification of lipid molecular species was achieved based on their *m/z* values and RT, and their distribution is visualized in a scatter plot in **Figure 2B**. This classification contributes to a detailed compositional understanding of lipid diversity among the sorghum cultivars.

To further explore the variation in lipid profiles across the six cultivars, sPLS-DA was conducted using MetaboAnalyst 5.0. The analysis, based on the first two

principal components (PC1 and PC2), accounted for 64.7% of the total variance and successfully separated the six cultivars into distinct clusters (**Figure 2C**). Replicate samples clustered closely, indicating good analytical reproducibility. Interestingly, MR43 exhibited a lipid profile clearly distinct from the other cultivars, suggesting significant compositional differences. The variables contributing most to the separation were visualized using a loading plot (**Figure 1D**), which revealed that FAHFA were key contributors to the separation pattern. This finding implies possible differences in lipid biosynthetic regulation between cultivars.

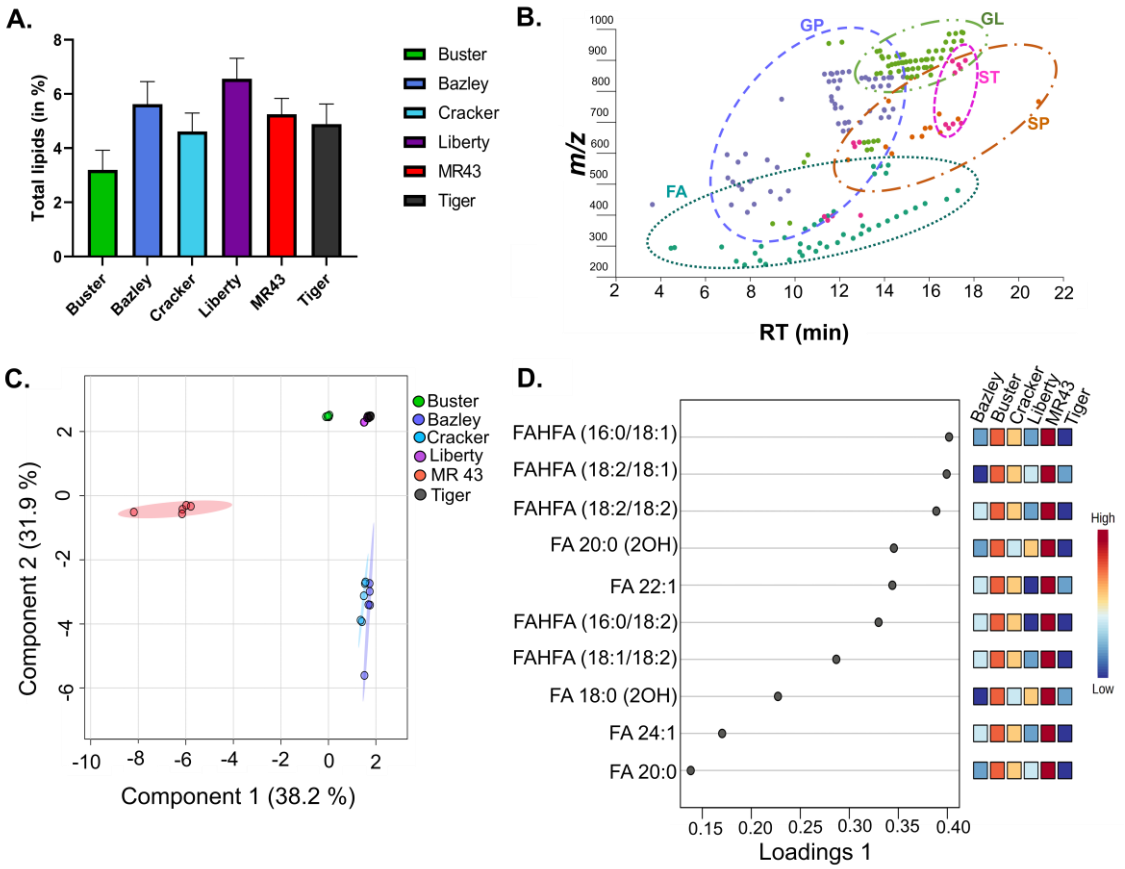

Figure 2: (A) Bar graph representing the total lipid content (%) of six sorghum cultivars on a fresh weight basis (n = 3). (B) Scatter plot displaying the distribution of lipid molecular species based on their mass-to-charge (*m/z*) ratios and retention times (RTs). (C) sPLS-DA score plot derived from lipidomic profiles of six sorghum cultivars, each dot represents an individual sample, with repeated samples clustering together. (D) Loading plot corresponding to the sPLS-DA, identifying the lipid molecular species responsible for the separation observed in the score plot.

A simplified lipid biosynthesis pathway schematic for plants, constructed based on Kyoto encyclopedia of genes and genomes (KEGG) pathway maps, is provided in **Figure 3**. This pathway illustrates the enzymatic routes through which key lipid classes are synthesized. Briefly, Acetyl-CoA serves as the precursor for free fatty acid (FFA)

synthesis, which may subsequently form FAHFAs, although the precise FAHFA biosynthesis pathway remains uncharacterized in plants. Additionally, Acetyl-CoA, in combination with glycerol-3-phosphate (G3P), gives rise to lysophosphatidic acid (LPA) and PA, which further convert into GLs and GPs. The pathway also shows the conversion of palmityl-CoA and serine into Cer of the SPs class. Based on the lipidomic profiles obtained in this study, it appears that certain biosynthetic pathways may be differentially regulated across the sorghum cultivars. For example, cultivars Buster and MR43 exhibited elevated levels of FFAs and FAHFAs compared to the other four cultivars, potentially indicating enhanced activity within the fatty acid biosynthesis pathway originating from Acetyl-CoA. In contrast, lower concentrations of Cer and HexCer were observed in Buster, Liberty, and Tiger, suggesting possible downregulation of the sphingolipid biosynthesis pathway, which also originates from Acetyl-CoA.

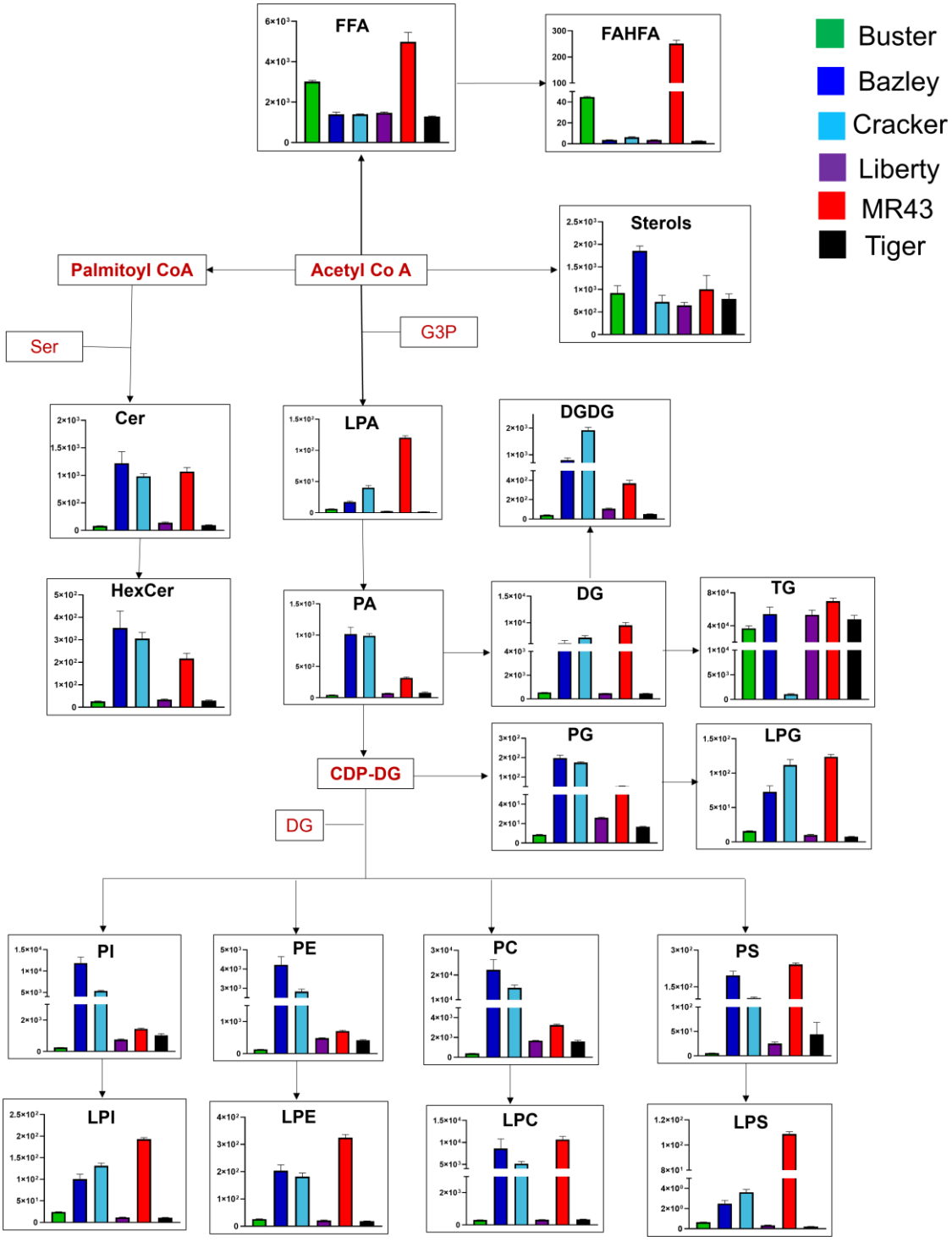

Figure 3: Schematic representation of plant lipid biosynthesis pathways relevant to sorghum grain lipidome profiles.

3.3.2 Lipid class distribution and fatty acid composition across six sorghum cultivars

In the untargeted lipidomic analysis of the six sorghum cultivars, a total of 43 fatty acid species were identified and classified into three major categories: SFAs, MUFAs, and PUFAs. SFAs, such as palmitic acid (FA 16:0), are characterized by the absence of double bonds in their carbon chain. In contrast, MUFAs, exemplified by oleic acid (FA 18:1), possess a single double bond typically located between the C9 and C10 positions. PUFAs contain multiple double bonds, which can be further grouped into two families: ω-3 (n-3) PUFAs, where the first double bond is located at the third carbon from the methyl end (e.g., linolenic acid; FA 18:3), and ω-6 (n-6) PUFAs, with the first double bond at the sixth carbon from the methyl end (e.g., linoleic acid; FA 18:2)[24]. The distribution of these three fatty acid classes across the cultivars is illustrated in **Figure 4A**. Among the cultivars, MR43 exhibited the highest levels of SFAs, MUFAs, and PUFAs, surpassing the other genotypes. This observation is consistent with earlier research on pigmented sorghum varieties, particularly those with red pericarps, which have been shown to contain elevated levels of these fatty acid classes[25].

The P:S ratio, a critical indicator of the nutritional and cardiovascular health potential of dietary lipids, was also determined for each cultivar and is presented in **Figure 4B**[26]. The cultivar Buster demonstrated the highest P:S ratio of 2.15, followed by MR43 (1.88), Cracker (1.51), Bazley (1.44), Tiger (1.43), and Liberty, which exhibited the lowest ratio of 1.36. Prior studies in animal models have suggested that maintaining a P:S ratio in the range of 1.0–1.5 is associated with a reduced risk of CVD[27]. These findings align with previous results obtained from studies of fish and seaweed lipidomes, where similarly favorable P:S values were observed, reinforcing the importance of this index in evaluating the health impacts of dietary fats[28,29].

The relative abundances of individual fatty acids, including bioactive FAHFAs, ω-6 PUFAs, ω-3 PUFAs, and the ω-6/ω-3 ratio, are shown in **Figure 4C** and **Figure 4D** as heatmaps. In these heatmaps, deep red indicates higher, and blue lower concentrations of the respective lipid species. The heatmaps revealed that palmitic acid, oleic acid, linoleic acid, and linolenic acid were consistently abundant in all cultivars, in agreement with earlier findings in sorghum lipid studies[25]. A detailed percentage distribution of SFAs, MUFAs, PUFAs (including ω-6 and ω-3 PUFAs), and FAHFAs is provided in **Table 1**. Among the cultivars, Buster showed a notably higher abundance of oleic acid, ω-6 PUFAs, and ω-3 PUFAs compared to the other genotypes. These unsaturated fatty acids are recognized for their antioxidant, anti-inflammatory, and cardio-protective properties[30]. Oleic acid, for instance, has been documented to reduce inflammatory responses, while linoleic acid (ω-6) has been shown to lower levels of pro-inflammatory cytokines such as tumor necrosis factor-alpha (TNF-α) and interleukin-1β (IL-1β), contributing to neuroprotection by reducing microglial activation[31,32]. Additionally, linolenic acid (ω-3) is known for its capacity to reduce the risk of CVD and arrhythmias, while also ω-3 fatty acids exhibit anti-cancer and anti-inflammatory properties[33,34]. Beyond these benefits, ω-3 PUFAs are essential for maintaining mental, immune, nervous system, visual, skeletal, and muscular health[35]. The analysis of the ω-6/ω-3 ratio among cultivars revealed that Bazley had the most favorable ratio at approximately 8:1, while Buster displayed the highest at around 10:1. An elevated ω-6/ω-3 ratio has been associated with increased susceptibility to inflammatory, allergic, and autoimmune conditions. Although no universal consensus exists regarding the ideal ratio for human health, dietary guidelines generally recommend maintaining a balance within the range of 1:1 to 4:1[36]. The structural identification of linolenic acid was confirmed via MS spectral analysis, with

representative spectra shown in **Figure 4D**. Among the cultivars, Bazley exhibited a particularly beneficial lipid composition, suggesting its potential as a functional grain for dietary interventions aimed at promoting health and preventing chronic diseases.

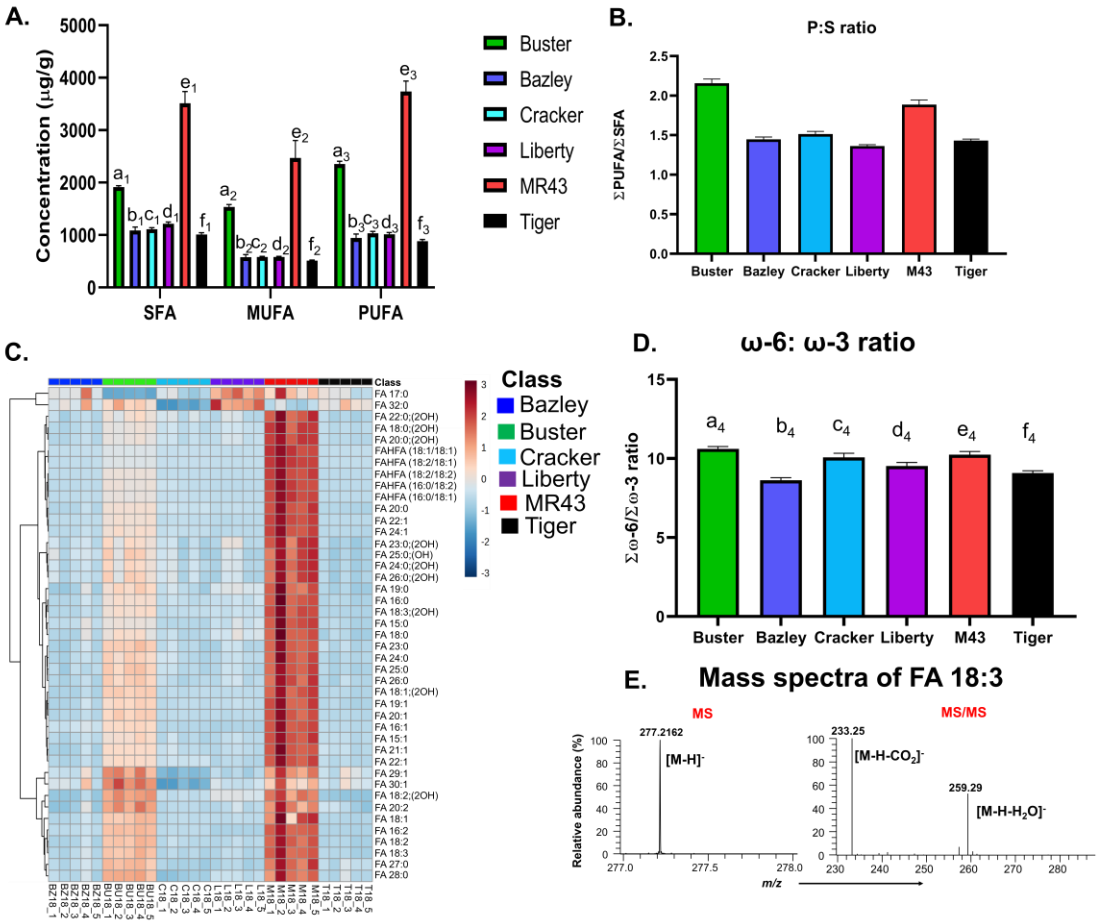

Figure 4: (A) Bar graph representing the relative abundance of saturated fatty acids (SFAs), monounsaturated fatty acids (MUFAs), and polyunsaturated fatty acids (PUFAs) identified in six sorghum cultivars. (B) Polyunsaturated to saturated fatty acid (P:S) ratio across cultivars, indicating nutritional value differences. Significant group comparisons are as follows: SFA: a_1-[b_1,c_1,d_1,e_1,f_1], i.e., group a_1, is significantly different from the groups shown in a square bracket, b_1-[e_1], c_1-[e_1], d_1-[e_1], e_1-[f_1], MUFA: a_2-[b_2,c_2,d_2,e_2,f_2], b_2-[e_2], c_2-[e_2], d_2-[e_2], e_2-[f_2], PUFA: a_3-[b_3,c_3,d_3,e_3,f_3], b_3-[e_3], c_3-[e_3], d_3-[e_3], e_3-[f_3]. (C)

Heatmap showing the relative abundance of individual fatty acids, including ω-3 and ω-6 PUFAs, FAHFAs, and other bioactive lipids. Red indicates higher, and blue lower concentrations of fatty acid molecular species. (D) ω-6 to ω-3 PUFA ratio in the six cultivars, highlighting nutritional balance differences, with Bazley showing the most favorable (lowest) ratio and Buster the highest. Significant group comparisons are as follows: a_4-[b_4, d_4, f_4], b_4-[c_4, d_4, e_4], c_4-[f_4], e_4-[f_4]. All the data are expressed as mean ± SEM (n = 5). Statistical significance was determined using two-way ANOVA with Tukey's multiple comparisons test. Different letters indicate significant differences at $p < 0.05$. (E) High-resolution mass spectrometry (MS) spectrum confirming the molecular identity of linolenic acid (FA 18:3) identified in sorghum cultivars.

Table 1: Major fatty acid with FAHFAs percentage composition of sorghum cultivars.

Fatty Acid	Buster (%)	Bazley (%)	Cracker (%)	Liberty (%)	MR43 (%)	Tiger (%)
Palmitic Acid	11.17	13.91	14.41	14.90	13.56	13.74
Stearic Acid	6.69	11.29	10.69	11.97	6.45	11.36
Oleic Acid	24.41	20.28	20.03	19.50	22.74	19.73
Linoleic Acid	34.89	31.31	32.98	31.13	31.65	31.92
Linolenic Acid	3.12	3.51	3.14	3.15	2.76	3.43
FAHFA	0.77	0.13	0.23	0.13	2.59	0.11
SFA	33.02	41.64	40.77	43.22	36.13	42.10
MUFA	26.46	22.18	21.34	20.62	25.40	21.31
PUFA	40.52	36.18	37.89	36.15	38.47	36.60

3.3.3 Correlation analysis of grain lipid classes in six sorghum cultivars

A comprehensive comparison of the major lipid classes, GP, SP, STs, and GL, across the six sorghum cultivars was conducted, and the findings are visualized as heatmaps in **Figures 5A-C**. Among these cultivars, MR43, Bazley, and Cracker exhibited substantially elevated levels of both GPs and SPs classes. Specifically, these cultivars

showed approximately 60-fold higher GPs concentrations and two-fold higher SP concentrations relative to Tiger, Liberty, and Buster. Within the GPs lipid class, PI and PC were the predominant lipid species in Bazley, collectively comprising nearly 90% of the total GPs. This result diverges somewhat from previous reports, where lysophosphatidylcholine (LPC) and PC were reported as the dominant GPs, accounting for around 80% of the total glycerophospholipids in sorghum[37]. This discrepancy highlights cultivar-specific variations in sorghum lipid composition and suggests possible genetic or environmental influences affecting lipid biosynthesis in these grains. The SPs lipid class, particularly ceramides, was also notably abundant in Bazley, MR43, and Cracker compared to the other cultivars. While studies on sphingolipids in sorghum are limited, recent reports have confirmed the presence of rare plant ceramides, termed phyto-ceramides, in various plant-derived materials such as wheat germs and coffee grounds. These lipids are known to be critical components of cellular membranes and play essential roles in maintaining skin permeability barrier function[38]. The high levels observed in select sorghum cultivars suggest an underexplored functional and nutritional role of these lipids in grains. Regarding the STs content, Bazley and MR43 demonstrated nearly two-fold higher levels of sitosterol (ST 29:1;O) compared to other cultivars. This observation aligns with earlier studies on sorghum distillers dried grains, where sitosterol was reported to account for 50% or more of the total plant sterols present in hexane extracts[39]. Additionally, sorghum kernel fractions such as wet-milled fiber and germ have been recognized as rich sources of free phytosterols and fatty acyl phytosterol esters[40]. Phytosterols are well-documented for their cholesterol-lowering effects, particularly their ability to reduce low-density lipoprotein cholesterol by inhibiting intestinal cholesterol absorption[41]. These results deepen our understanding of the phytosterol diversity in

sorghum and support its potential health benefits.

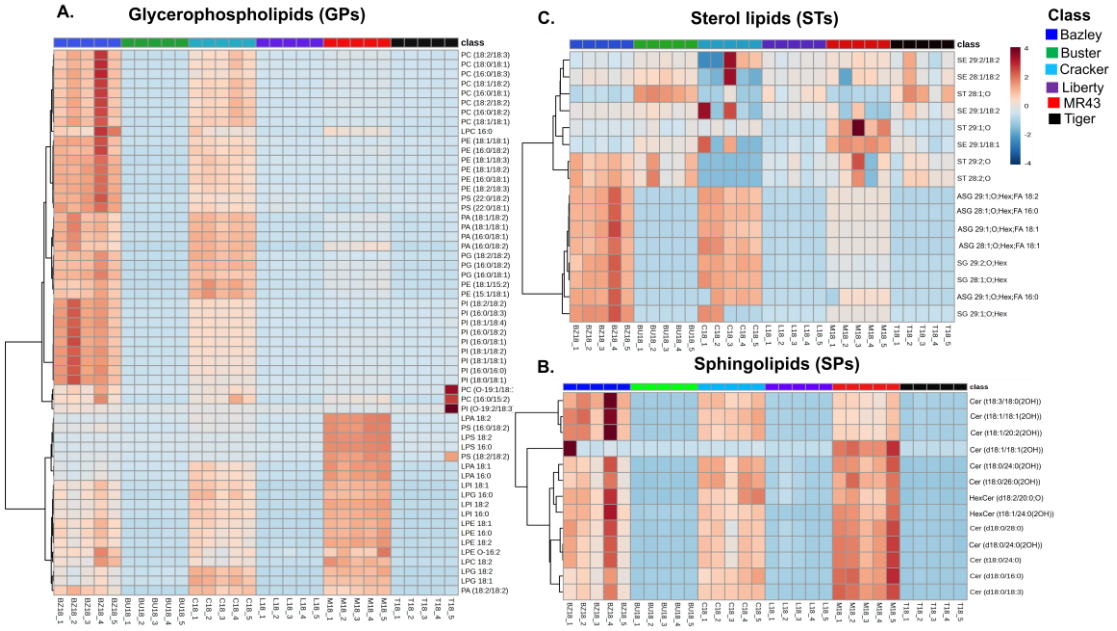

Figure 5: (A) Heatmap representing the relative abundance of major glycerophospholipid classes (GPs) in six sorghum cultivars, (B) Sphingolipid (SP), & (C) Sterol lipids (ST).

Further insights into GLs concentrations are provided in **Figure 6A**, which illustrates the relative abundance of GLs in the cultivars. MR43 and Bazley exhibited higher levels of GLs compared to the other cultivars. Among these, TG was the most abundant component, with MR43 showing the highest concentration and Cracker the lowest. These findings are consistent with previous research reporting TG as the predominant lipid class in grain sorghum oil fractions, with palmitic, oleic, and linoleic acids identified as the primary fatty acids[5]. Notably, triacylglycerol (TG 54:2), consisting of 54 acyl chain carbons and two double bonds, was absent across all six cultivars. This is a relevant finding since previous studies have associated elevated levels of TG (54:2) in plasma with an increased risk of CVD, particularly in individuals with T2D[42]. Its absence in these sorghum cultivars may indicate a favorable lipid profile regarding CVD

risk.

Examining the contribution of ω-6 and ω-3 PUFAs within the structural components of GPs and GLs, our data revealed that in GLs, the combined concentration of these essential fatty acids was more than four times higher than in GPs (**Figures 6B** and **6C**). This indicates that GLs serve as a richer dietary source of PUFAs in sorghum. Such a distribution is nutritionally valuable, as PUFAs are crucial for maintaining membrane fluidity, flexibility, and cell signaling functions[43]. These results are consistent with the known importance of linoleic acid and linolenic acid, which serve as primary precursors for ω-6 and ω-3 PUFAs, respectively[44]. Cereal lipids, including those from sorghum, are particularly beneficial when they are enriched in these essential fatty acids. The comparatively higher abundance of these fatty acids within the GLs class in our study reinforces the relevance of lipid profile variations among cultivars and emphasizes the potential health benefits associated with the dietary consumption of sorghum grain lipids.

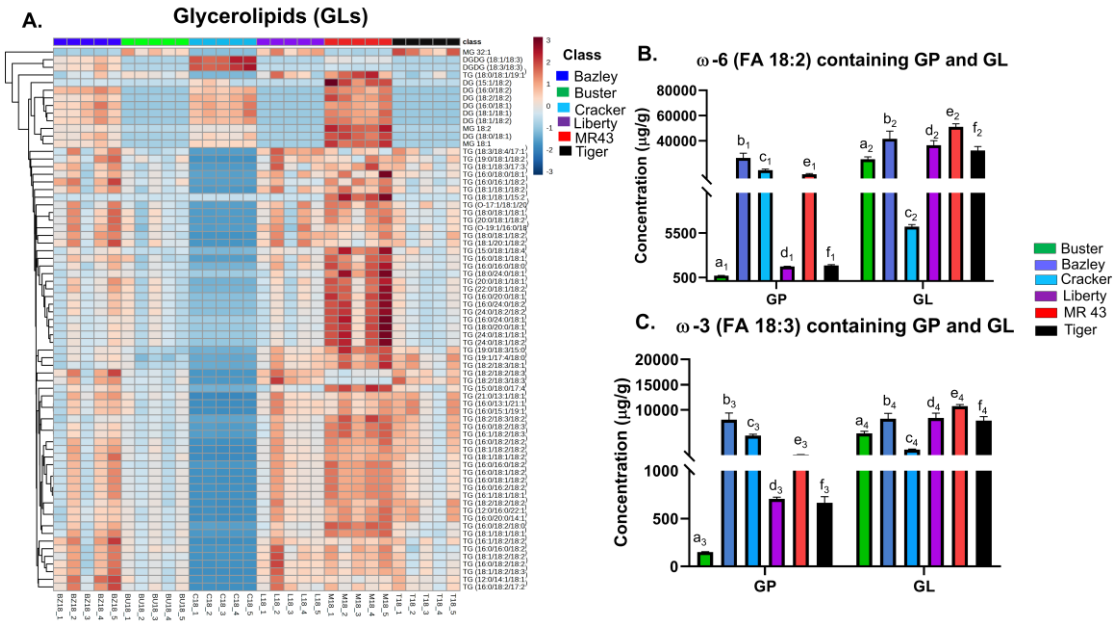

Figure 6: (A) Heatmap illustrating the relative abundance of glycerolipids (GLs). (B) Bar graph showing the concentrations of ω-6 and ω-3 PUFAs within glycerolipids (GLs) of each cultivar. (C) Bar graph displaying the corresponding concentrations of ω-6 and ω-3 PUFAs within glycerophospholipids (GPs). Significant groups for GP: a_1-[b_1, c_1], b_1-[d_1, e_1, f_1], c_1-[d_1, f_1]; for GL: a_2-[b_2, c_2, d_2, e_2], b_2-[c_2], c_2-[d_2, e_2, f_2], d_2-[e_2], e_2-[f_2]. (C). Concentrations of ω-3 PUFAs (linolenic acid, FA (18:3)) in GP and GL. Significant groups for GP: a_3-[b_3], b_3-[d_3, e_3, f_3], for GL: a_4-[b_4, c_4, d_4, e_4, f_4], b_4-[c_4], c_4-[d_4, e_4, f_4]. Data are expressed as mean ± SEM (n = 5). Statistical significance was determined using two-way ANOVA with Tukey's multiple comparison test. Values with different letters indicate significant differences at $p < 0.05$.

3.3.4 Identification and structural characterization of fatty acid esters of hydroxy fatty acids (FAHFAs) in sorghum cultivars

FAHFAs represent a recently recognized family of bioactive lipids with promising therapeutic potential for addressing lipid oxidation, diabetes, obesity-associated

inflammation, and cancer. Although previous studies have documented the occurrence of FAHFAs in a range of plant-based foods such as vegetable oils, grains, cereals, fruits, teas, and fermented products, evidence of their presence in sorghum has been lacking[45]. Several cereals, including rice bran, fermented brown rice, oats, and wheat, have been confirmed as dietary sources of FAHFAs, with these compounds found to exist in multiple families and regioisomeric forms[46,47]. Despite this, no prior research has identified or characterized FAHFAs in sorghum grain.

In the present study, five distinct FAHFA molecular species were successfully identified and characterized in the grains of six sorghum cultivars. The distribution of these FAHFAs among the different cultivars is presented in **Table 1**, which reveals that MR43 exhibited the highest total FAHFA content relative to the other varieties. EICs and representative chemical structures of the identified FAHFAs are displayed in **Figure 7A**. The identities of these compounds were further validated using high-resolution MS and MS/MS analyses, as shown in **Figure 7B**. All FAHFAs in this study ionized in negative mode, producing $[M-H]^-$ precursor ions. Palmitic acid ester of hydroxy-linoleic acid (PAHLA) produced an $[M-H]^-$ ion at *m/z* 533.4563, with its MS/MS fragmentation generating ions at *m/z* 295 and 255, corresponding to the loss of hydroxy-linoleic acid and palmitic acid, respectively. A subsequent loss of a water molecule from *m/z* 295 produced an ion at *m/z* 277, confirming the identification as PAHLA. Liu et al. recently reported that increased plasma levels of PAHLA are associated with early-stage colorectal cancer (CRC), indicating its potential as a biomarker for early detection of CRC[48]. Similarly, OAHOA exhibited an $[M-H]^-$ ion at *m/z* 561.4875, with fragmentation ions at *m/z* 297 and 281 resulting from the losses of hydroxy-oleic acid and oleic acid, respectively. The further loss of water from *m/z* 297 generated *m/z* 279, verifying the

compound as OAHOA. Matsuzawa et al. identified six different FAHFA families in rice, with OAHOA representing the most prevalent one[49]. Linoleic acid ester of hydroxy-oleic acid (LAHOA) produced $[M-H]^-$ at *m/z* 559.4723, and MS/MS spectra showed characteristic fragment ions at *m/z* 297 and 279, indicating the sequential loss of hydroxy-oleic acid and linoleic acid. The loss of water from *m/z* 297 confirmed LAHOA's identity. Interestingly, LAHOA has been previously detected in both walnut oil and raw almond oil[50]. Following a similar fragmentation pattern, linoleic acid ester of hydroxy-linoleic acid (LAHLA) exhibited $[M-H]^-$ at *m/z* 557.4564. The MS/MS spectra revealed losses at *m/z* 295 and 279, corresponding to hydroxy-linoleic acid and linoleic acid. Further dehydration of *m/z* 295 yielded a fragment at *m/z* 277, confirming the structure as LAHLA. Previous research on nut and oat oils revealed high levels of unsaturated FAHFAs, with LAHLA being particularly abundant and recognized for its anti-inflammatory effects[51]. Lastly, palmitic acid ester of hydroxy-oleic acid (PAHOA) displayed an $[M-H]^-$ ion at *m/z* 535.4718, with fragment ions at *m/z* 297 and 255, attributed to the loss of hydroxy-oleic acid and palmitic acid, respectively. The subsequent water loss yielded a peak at *m/z* 279, confirming PAHOA. PAHOA has also been detected in a variety of plant-based foods, including fruits, vegetables, and cereals[52].

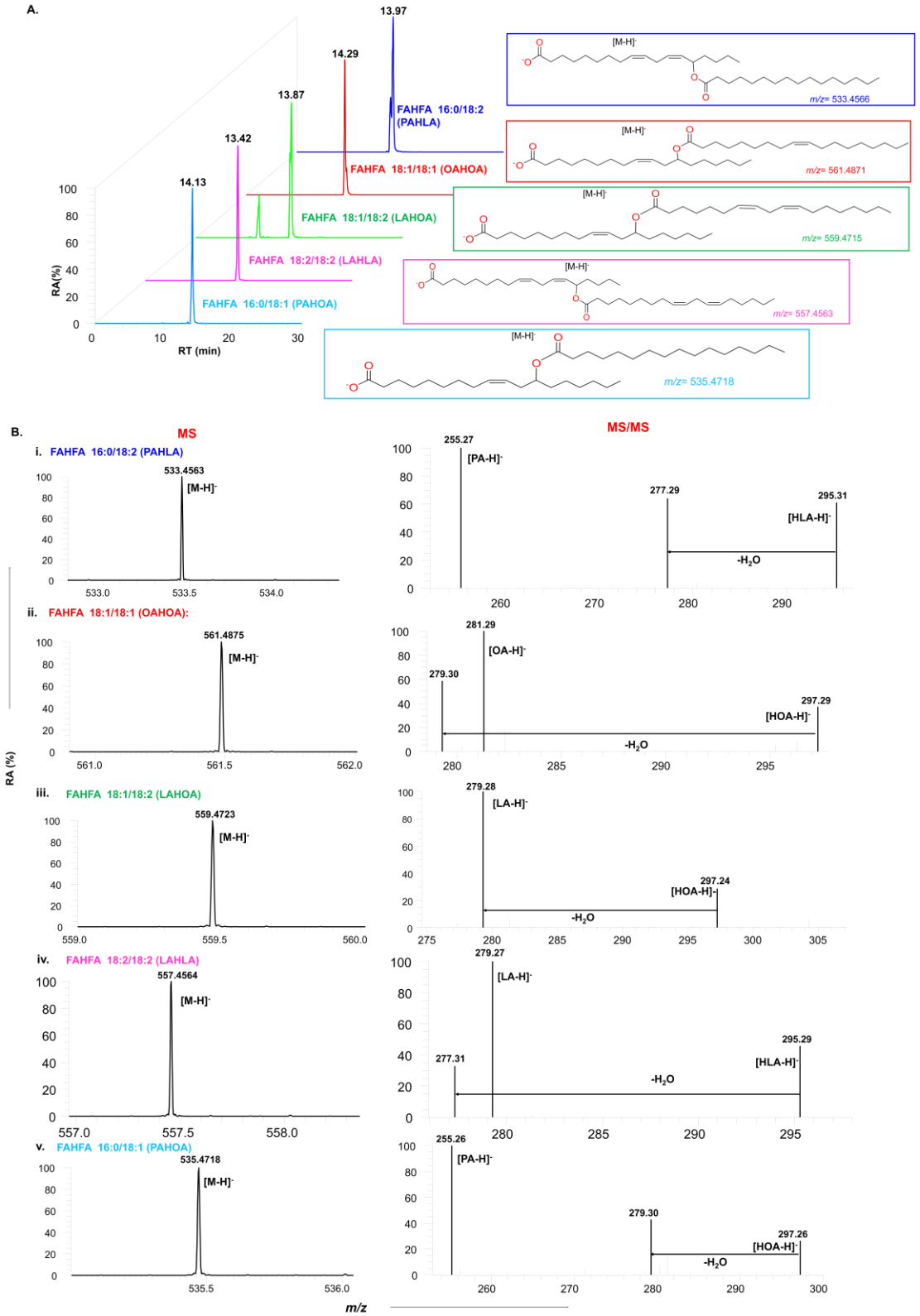

Figure 7: (A) EICs showing the presence of five newly characterized FAHFA species across six sorghum cultivars, alongside their chemical structures. (B) MS and MS/MS

spectra confirming the identity of these FAHFAs in negative ionization mode through characteristic fragment ion losses. (i) Palmitic acid ester of hydroxy-linoleic acid (PAHLA), (ii) oleic acid ester of hydroxy-oleic acid (OAHOA), (iii) linoleic acid ester of hydroxy-oleic acid (LAHOA), (iv) linoleic acid ester of hydroxy-linoleic acid (LAHLA), and (v) palmitic acid ester of hydroxy-oleic acid (PAHOA) were identified.

To pinpoint the hydroxylation positions within these FAHFAs, DMED derivatization coupled with MS^n analysis was conducted using the MR43 cultivar, which contained the highest FAHFA content. This analysis was benchmarked against a DMED-labeled 12-OAHOA standard, with fragmentation patterns compared to confirm hydroxylation sites (**Figure 8A**)[53,54]. DMED-labeled 12-OAHOA ionized in positive mode to produce an $[M+H]^+$ ion at *m/z* 633.5934. The loss of the dimethylamino group (45 Da) resulted in *m/z* 588, with subsequent fragmentation generating ions at *m/z* 351 (loss of oleoyl group) and 306 (loss of oleoyl group with dimethylamino group). Further, the MS^3 analysis of *m/z* 306 fragmentation yielded characteristic ions at *m/z* 208 ($C_{13}H_{22}NO^+$), *m/z* 98 ($C_7H_{14}O^{\cdot+}$), and *m/z* 222 ($C_{14}H_{24}NO^+$), confirming hydroxylation at the C12 position. The structure was confirmed to be 12-OAHOA. A similar fragmentation profile was observed for DMED-labeled OAHOA, PAHOA, and LAHOA in the sorghum MR43 sample, confirming that these FAHFAs shared a hydroxylation site at C12 (**Figure 8B**). In contrast, LAHLA showed a distinct fragmentation pattern, with DMED-labeled $[M+H]^+$ at *m/z* 629.5635 producing a fragment at *m/z* 584 (loss of 45 Da), and product ions at *m/z* 351 (loss of the linoleoyl group) and *m/z* 349 (loss of $C_{23}H_{41}O_2^+$), confirming the hydroxyl group position at C14. Furthermore, MS^3 fragmentation of *m/z* 306 (loss of linoleoyl group with the dimethylamino group) generated diagnostic ions at *m/z* 208 ($C_{13}H_{22}NO^+$), *m/z* 98 ($C7H14O^{\cdot+}$), *m/z* 222 ($C_{14}H_{24}NO^+$), *m/z* 236 ($C_{15}H_{26}NO^+$), and *m/z*

250 ($C_{16}H_{28}NO^{+}$), conclusively identifying the position of hydroxylation as 14th and structure as 14-LAHLA. This represents the first report of these FAHFA structures in sorghum grain, greatly expanding current knowledge of bioactive lipids in cereals and providing new insights into the potential health-promoting properties of sorghum.

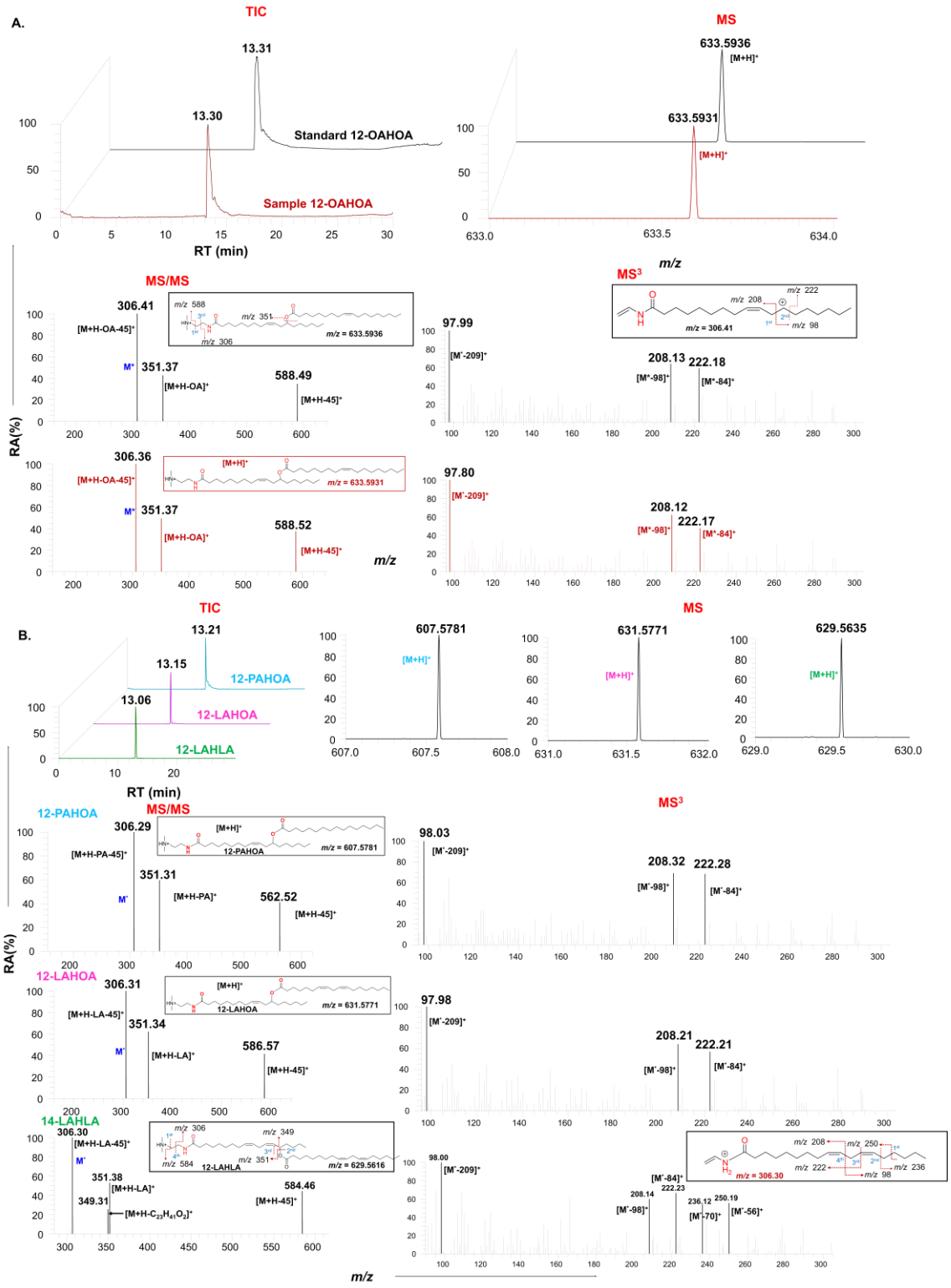

Figure 8: (A) EIC and MSn spectra of DMED-labeled 12-OAHOA standard and corresponding FAHFAs from MR43 sorghum. (B) EIC and MSn spectra of DMED-

labeled LAHLA from MR43 sorghum.

3.4 Limitations

This study provides important insights into the distribution and concentration of FAHFAs in different sorghum cultivars, offering a valuable first step in understanding the diversity of these bioactive lipids in sorghum grain. While our identification and detailed profiling of FAHFAs add new information to the sorghum lipidome, several limitations must be acknowledged. Firstly, the grain samples were collected from a single growing season and location. As lipid composition is known to vary with agronomic conditions, harvest stage, and post-harvest storage, these factors were not addressed here. Future studies incorporating multi-year, multi-location trials would help capture broader variability and improve the generalizability of these findings. Additionally, the quantitative data obtained were semi-quantitative, as internal standards were added after homogenization to prevent their loss during sample preparation, potentially affecting accuracy. The lack of commercial FAHFA standards also necessitated reliance on MS/MS spectral interpretation for identification, limiting absolute quantification. Moreover, due to the low abundance of PAHLA in the samples, its hydroxylation position could not be confirmed. Future research should address these limitations, including wider sampling, improved standard availability, and absolute quantification, to advance our understanding of sorghum lipidomes and the functional significance of FAHFAs.

3.5 Conclusion

Our comprehensive lipidomic analysis of six commercial sorghum cultivars uncovered substantial diversity in their lipid molecular profiles, highlighting distinct biochemical characteristics unique to each variety. Through multivariate data analysis, clear differences in lipid composition were observed, providing valuable insights into the nutritional qualities and potential health-promoting properties of these grains. The discovery and structural characterization of FAHFAs in sorghum grains using LC/MS and derivatization techniques marks an important contribution to the expanding field of plant lipidomics. Notably, cultivar MR43 demonstrated the greatest variability in both total lipid content and bioactive lipid composition, particularly in its FAHFA content. Furthermore, variations in key nutritional lipid indices among cultivars were observed. Cultivar Bazley displayed the most favorable ω-6 to ω-3 fatty acid ratio, while Cracker, Bazley, Tiger, and Liberty exhibited optimal P:S ratios, both of which are important indicators of dietary lipid quality. These findings reinforce the nutritional significance of sorghum and its potential as a functional food ingredient within the human diet. Building on this foundation, future work will extend beyond sorghum to explore similar bioactive lipid compounds in a variety of cereals and food crops. By adopting a broader foodomics approach, this research aims to expand the current understanding of lipid diversity within staple grains, offering valuable perspectives on their roles in nutrition, agriculture, and health. This study contributes to the growing body of evidence supporting the integration of lipidomics into food science and nutrition research, paving the way for more targeted, health-oriented dietary recommendations.

3.6 References:

1. Anglani, C. (1998). Sorghum for human food–A review. Plant Foods for Human Nutrition, 52, 85-95.
2. Cedrez, C. B., Chamberlin, J., & Hijmans, R. J. (2020). Seasonal, annual, and spatial variation in cereal prices in Sub-Saharan Africa. Global Food Security, 26, 100438.
3. Ofosu, F. K., Elahi, F., Daliri, E. B. M., Tyagi, A., Chen, X. Q., Chelliah, R., Kim, J. H., Han, S. I., & Oh, D. H. (2021). UHPLC-ESI-QTOF-MS/MS characterization, antioxidant and antidiabetic properties of sorghum grains. Food chemistry, 337, 127788.
4. Shim, T. J., Kim, T. M., Jang, K. C., Ko, J. Y., & Kim, D. J. (2013). Toxicological evaluation and anti-inflammatory activity of a golden gelatinous sorghum bran extract. Bioscience, Biotechnology, and Biochemistry, 77(4), 697-705.
5. Lee, B. H., Carr, T. P., Weller, C. L., Cuppett, S., Dweikat, I. M., & Schlegel, V. (2014). Grain sorghum whole kernel oil lowers plasma and liver cholesterol in male hamsters with minimal wax involvement. Journal of functional foods, 7, 709-718.
6. Smolensky, D., Rhodes, D., McVey, D. S., Fawver, Z., Perumal, R., Herald, T., & Noronha, L. (2018). High-polyphenol sorghum bran extract inhibits cancer cell growth through ROS induction, cell cycle arrest, and apoptosis. Journal of Medicinal Food, 21(10), 990-998.
7. Pontieri, P., Mamone, G., De Caro, S., Tuinstra, M. R., Roemer, E., Okot, J., Vita, P. D., Ficco, D. B. M., Alifano, P., Pignone, D., Massardo, D. R., & Del Giudice, L. (2013). Sorghum, a healthy and gluten-free food for celiac patients as demonstrated by genome, biochemical, and immunochemical analyses. Journal of Agricultural and Food Chemistry, 61(10), 2565-2571.

8. Goyal, M.; R. S. Sohu; R. Bhardwaj; B. S. Gill; M. Goyal. Genetic Variance and Predicted Response for Three Types of Recurrent Selection Procedures in Forage Sorghum [Sorghum Bicolor (L.) Moench]. Range Management and Agroforestry 2020, 41 (1), 43–51.
9. Goyal, M., Sohu, R. S., Bhardwaj, R., Gill, B. S., & Goyal, M. (2020). Genetic variance and predicted response for three types of recurrent selection procedures in forage sorghum [Sorghum bicolor (L.) Moench]. Range Management and Agroforestry, 41(1), 43-51.
10. Rooney, L. W., & Serna-Saldivar, S. O. (2000). Sorghum. In Handbook of cereal science and technology, Revised and expanded (pp. 149-175). CRC Press.
11. Hwang, K. T., Cuppett, S. L., Weller, C. L., & Hanna, M. A. (2002). Properties, composition, and analysis of grain sorghum wax. Journal of the American Oil Chemists' Society, 79(6), 521-527.
12. Policosanol Contents and Compositions in Wax-Like Materials Extracted from Selected Cereals of Korean Origin.
13. Mehmood, S., Orhan, I., Ahsan, Z., Aslan, S., & Gulfraz, M. (2008). Fatty acid composition of seed oil of different Sorghum bicolor varieties. Food chemistry, 109(4), 855-859.
14. Pontieri, P., Di Fiore, R., Troisi, J., Bean, S. R., Roemer, E., Okot, J., Alifano, P., Pignone, D., Giudice, L. D., & Rita Massardo, D. (2011). Chemical composition and fatty acid content of white food sorghums grown in different environments. Maydica, 56(1), 51.
15. Zbasnik, R., Carr, T., Weller, C., Hwang, K. T., Wang, L., Cuppett, S., & Schlegel, V. (2009). Antiproliferation properties of grain sorghum dry distiller’s grain lipids in

Caco-2 cells. Journal of agricultural and food chemistry, 57(21), 10435-10441.

16. Desta, K. T., Choi, Y. M., Shin, M. J., Yoon, H., Wang, X., Lee, Y., Yi, J., & Lee, S. (2023). Comprehensive evaluation of nutritional components, bioactive metabolites, and antioxidant activities in diverse sorghum (Sorghum bicolor (L.) Moench) landraces. Food Research International, 173, 113390.
17. Treviño-Salinas, M., Perales-Torres, A., Castillo-Ruíz, O., Montes-García, N., Lizarazo-Ortega, C., Navarro-Cortez, R., & Rodríguez-Castillejos, G. (2021). Proximal analysis and profile of fatty acids on six varieties of white grain sorghum with potential use in human consumption. CyTA-Journal of Food, 19(1), 547-551.
18. Kang, J., Price, W. E., Ashton, J., Tapsell, L. C., & Johnson, S. (2016). Identification and characterization of phenolic compounds in hydromethanolic extracts of sorghum wholegrains by LC-ESI-MSn. Food chemistry, 211, 215-226.
19. Suganyadevi, P., Saravanakumar, M., & Mohandas, S. (2021). Characterization of anthocyanin from red sorghum (Sorghum bicolor) bran by liquid chromatography-electron spray ionization mass spectrometry analysis. European Journal of Mass Spectrometry, 27(2-4), 107-114.
20. B. Gowda, S. G., Fuda, H., Tsukui, T., Chiba, H., & Hui, S. P. (2020). Discovery of eicosapentaenoic acid esters of hydroxy fatty acids as potent Nrf2 activators. Antioxidants, 9(5), 397.
21. Bligh, E. G., & Dyer, W. J. (1959). A rapid method of total lipid extraction and purification. Canadian journal of biochemistry and physiology, 37(8), 911-917.
22. B. Gowda, S. G., Gowda, D., Liang, C., Li, Y., Kawakami, K., Fukiya, S., Yokota, A., Chiba, h., & Hui, S. P. (2020). Chemical labeling assisted detection and identification of short chain fatty acid esters of hydroxy fatty acid in rat colon and

cecum contents. Metabolites, 10(10), 398.

23. Johnston, D. J., & Moreau, R. A. (2017). A comparison between corn and grain sorghum fermentation rates, distillers dried grains with solubles composition, and lipid profiles. Bioresource Technology, 226, 118-124.
24. Coniglio, S., Shumskaya, M., & Vassiliou, E. (2023). Unsaturated fatty acids and their immunomodulatory properties. Biology, 12(2), 279.
25. Pontieri, P., Troisi, J., Calcagnile, M., Bean, S. R., Tilley, M., Aramouni, F., Boffa, A., Pepe, G., Campiglia, P., Del Giudice, F., Chessa, A. L., Smolensky, D., Aletta, M., Alifano, P., & Del Giudice, L. (2022). Chemical composition, fatty acid and mineral content of food-grade white, red and black sorghum varieties grown in the mediterranean environment. Foods, 11(3), 436.
26. Kang, M. J., Shin, M. S., Park, J. N., & Lee, S. S. (2005). The effects of polyunsaturated: saturated fatty acids ratios and peroxidisability index values of dietary fats on serum lipid profiles and hepatic enzyme activities in rats. British journal of nutrition, 94(4), 526-532.
27. Gowda, S. G. B., Minami, Y., Gowda, D., Furuko, D., Chiba, H., & Hui, S. P. (2021). Lipidomic analysis of non-esterified furan fatty acids and fatty acid compositions in dietary shellfish and salmon by UHPLC/LTQ-Orbitrap-MS. Food Research International, 144, 110325.
28. Gowda, S. G. B., Yifan, C., Gowda, D., Tsuboi, Y., Chiba, H., & Hui, S. P. (2022). Analysis of antioxidant lipids in five species of dietary seaweeds by liquid chromatography/mass spectrometry. Antioxidants, 11(8), 1538.
29. Troesch, B., Eggersdorfer, M., Laviano, A., Rolland, Y., Smith, A. D., Warnke, I.,Weimann, A., & Calder, P. C. (2020). Expert opinion on benefits of long-chain

omega-3 fatty acids (DHA and EPA) in aging and clinical nutrition. Nutrients, 12(9), 2555.

30. Eastman, A. J., Moore, R. E., Townsend, S. D., Gaddy, J. A., & Aronoff, D. M. (2021). The influence of obesity and associated fatty acids on placental inflammation. Clinical therapeutics, 43(2), 265-278.
31. Tan, B., Wang, Y., Zhang, X., & Sun, X. (2022). Recent studies on protective effects of walnuts against neuroinflammation. Nutrients, 14(20), 4360.
32. Zhang, W., Li, R., Li, J., Wang, W., Tie, R., Tian, F., Liang, X., Xing, W., He, Y., Yu, L., Xi, M., Wang, S., Zheng, Q., & Zhang, H. (2013). Alpha-linolenic acid exerts an endothelial protective effect against high glucose injury via PI3K/Akt pathway. PloS one, 8(7), e68489.
33. Mason, R. P., Jacob, R. F., Shrivastava, S., Sherratt, S. C., & Chattopadhyay, A. (2016). Eicosapentaenoic acid reduces membrane fluidity, inhibits cholesterol domain formation, and normalizes bilayer width in atherosclerotic-like model membranes. Biochimica et Biophysica Acta (BBA)-Biomembranes, 1858(12), 3131-3140.
34. Djuricic, I., & Calder, P. C. (2021). Beneficial outcomes of omega-6 and omega-3 polyunsaturated fatty acids on human health: An update for 2021. Nutrients, 13(7), 2421.
35. DiNicolantonio, J. J., & O'Keefe, J. (2021). The importance of maintaining a low omega-6/omega-3 ratio for reducing the risk of autoimmune diseases, asthma, and allergies. Missouri medicine, 118(5), 453.
36. Osagie, A. U. (1987). Total lipids of sorghum grain. Journal of agricultural and food chemistry, 35(4), 601-604.

37. Reisberg, M., Arnold, N., Porzel, A., Neubert, R. H., & Dräger, B. (2017). Production of rare phyto-ceramides from abundant food plant residues. Journal of Agricultural and Food Chemistry, 65(8), 1507-1517.
38. Leguizamón, C., Weller, C. L., Schlegel, V. L., & Carr, T. P. (2009). Plant sterol and policosanol characterization of hexane extracts from grain sorghum, corn and their DDGS. Journal of the American oil chemists' society, 86, 707-716.
39. Singh, V., Moreau, R. A., & Hicks, K. B. (2003). Yield and phytosterol composition of oil extracted from grain sorghum and its wet-milled fractions. Cereal chemistry, 80(2), 126-129.
40. Ferguson, J. J., Stojanovski, E., MacDonald-Wicks, L., & Garg, M. L. (2018). Curcumin potentiates cholesterol-lowering effects of phytosterols in hypercholesterolaemic individuals. A randomised controlled trial. Metabolism, 82, 22-35.
41. Taya, N., Katakami, N., Omori, K., Hosoe, S., Watanabe, H., Takahara, M., M., Miyashita, K., Nishizawa, H., Konya, Y., Obara, S., Hidaka, A., Nakao, M., Takahashi, M., Izumi, Y., Shimomura, I., & Bamba, T. (2023). Change in fatty acid composition of plasma triglyceride caused by a 2 week comprehensive risk management for diabetes: A prospective observational study of type 2 diabetes patients with supercritical fluid chromatography/mass spectrometry-based semi-target lipidomic analysis. Journal of Diabetes Investigation, 14(1), 102-110.
42. Balić, A., Vlašić, D., Žužul, K., Marinović, B., & Bukvić Mokos, Z. (2020). Omega-3 versus omega-6 polyunsaturated fatty acids in the prevention and treatment of inflammatory skin diseases. International journal of molecular sciences, 21(3), 741.
43. Narducci, V., Finotti, E., Galli, V., & Carcea, M. (2019). Lipids and fatty acids in

Italian durum wheat (Triticum durum Desf.) cultivars. Foods, 8(6), 223.

44. Olajide, T. M., & Cao, W. (2022). Exploring foods as natural sources of FAHFAs—A review of occurrence, extraction, analytical techniques and emerging bioactive potential. Trends in Food Science & Technology, 129, 591-607.
45. Watanabe, A., Balas, L., Saigusa, D., Ogura, J., Durand, T., Mano, N., & Yamaguchi, H. (2022). Analytical evaluation of fatty acid esters of hydroxy fatty acid quantity in fermented brown rice and rice bran (FRBA). Food Chemistry Advances, 1, 100040.
46. Liberati-Čizmek, A. M., Biluš, M., Brkić, A. L., Barić, I. C., Bakula, M., Hozić, A., & Cindrić, M. (2019). Analysis of fatty acid esters of hydroxyl fatty acid in selected plant food. Plant foods for human nutrition, 74, 235-240.
47. Liu, T., Tan, Z., Yu, J., Peng, F., Guo, J., Meng, W., Chen, Y., Rao, T., Liu, Z., & Peng, J. (2020). A conjunctive lipidomic approach reveals plasma ethanolamine plasmalogens and fatty acids as early diagnostic biomarkers for colorectal cancer patients. Expert review of proteomics, 17(3), 233-242.
48. Matsuzawa, Y., Higashi, Y., Takano, K., Takahashi, M., Yamada, Y., Okazaki, Y., Nakabayashi, R., Saito, K., & Tsugawa, H. (2021). Food lipidomics for 155 agricultural plant products. Journal of Agricultural and Food Chemistry, 69(32), 8981-8990.
49. Takumi, H., Kato, K., Ohto-N, T., Nakanishi, H., Kamasaka, H., & Kuriki, T. (2021). Analysis of fatty acid esters of hydroxyl fatty acid in nut oils and other plant oils. Journal of Oleo Science, 70(12), 1707-1717.
50. Paluchova, V., Vik, A., Cajka, T., Brezinova, M., Brejchova, K., Bugajev, V., Draberova, L., Draber, P., Buresova, J., Kroupova, P., Bardova, K., Rossmeisl, M., Kopecky, J., Hansen, T. V., & Kuda, O. (2020). Triacylglycerol-rich oils of marine

origin are optimal nutrients for induction of polyunsaturated docosahexaenoic acid ester of hydroxy linoleic acid (13-DHAHLA) with anti-inflammatory properties in mice. Molecular Nutrition & Food Research, 64(11), 1901238.

51. Ding, J., Kind, T., Zhu, Q. F., Wang, Y., Yan, J. W., Fiehn, O., & Feng, Y. Q. (2020). In-silico-generated library for sensitive detection of 2-dimethylaminoethylamine derivatized FAHFA lipids using high-resolution tandem mass spectrometry. Analytical chemistry, 92(8), 5960-5968.
52. An, N., Wang, Y., He, D. X., Mei, P. C., Zhu, Q. F., & Feng, Y. Q. (2023). A dataset of branched fatty acid esters of hydroxy fatty acids diversity in foods. Scientific Data, 10(1), 790.

Chapter 4

Bioactive Lipids and Glycemic Impact of Pigmented Japonica Rice for Metabolic Health

4.1 Introduction

Rice, a staple crop cultivated in over 100 countries, is a cornerstone of global nutrition, with Asia contributing 90% of its global production. It belongs to the Poaceae family and includes two primary species, *Oryza sativa* (Asian rice) and *Oryza glaberrima* (African rice)[1]. Within *O. sativa*, the subspecies *indica* and *japonica* offer diverse agronomic and nutritional traits[2]. Rice undergoes processing to produce two primary forms: brown and white rice. Brown rice retains its nutrient-rich bran layer, a valuable source of dietary fiber, essential vitamins, and healthy fats. In contrast, white rice undergoes additional milling to remove the bran and germ, resulting in a product with a longer shelf life but reduced nutritional content[3]. Beyond these traditional forms, pigmented rice varieties such as red, purple, and black rice are gaining increasing attention as functional foods. These varieties are renowned for having a substantial amount of bioactive compounds, such as phenolic acids and anthocyanins, which give them their vivid colors and strong antioxidant capabilities[4,5].

Nutritionally, rice comprises approximately 85-90% starch, 7-12% protein, and 0.2-3.4% lipids, along with vitamins and trace elements[6]. While lipids constitute a relatively small proportion of rice, they play a crucial role in its nutritional profile and functional properties. These lipids are vital for maintaining cell membrane integrity, serving as a reservoir for energy storage, and facilitating signal transduction processes[7]. Furthermore, they significantly impact the grain's quality and nutritional value[7]. Brown rice contains 1.7-3.4% lipids, primarily concentrated in the embryo, husk, and aleurone layer, while polished rice retains 0.1-1.52%, mostly in the aleurone layer[8]. Lipids in rice are broadly categorized as starch lipids (SLs) and non-starch lipids (NSLs). SLs, forming starch-lipid complexes predominantly with palmitic and linoleic acids, account for 0.21-0.76% of the

grain endosperm. In contrast, NSLs, contributing 2.9-3.4% in the aleurone layer, include free fatty acids and glycerolipids like oleic acid, linoleic acids, and palmitic acids, with minor components such as stearic and alpha-linolenic acids[9]. Importantly, unsaturated fatty acids in rice lipids have been shown to slow oxidative degradation, extend shelf life, minimize food loss, and safeguard the grain's nutritional and safety attributes[10].

Besides lipids, starch, the dominant component of rice, is rapidly digested in the gastrointestinal tract, leading to a high glycemic index (GI) in humans[11]. White rice, with a GI of 83.40 ± 15.93, is classified as a high-GI food, posing risks for metabolic disorders such as obesity and CVD[12,13]. GI, defined as the incremental area under the blood glucose curve after consuming a test food with 50 g of carbohydrates compared to a reference food, provides a standardized measure of postprandial blood glucose response[14]. However, previous studies explained that various factors, including cooking methods, storage conditions, antioxidant components in pigmented rice, and industrial treatments, influence rice GI[15-19].

Emerging evidence suggests that rice lipids, particularly fatty acids, and cooking oils, can modulate the glycemic response by forming complexes with starch, especially amylose, and occasionally amylopectin[20,21]. Recent advances in lipidomics facilitated by metabolomics techniques have expanded the approach to investigating dietary lipids in food[7-9,22-24]. Advancements in gas chromatography-mass spectrometry have revealed that lipids and lipid-derived volatiles such as aldehydes, alcohols, and ketones are the key contributors to rice flavor in cooked rice under different storage conditions and temprature[8,22,23]. The present research uses a highly sensitive Q-extractive Orbitrap/MS and UPLC coupled with Q-TOF spectrometry method for comprehensive lipidomics profile analysis in rice, linking lipids to evaluate grain quality as well as their changes

during storage respectively[7,24]. For instance, lipidomics analysis using UPLC-Q-exactive orbitrap/MS identified 13 SLs and 395 NSLs and their changes over time during storage[9].

Previous studies have extensively analyzed lipid-derived volatiles and their role in flavor and storage stability, yet the correlation between lipids, starch digestibility, and GI remains underexplored, particularly for *japonica* rice. Furthermore, most research has focused on *indica* varieties, leaving a significant knowledge gap regarding *japonica* rice's nutritional and metabolic attributes.

This study addresses these gaps by analyzing the lipidome of 56 *japonica* cultivars using HPLC /LTQ-orbitrap mass spectrometry, identifying health-promoting lipids and metabolites. *In-vitro* assays further compared starch digestibility and estimated GI of selected pigmented *japonica* and *indica* rice, providing a comprehensive understanding of their nutritional and metabolic profiles.

4.2 Materials and methods

4.2.1 Sample collection and preparation:

The 56 *japonica* rice cultivars analyzed in this study were sourced from various prefectures across Japan and represent commercially available varieties purchased from an online store. Detailed information about each cultivar, including pigmentation, collection location, and farming practices (organic or inorganic), is presented in **Table 1**. Each cultivar has been assigned a serial number for ease of reference throughout the study, for example, Koshihikari from Shikoku and Niigata prefecture is assigned serial numbers 4 and 16, respectively. Additionally, *indica* brown rice and parboiled rice were also procured from online stores for comparative *in-vitro* assay analyses. The study design, along with the map showing the origin of each *japonica* cultivars, is demonstrated in

Figure 1.

Around 500 g of each *japonica* rice cultivar was ground to make powder. The grains were powdered using a blender and kept in Falcon tubes at -80ºC conditions for lipid extraction as well as for total starch (TS) assay. 100 g of the brown rice-55 and *indica* brown rice were passed through a McGill Miller No. 2 (Grainman Mfg. Inc., USA) to obtain milled rice. These milled rice samples were kept in Ziplock bags in a freezer until further use in starch digestibility experiments.

For resistant starch (RS) assay and *in-vitro* starch digestibility experiments, brown (cv 55,48), red (cv 19,40), green (cv 24,41), black (cv 15,42), milled and par-boiled *indica* rice grains were cooked in beakers as per a previous study with minor modifications[25]. In brief, for cooking 10 g of rice grains, the sample was washed and pre-soaked in 20 mL of distilled water for 30 min before cooking. The beaker was placed in a pressure cooker containing 500 mL of distilled water, cooked for 20 min, and allowed to stand for 10 min without removing the aluminum foil. Afterward, the beaker was then taken out of the rice cooker, placed in a Kim wipe to remove the excess surface water, and allowed to cool down.

Table 1: Cultivars name and origin

Sl. No.	Cultivars name	Farming method	Pigmentation	Region	Prefecture
1	Akisakari	Organic	Brown	Kagawa	Shikoku
2	Masshigura	Organic	Brown	Aomori	Tohoku
3	Asahinoyme	Organic	Brown	Gunma	Kanto
4	Koshihikari	Organic	Brown	Kagawa	Shikoku
5	Hinohikari	Organic	Brown	Kagawa	Shikoku
6	Hitomebore	Organic	Brown	Yamagata	Tohoku
7	Haenuki	Organic	Brown	Yamagata	Tohoku
8	Sasanishiki	Organic	Brown	Yamagata	Tohoku
9	Tsuyahime	Organic	Brown	Yamagata	Tohoku
10	Dewanomochi	Organic	Brown	Yamagata	Tohoku
11	Akitakomachi	Organic	Brown	Akita	Tohoku
12	Kinunohada	Organic	Brown	Akita	Tohoku
13	Yumeobako	Organic	Brown	Akita	Tohoku
14	Awayukikomachi	Organic	Brown	Akita	Tohoku
15	Kuromai Kakumai	Organic	Black	Shizuoka	Chubu
16	Koshihikari	Organic	Brown	Niigata	Chubu
17	Red rice	Inorganic	Red rice	Yamaguchi	Chugoku
18	Black rice (Shikokuen)	Organic	Black	Kagawa	Shikoku
19	Ancient Red rice	Inorganic	Red	Shizuoka	Chubu
20	Sasanishiki	Inorganic	Brown	Miyagi	Tohoku
21	Nikomara	Organic	Brown	Kumamoto	Kyushu
22	Seiten no Hekireki	Inorganic	Brown	Aomori	Tohoku
23	Yanagimochi	Organic	Brown	Niigata	Chubu
24	Midori mai	Inorganic	Green	Shizuoka	Chubu
25	Daishimochimogi	Inorganic	Brown	Shizuoka	Chubu
26	Ikuhikari	Inorganic	Brown	Kagoshima	Kyushu
27	Sagabiyori	Inorganic	Brown	Saga	Kyushu
28	Hitomebore	Inorganic	Brown	Miyagi	Tohoku
29	Tsugaru Roman	Inorganic	Brown	Aomori	Tohoku

Sl. No.	Cultivars name	Farming method	Pigmentation	Region	Prefecture
30	Mix Brown rice	Inorganic	Brown	Fukushima	Tohoku
31	Haenuki	Inorganic	Brown	Yamagata	Tohoku
32	Milky Queen	Inorganic	Brown	Iwate	Tohoku
33	Mori no Kumasan	Inorganic	Brown	Kumamoto	Kyushu
34	Brown rice	Inorganic	Brown	Kyoto	Kansai
35	Mizukagami	Inorganic	Brown	Shiga	Kansai
36	Mebuki Komachi (Asamurasaki)	Organic	Black	Akita	Tohoku
37	Koshihikari	Inorganic	Brown	Kyoto	Kansai
38	Fusanomochi	Organic	Brown	Chiba	Kanto
39	Koinoyokan	Organic	Brown	Hiroshima	Chugoku
40	Red rice	Organic	Red	Chiba	Kanto
41	Green rice	Organic	Green	Chiba	Kanto
42	Black rice	Organic	Black	Chiba	Kanto
43	Asahi	Inorganic	Brown	Okayama	Chugoku
44	Hanaechizen	Inorganic	Brown	Fukui	Chubu
45	Yumegokochi	Organic	Brown	Ishikawa	Chubu
46	Kinnoibaki	Inorganic	Brown	Miyagi	Tohoku
47	Oborozuki	Organic	Brown	Hokkaido	Hokkaido
48	Nanatsuboshi	Inorganic	Brown	Hokkaido	Hokkaido
49	Okayamaasahi	Organic	Brown	Tottori	Chugoku
50	Yumeperika	Inorganic	Brown	Hokkaido	Hokkaido
51	Genki Tsukushi	Inorganic	Brown	Fukuoka	Kyushu
52	Tottoriasahi	Organic	Brown	Tottori	Chugoku
53	Ancient rice mix	Organic	Brown	Chiba	Kanto
54	Hashitsumo	Inorganic	Brown	Gifu	Chubu
55	Koshihikari	Organic	Brown	Chiba	Kanto
56	Hinohikari	Organic	Brown	Kumamoto	Kyushu

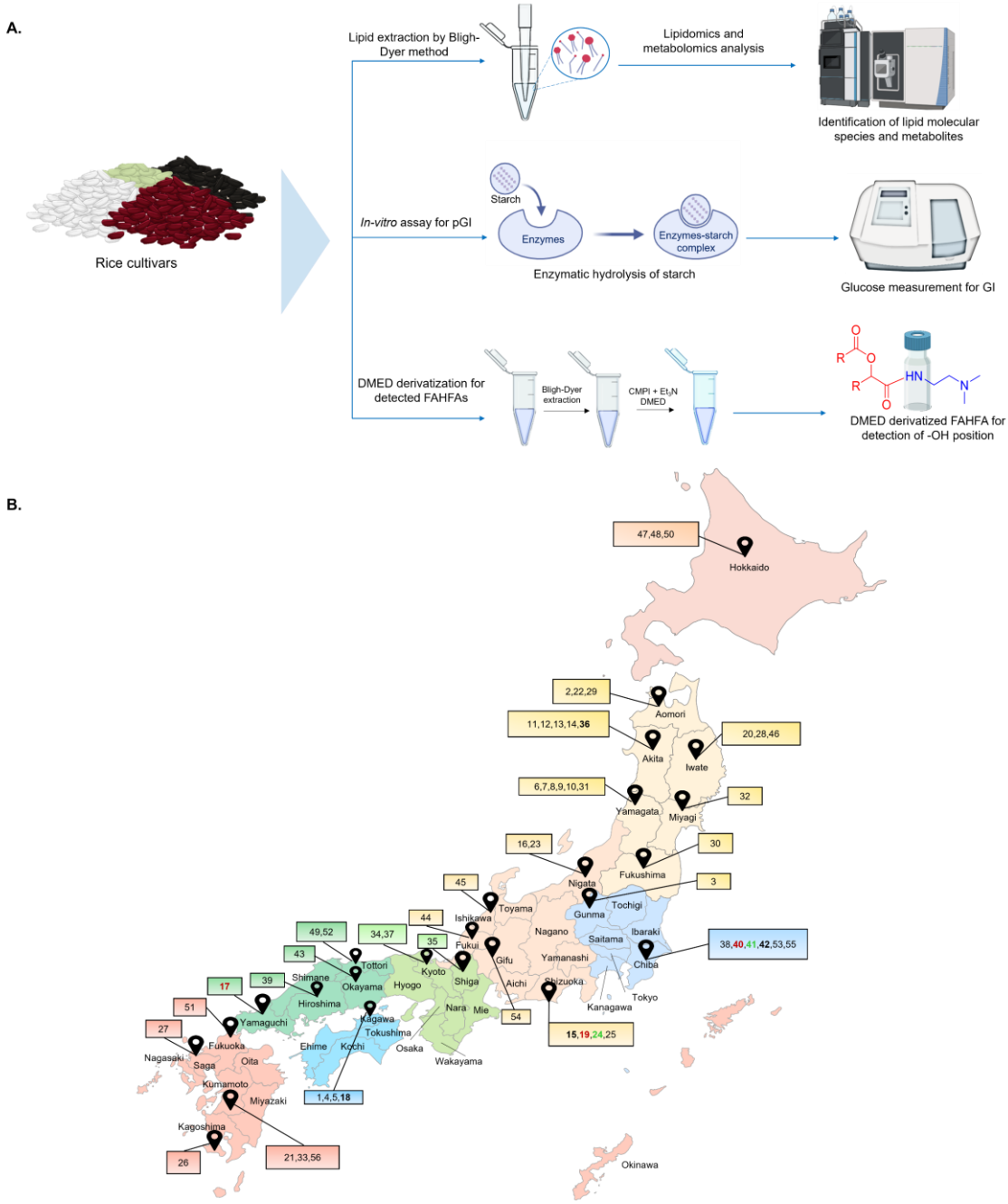

Figure 1: Study workflow and collection of 56 *japonica* rice cultivars. (A) Study design of the 56 *japonica* rice cultivars. Lipidomics and metabolomics analysis were performed for the 56 *japonica* cultivars. The *in-vitro* assay for predicted glycemic index (pGI) calculation was only performed for the selected pigmented *japonica* rice (two of each from brown, black, red, and green rice) and two cultivars of Indica rice. The DMED

derivatization was carried out with a single cultivar of rice to detect the position of the -OH group in the identified FAHFAs. (B) Map of Japan highlighting the prefectures where the rice cultivars were collected. The bold black numbers indicate black rice cultivars (n=4), while bold green (n=2) and red numbers (n=3) represent green and red rice cultivars, respectively. Non-bold numbers correspond to brown rice (n=47) cultivars. The list of the names of each rice cultivar, along with their serial numbers for reference, is given in **Table 1**.

4.2.2 Materials:

The LC/MS-grade solvents used in this study, including isopropyl alcohol, chloroform, and methanol, were the same as those described in **Chapter 2, Section 2.2.2**. Similarly, ammonium acetate solution (1 M) used as an LC/MS eluent additive, the EquiSPLASH LIPIDOMIX quantitative standard, and deuterated oleic acid (OA-d9) internal standard were obtained from the same suppliers as previously detailed in **Chapter 2, Section 2.2.2**. The derivatization of FAHFAs using DMED was obtained from the same suppliers as described in **Chapter 3, Section 3.2.1**.

Additionally, the FAHFA standard, 12-OAHOA , was synthesized in our laboratory following the protocol described in our previous research[26]. Similarly, the FAHFA standard 2-OAHNA (oleic acid esters of 2-hydroxy nonanoic acid) was synthesized in our laboratory following the protocol outlined in our recent research paper[27].

The D-glucose assay kit was purchased (GOPOD Format, K-GLU; Megazyme, Ireland; SKU: 700004297). The enzymes α-amylase (from *Aspergillus oryzae*) and amyloglucosidase (AMG; from *Aspergillus niger*) were also obtained from Megazyme (SKU: 700004188 and 700004182, respectively). Pepsin, was sourced from Sigma-

Aldrich (CAS-No.: 9001-75-6).

4.2.3 Lipid extraction, total lipid extraction, and DMED derivatization:

The lipid extraction procedure for pigmented *japonica* rice cultivars was performed following the same modified Bligh-Dyer method described in **Chapter 3, Section 3.2.2**. This included sample homogenization with ceramic beads, solvent extraction using methanol, chloroform, and water, phase separation, and collection of the lipid-rich fraction, as detailed in the previously mentioned section.

The total lipid content analysis and DMED derivatization of FAHFAs were also carried out according to the protocols described in **Chapter 3**, **Sections 3.2.3** and **3.2.4**, respectively. In this study, derivatization was specifically performed on a single pigmented *japonica* rice cultivar, green rice-24, selected based on its distinct lipidomic profile.

4.2.4 Synthesis of 2-OAHNA:

The synthesis of 2-OAHNA was carried out following the procedures described in a previous study on short-chain fatty acid esters of hydroxy fatty acids[27]. Briefly, 500 mg of nonanoic acid (FA 9:0) was placed in a round-bottom flask, and red phosphorus (1.3 eq.) was added. The mixture was heated to 95°C under a reflux condenser. Bromine water (3 eq.) was added dropwise, and the reaction was stirred at 95°C for 6 hrs. After cooling to room temperature, 20 mL of water was added, and the mixture was stirred for 20 min. The reaction mixture was then extracted with diethyl ether to obtain 2-bromononanoic acid. To synthesize 2-hydroxy nonanoic acid (2-HNA), the 2-bromononanoic acid was treated with excess 2 M NaOH (2 eq.) and refluxed at 85°C for 30 hours. The progress of the reaction was monitored using thin-layer chromatography. Upon completion, the reaction was cooled to room temperature and acidified with 2 M HCl. The resulting

mixture was extracted with diethyl ether, and the ether layer was dried over anhydrous sodium sulfate. The solvent was removed under reduced pressure, and the residue was purified by column chromatography using chloroform and methanol (97:3, v/v) to yield 2-HNA. For the esterification step, 100 mg of 2-HNA was dissolved in dichloromethane, and pyridine (100 μL per 50 mg of 2-HNA) was added. Oleoyl chloride (2 eq.) was then added dropwise at 0°C, and the reaction was stirred at room temperature overnight. The reaction mixture was extracted with dichloromethane and purified by silica gel column chromatography using chloroform and methanol (95:5, v/v) to yield 2-OAHNA. The final product was characterized by high-resolution electrospray ionization mass spectrometry (HR-ESI-MS), proton nuclear magnetic resonance (^{1}H NMR), and carbon-13 nuclear magnetic resonance (^{13}C NMR) to confirm its structure and purity.

4.2.6 LC/MS analysis:

The LC-MS analysis of lipid extracts and DMED-derivatized FAHFAs from pigmented *japonica* rice cultivars was performed using the same method described in **Chapter 3**, **Section 3.2.5**.

4.2.7 Total starch quantification:

TS content of the rice flour was determined using the standard protocol provided in the Megazyme K-TSTA kit (Megazyme, Ireland). Briefly, 100 mg of rice flour was weighed into a 15 mL Falcon tube. To this, 0.2 mL of 80% ethanol was added, followed by 2 mL of cold 1.7 M NaOH solution. The mixture was placed on a magnetic stirrer and stirred in an ice bath for 15 min until completely dissolved. Next, 8 mL of 0.6 M CH_3COONa buffer (pH 3.8) was added, and the solution was mixed using a vortex shaker. Subsequently, 0.1 mL of each α-amylase (3000 U/mL) and AMG (3300 U/mL) were added to the mixture, followed by brief mixing for 5s. The container was then transferred

to a 50°C water bath and incubated for 30 min. After the incubation, the solution was removed from the water bath and centrifuged at 7000 g for 5 min. The supernatant (1 mL) was transferred into a fresh tube and mixed with 4 mL of 0.1 M CH_3COONa buffer (pH 5.0). Aliquots of 0.1 mL were transferred from the solution, and 3 mL of GOPOD reagent was added to each aliquot. The mixture was incubated for 20 minutes at 50°C. The absorbance of the resulting solution was measured at 510 nm using a UV spectrophotometer (V-530, Jasco, Tokyo, Japan). The starch content was calculated according to the formula provided in the Megazyme K-TSTA kit.

4.2.8 *In-vitro* starch hydrolysis index and estimated glycemic index determination:

In-vitro starch digestibility and estimated glycemic index (eGI) were determined according to the protocol outlined by Goñi et al[28]. Briefly, 2 g of cooked rice was homogenized using a mortar and pestle to obtain a slurry. A 100 mg portion of the slurry was transferred to a 15 mL Falcon tube. To this, 10 mL of 1 M HCl–KCl buffer was added, and the mixture was thoroughly mixed. Next, 0.2 mL of pepsin solution (1 g of pepsin dissolved in 10 mL of 1 M HCl/KCl buffer, pH 1.5) was added to each tube, and the mixture was incubated at 40°C for 60 min in a shaking water bath. After incubation, the volume was increased to 25 mL by adding 15 mL of 0.1 M tris-maleate buffer (pH 6.9) and stirring thoroughly. Immediately, 5 mL of α-amylase solution (10 mg/mL in 0.1 M tris-maleate buffer, providing 2.6 IU of activity) was added to each tube. The enzyme-treated samples were incubated in a shaking water bath at 37°C for 3 hrs. At predetermined intervals (0, 30, 60, 90, 120, 150, and 180 min), 1 mL aliquots were collected in triplicates for glucose quantification. For the estimation of rapidly digestible starch (RDS) and slowly digestible starch (SDS) fractions, additional 1 mL aliquots were collected after 20 min (G20) and 120 min (G120) of incubation, respectively. The enzyme

reaction was stopped by boiling the collected aliquots at 100°C for 5 min. A final incubation was performed at 60°C for 45 min by adding 1 mL of 0.4 M CH_3COONa buffer (pH 4.75) and 80 µL of AMG solution (3300 U/mL) to each aliquot. After centrifugation at 2000 g for 10 min, 100 µL of the supernatant was used for glucose measurement. The starch digestion rate was calculated as the % of TS hydrolyzed at each 30-minute interval from 0 to 180 minutes. The TS in each sample was determined using the equation, which is as follows[25]:

$$\%\ \text{starch} = \Delta A \times F \times \left(\frac{100}{0.1}\right) \times \left(\frac{1}{1000}\right) \times \left(\frac{100}{W}\right) \times \left(\frac{162}{180}\right)$$

where ΔA= averaged absorbances read against the reagent blank

F=100 µg of glucose divided by the GOPOD absorbance obtained for this solution

W=weight of the test portion of starch analyzes

The rate of starch digestion was expressed as the % of starch hydrolyzed relative to the total starch content, determined at various time points, using the following equation:

$$\%\ \text{of starch hydrolysis} = \left(\%\ \text{of starch hydrolysis at certain}\ \frac{\text{time}}{\text{total}}\ \text{strach}\ (\%)\right) \times 100$$

The % of starch hydrolyzed at each time point was plotted against time (in min) starting from 0 min. The area under the curve (AUC) for each cooked rice sample was then calculated using GraphPad Prism 8. The *in-vitro* starch hydrolysis index (HI) was determined by comparing the total glucose released from the hydrolyzed rice samples over the 0-180 min period to that released from hydrolyzed corn starch, which was analyzed under identical conditions. HI was expressed as a percentage, as shown below:

$$\text{HI} = \left(\text{AUC of}\ \frac{\text{sample}}{\text{AUC}}\ \text{of corn starch}\right) \times 100$$

The eGI of the pigmented and milled rice samples was estimated according to the proposed equation of Goñi et al. The equation is as follows:

$$eGI = 39.71 + (0.549 \times HI)$$

4.2.9 Resistant starch assay:

The RS content of cooked rice was determined following the standard protocol outlined in the Megazyme Assay Kit (Megazyme International, Wicklow, Ireland). First, 100 mg of homogenized rice sample was transferred into Falcon tubes, ensuring no residue remained adhered to the tube walls. To each sample, 4 mL of pancreatic α-amylase (10 mg/mL) containing 3 U/mL AMG was added, followed by thorough mixing and incubation in a shaking water bath at 37 °C for 16 hrs. After the incubation, 4 mL of absolute ethanol was added to each tube and mixed vigorously. The tubes were then centrifuged at 1500g for 10 min. The supernatant was decanted, and the pellets were re-dissolved in 2 mL and 6 mL ethanol (50%) aliquots, with continuous stirring and centrifugation after each addition. Next, 2 mL of 2M KOH solution was added to the tubes, which were stirred for 25 min in an ice bath to dissolve the pellets. Following this, 8 mL of 1.2M CH_3COONa buffer (pH 3.8) was added to each tube, and the contents were stirred on a magnetic stirrer. To the mixture, 0.1 mL of AMG solution (3300 U/mL) was added, followed by further stirring. The tubes were then incubated in a water bath at 50 °C for 30 min. After incubation, a 0.1 mL aliquot was taken from each tube and centrifuged at 2000g for 10 min. To each aliquot, 3 mL of GOPOD reagent was added in triplicate, and the mixture was incubated at 50 °C for 20 min. Absorbance was measured at 510 nm against a reagent blank, and the RS content was calculated according to the formula provided in the kit manual.

4.2.10 Statistical Analysis

The lipidomics data set included molecular species of lipids identified in both positive and negative ionization modes. Data visualization was performed using Microsoft Excel

2021, with results presented as mean ± SEM. For statistical analysis, one-way ANOVA was conducted using GraphPad Prism 8, to determine significant differences between experimental groups. To explore data variation and patterns, MetaboAnalyst (version 6.0) was used for sPLS-DA, orthogonal partial least-squares discriminant analysis (OPLS-DA), and to generate heatmaps. These tools allowed for a comprehensive understanding of molecular lipid species' patterns and variations. Z-score normalization was performed using Microsoft Excel 2021.

4.3 Results and discussion

4.3.1 Discriminative potential of *japonica* cultivars based on lipidomics profiles: The role of pigmentation, geographic origin, and farming practices:

The lipidomics profiles of 56 *japonica* rice cultivars were analyzed to explore variations in lipid composition driven by pigmentation, geographic origin, and farming methods. Cultivars were categorized into four pigmentation types: black, red, brown, and green (**Table 1**). Multivariate analysis, particularly the sPLS-DA plot (**Figure 1A**), provided insights into the lipidomic differences among these pigmentation groups. The results indicate that brown rice cultivars exhibit a slightly distinct lipidome compared to black, red, and green rice cultivars. The two principal components in the sPLS-DA model account for a combined contribution rate of 26.5%, reflecting a high degree of similarity among the samples overall. The loading plot (**Appendix 1A**) reveals that FFA, Cer, and phytosphingosine are the key metabolites driving this distinction. Interestingly, geographic origin further influenced the lipid profiles within specific pigmentation groups. Black rice cultivars from the Shikoku region, for example, displayed unique lipid profiles compared to those from the Chubu region (**Figure 1B**), with the first two PC accounting

for 59.7% of the variation. GLs were identified as the primary metabolites contributing to this regional variation (**Appendix 1B**). Similar regional differences were noted for red and green rice cultivars **(Figures 1C** and **1D**), with corresponding loading plots (**Figures S1C** and **S1D**) supporting these findings. In contrast, brown rice cultivars exhibited minimal regional variation, with the first two components contributing 28.4% of the total variance, indicating high lipidomic similarity across regions (**Figure 1E** and **Appendix Figure 1E**).

In addition to pigmentation and geographic origin, farming methods also shaped the lipid profiles of *japonica* rice cultivars. Cultivars were categorized based on their organic (natural farming practices) and inorganic (conventional farming practices). The OPLS-DA plot (**Figure 1F**) demonstrates subtle differences between the two groups, with T-scores of 4.4% and 12.4% for the first two components, respectively. FAs and GPs were identified as the primary contributors to the observed separation (**Appendix Figure 1F**). These differences align with previous studies that suggest nitrogen fertilizer application and planting density significantly influence metabolite abundance and diversity, particularly lipid metabolites such as physapubescin and 2-undecen-1-ol, which are crucial for determining rice quality[29].

Environmental factors like irrigation practices may also contribute to the observed lipidomic variation in cultivars. For example, a recent study on alternate wetting and drying (AWD) irrigation regimes showed that moderate AWD conditions (AWMD) significantly enhanced rice cooking and eating quality by altering lipid subclasses, including TGs, DGs, Cer, PC, and digalactosyldiacylglycerol[30]. These findings highlight the interconnected influence of pigmentation, region, and farming methods on the lipid profiles of *japonica* rice cultivars, which in turn shape rice quality and nutritional

attributes. Understanding region-specific lipidomic variations could help develop rice varieties that are specific to specific regions, potentially enhancing both cooking and nutritional qualities.

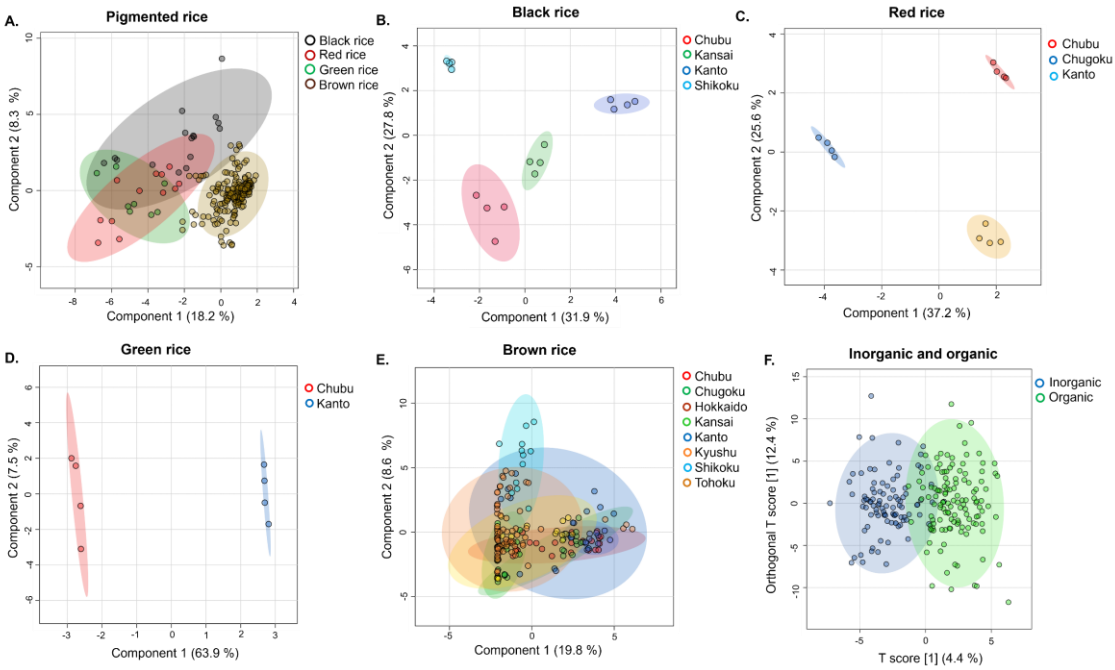

Figure 2: Multivariate analysis of rice cultivars. (A) Sparse Partial Least Squares Discriminant Analysis (sPLS-DA) score plot illustrating the separation of rice cultivars based on pigmentation. (B) sPLS-DA plot showing the regional variation among black rice cultivars, with differentiation based on their prefecture of origin. (C, D, E) sPLS-DA plots depicting the differentiation of red, green, and brown rice cultivars, respectively, based on their prefecture of origin. (F) Orthogonal Partial Least Squares Discriminant Analysis (OPLS-DA) score plot demonstrating the differentiation between cultivars based on farming methods (organic vs. inorganic).

4.3.2 Lipid class distribution and nutritional profile: Distinct patterns in pigmented rice cultivars

A comprehensive lipidomics analysis across *japonica* rice cultivars revealed a total of 198 lipid molecular species, categorized into five major lipid classes: FAs, GPs, SPs, GLs, and STs. The major lipid class distribution among pigmented rice cultivars, illustrated in **Figure 3A**, highlights variations in lipid class composition. Among these, GLs constituted the largest proportion of total lipids, with brown rice exhibiting the highest GLs content (85.25%) compared to other cultivars. Black rice, however, displayed the highest percentage of GPs (14.85%), while red rice was characterized by the highest proportion of FAs (21.15%). Notably, green rice exhibited elevated levels of SPs (0.27%) and STs (0.14%), distinguishing it from the other pigmented rice varieties. These findings are consistent with earlier reports, such as those by Yoshida et al. (2012), which documented higher GPs content in black rice, underscoring its potential roles in membrane stability and stress tolerance. Similarly, the elevated FAs levels observed in red rice align with its association with antioxidant lipids[31].

The nutritional profile of these *japonica* cultivars, depicted in **Figure 3B**, underscores the variations in total lipid percentage, the P:S ratio, and the ω-6: ω-3 fatty acid ratios. Red rice demonstrated a significantly higher total lipid percentage than brown and black rice, while green rice exhibited the lowest lipid content among all cultivars. These results corroborate previous studies suggesting that pigmented rice cultivars generally have higher lipid content compared to non-pigmented varieties[32,33]. Including green rice in the analysis expands the current understanding of lipid content variations in pigmented rice cultivars.

Among the FAs class of lipids, a total of 39 fatty acids were identified, classified

as SFAs and PUFAs based on the absence or presence of double bonds, respectively. The P:S ratio, a critical index for evaluating cardiovascular health, is shown in **Figure 3B(ii)**[34,35]. Green rice had the highest ratio (1.49), followed by black (0.96), red (0.72), and brown rice (0.51). All cultivars exceeded the generally recommended P:S ratio of ≥0.4, indicating their potential protective effects against CVD and related complications[34-37].

PUFAs were further categorized into ω-6 and ω-3 fatty acids based on the position of the first double bond. The ω-6: ω-3 ratio, depicted in **Figure 3B(iii)**, ranged from 5.5 in brown rice to 9.5 in both black and green rice. While high ω-6: ω-3 ratios are typical of Western diets and associated with an increased risk of inflammatory diseases, lower ratios (1:1 to 4:1) are generally considered more beneficial, depending on the disease under consideration[38]. Although the ratios in these rice cultivars are higher than ideal, they provide a baseline for considering dietary balance and cultivar selection.

Nutritional indices, including the health promotion index (HPI), atherogenicity index (AI), and hypo/hypercholesterolemic (HH) ratio, reveal notable functional differences among the pigmented rice cultivars (**Figure 3B(iv-vi)**). The HPI, which evaluates the overall nutritional value of the lipid profile, was highest in green rice (1.50), followed by black rice (0.90), red rice (0.71), and brown rice (0.50). A higher HPI reflects a superior balance of beneficial fatty acids, highlighting green and black rice as nutritionally superior options. Notably, while HPI has traditionally been used to evaluate the nutritional quality of foods like milk and fish (ranging from 0.16-3.30), its application in rice lipidomics demonstrates the versatility of this index in assessing plant-based dietary components[36,39]. The AI, which reflects the balance between pro-atherogenic SFAs and anti-atherogenic unsaturated fatty acids, was highest in brown rice (2.57)[40]. Red rice followed with an AI

of 1.93, while black and green rice exhibited considerably lower values of 1.25 and 0.77, respectively. A lower AI indicates a reduced risk of atherosclerosis and CVD, as supported by studies on low-AI dietary oils such as rapeseed oil[40]. These findings suggest that green and black rice, with their low AI values, may be more suitable for heart-healthy diets. Additionally, the observed lower AI in black rice aligns with prior research showing that black rice extract supplementation effectively reduces AI and lipid levels in hypercholesterolemic models, underscoring its potential as a functional food for managing cardiovascular risks[41]. The HH ratio, indicative of the cholesterol-modulating effects of specific FFA, was highest in green rice (3.15), followed by black rice (2.05), red rice (1.60), and brown rice (1.18). A higher HH ratio is associated with a favorable balance between hypo- and hypercholesterolemic fatty acids, promoting healthier cholesterol metabolism. The significantly higher HH ratio observed in green rice emphasizes its potential as a dietary component for improving lipid profiles and reducing cholesterol-related health risks.

Together, these indices illustrate the distinct nutritional profiles of the pigmented rice varieties. Green and black rice emerge as nutritionally advantageous, given their low AI, high HH ratio, and elevated HPI values, suggesting their potential for incorporation into functional diets aimed at cardiovascular health and lipid management. In contrast, brown and red rice, with higher AI and lower HH and HPI values, maybe more suited for dietary applications where energy density and other functional properties are prioritized.

The heatmap in **Figure 3C** provides a detailed visualization of FA concentrations, revealing distinct patterns among the pigmented rice cultivars. The concentration here taken into consideration is the average of all the cultivars. Green and red rice demonstrated greater diversity in lipid classes, encompassing SFAs, PUFAs, and

bioactive lipids such as FAHFAs. In contrast, black rice exhibited a predominance of SFAs, while brown rice was enriched in FAHFAs. These findings align with previous studies highlighting cultivar-dependent variations in rice lipid profiles and the functional significance of specific lipid classes in health and stress tolerance[42,43]. Key FFA identified included myristic (C14:0), palmitic (C16:0), stearic (C18:0), and arachidic (C20:0) acids, alongside MUFAs like palmitoleic (C16:1) and oleic (C18:1) acids, and PUFAs such as linoleic (C18:2) and gamma-linolenic (C18:3) acids. These findings are consistent with earlier reports identifying these fatty acids as dominant in rice lipids, with variations attributed to genetic differences among cultivars[43]. Including green rice in this study adds a novel dimension, as previous lipidomics research has largely overlooked this variety. The detection of FAHFAs in pigmented rice cultivars, reported here for the first time, expands the understanding of bioactive lipid diversity in rice. While FAHFAs have been previously identified in fermented brown rice, their presence in pigmented rice varieties underscores their potential contribution to the health-promoting properties of these cultivars[44,45]. A detailed discussion about the bioactive FAHFAs is mentioned in **section 3.5**. These findings underscore the unique lipidomic signatures of pigmented rice varieties and provide a deeper understanding of their potential health benefits and applications.

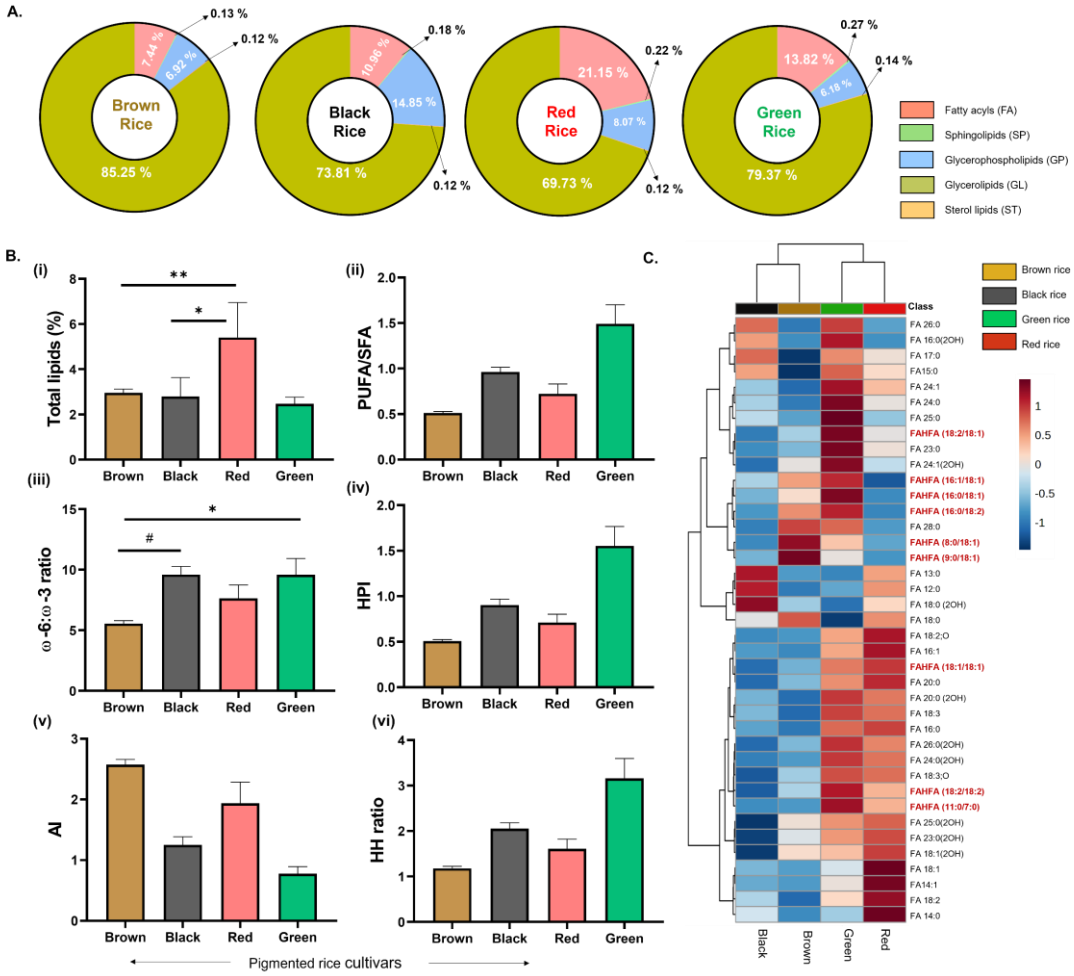

Figure 3: Distribution of lipid classes, nutritional indices, and heatmap visualization of pigmented rice cultivars (A) Donut chart showing the percentage distribution of lipid classes in pigmented rice cultivars.(B) Bar plots representing:(i) Total lipid percentage,(ii) Polyunsaturated fatty acids (PUFA) to saturated fatty acids (SFA) ratio,(iii) ω-6 to ω-3 fatty acid ratio,(iv) Health Promotion Index (HPI),(v) Index of Atherogenicity (IA), and(vi) Hypocholesterolemic/Hypercholesterolemic (H/H) ratio.(C) Heatmap illustrating the concentration of fatty acyls across pigmented rice cultivars. All the data are expressed as mean ± SEM (n = 4). Statistical significance was determined using one-way ANOVA with Tukey's multiple comparisons test. The significant differences are *p < 0.05, **p<0.01 and #p<0.0001.

4.3.3 Heatmap analysis of lipid classes: Insights into GP, GL, ST, and SP variations in pigmented rice

The heatmap visualization of major lipid classes presented in **Figure 4**, highlights the distinct lipid profiles across pigmented rice cultivars, revealing key differences in their lipidomic landscapes.

Among GLs, TGs exhibited the highest diversity, with red and black rice displaying the most variation, followed by brown rice, while green rice showed the least diversity (**Figure 4A**). This predominance of TGs aligns with previous findings, which reported TGs as the dominant lipid component in *japonica* rice bran, contributing 84.9–86.0% of the total lipid weight[46]. The higher diversity in red and black rice suggests a greater potential for energy storage and metabolic activity, while the lower diversity in green rice may reflect differences in lipid metabolism specific to this cultivar. GPs, vital structural constituents of cellular membranes, play a critical role in maintaining cellular homeostasis[47]. In this study, GPs were predominantly composed of phospholipids (PLs) such as PC, PI, and PE, which together accounted for the majority of this lipid class (**Figure 4B**). These findings align with earlier reports highlighting PC, PE, and PI as the principal PLs in oil-rich rice bran and germ, constituting 80% of total PLs[46]. Dietary PLs have been associated with health benefits, including protection against coronary heart disease, cancer, and inflammation, suggesting that incorporating PL-rich cultivars like red, brown, and black rice into diets could provide functional health benefits[48]. Notably, one species of CL, a mitochondria-specific dimeric PL critical for mitochondrial function and cellular signaling, was also identified in this study[49]. STs, primarily phytosterols, showed varying distributions among the cultivars (**Figure 4C**). Green and black rice had the highest phytosterol content, followed by brown rice, with red rice exhibiting the

lowest levels. Detected phytosterols included campesterol (ST 28:1), sitosterol (ST 29:1), and stigmasterol derivatives (SG 29:2; O; Hex, SG 29:1; O; Hex, and SG 28:1; O; Hex). These results align with prior studies identifying similar phytosterols in rice, including pigmented red rice[50,51]. SPs were predominantly composed of Cer and phytosphingosine, with black rice showing the highest levels, followed by red, brown, and green rice **(Figure 4D**). Two species of HexCer were also detected. SPs, including Cer and HexCer, are essential for cellular signaling and structural integrity of the lipid bilayer[52]. The higher abundance of these lipids in black rice suggests its superior capacity for cellular protection and stress response, further differentiating its lipid profile from the other cultivars.

In addition to lipid class variations, **Appendix Figure 2** presents a heatmap analysis of 57 metabolites, including sugars, flavonoids, and phenols, identified in pigmented rice cultivars. Brown rice exhibited the highest abundance of these metabolites, followed by black, green, and red rice. The elevated levels of bioactive metabolites in brown and black rice further enhance their functional and nutritional value. Overall, the heatmap analysis underscores the distinctive lipidome profiles of pigmented rice cultivars, highlighting variations in lipid class composition across the varieties. These insights provide a strong foundation for understanding the functional and nutritional implications of pigmented rice lipids, emphasizing their potential applications in health-oriented diets and functional food development.

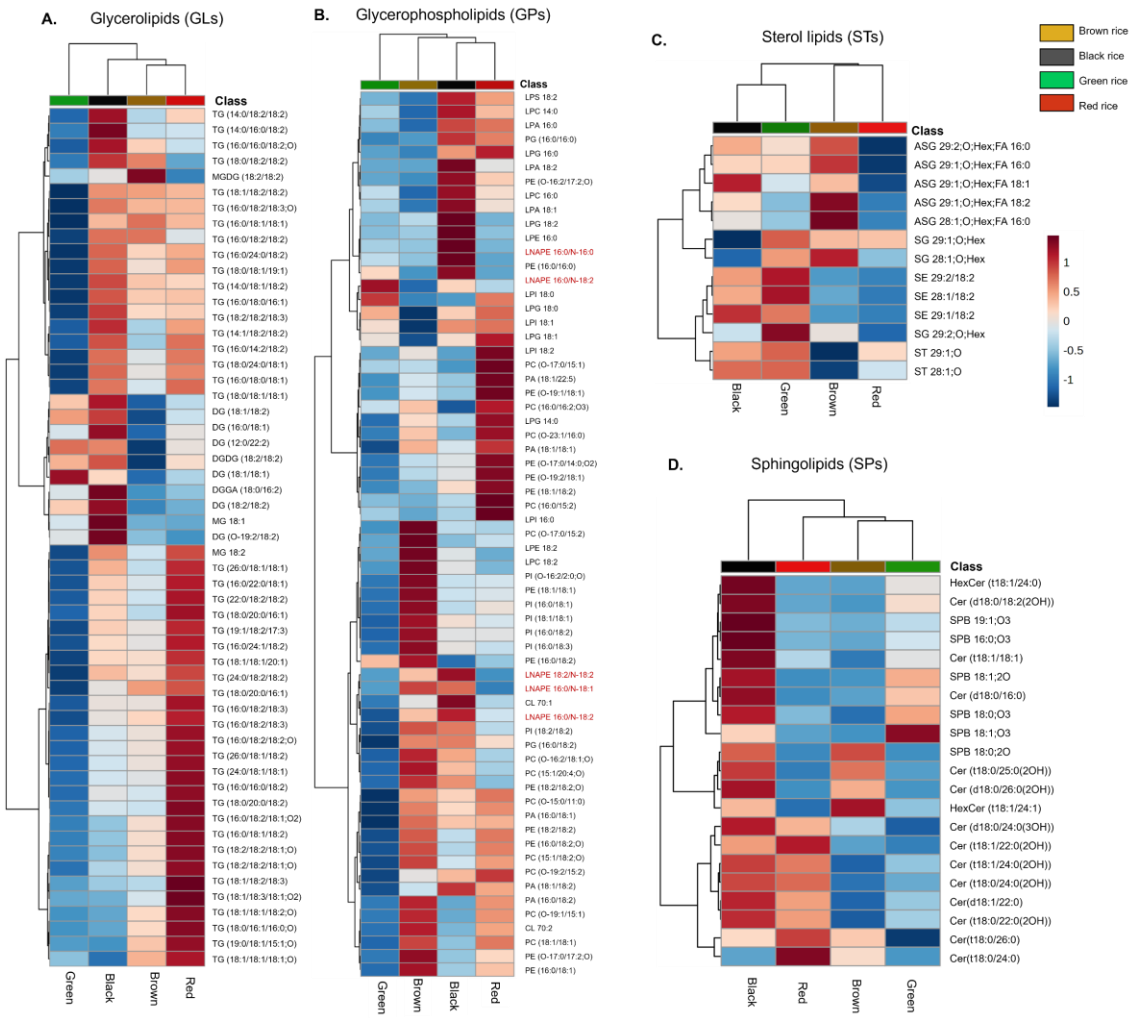

Figure 4: Heatmaps of three major lipid classes in 56 rice cultivars based on pigmentation. (A) Heatmap showing the concentration of glycerolipids (GLs) (B) Heatmap displaying the concentration of glycerophospholipids (GPs), (C) Heatmap displaying the concentration of sterol lipids (STs), and (D) Heatmap illustrating the concentration of sphingolipids (SPs) across rice cultivars.

4.3.4 MS fragmentation analysis: Insights into LNAPE abundance in black rice

PLs, a critical subset of the GPs major class, comprise up to 10% of the total lipid content in rice grains[2]. Among these, N-acyl-lysophosphatidylethanolamines (LNAPE) are partially hydrolyzed derivatives of N-acyl-phosphatidylethanolamines (NAPE).

Although LNAPE belong to the PE family, their defining feature is the esterification of the amine group with fatty acids[36]. NAPE have been detected in diverse biological membranes, including those of humans, animals, plants, and prokaryotic cells[36,53-55]. In cereals such as wheat and oats, NAPE contribute significantly to the polar lipid content, comprising 3–5%[56,57]. The most common NAPE species in these grains include those containing N-acylated fatty acids such as 16:0, 18:1, 18:2, and 18:3[57]. Previous studies on *japonica* rice grains have identified LNAPEs, but the comprehensive characterization of these lipids in pigmented rice cultivars remains unexplored[58]. NAPE are biologically significant, playing roles in regulating food intake, neuroprotection, cell proliferation, and pain modulation[55]. However, there is limited information about their sources and diversity, particularly in pigmented rice.

The structural characterization of these lipids was particularly challenging due to their close similarity with PEs, which are the second most abundant lipid class in eukaryotic cells. This structural resemblance often leads to difficulties in differentiating the relatively less abundant LNAPE from overlapping PE isomers within the same extract. In our earlier work, signals corresponding to these compounds were detected, but precise identification was hindered by unresolved chromatographic peaks and overlapping mass spectra.

To address this issue, the current study employed a recently established, specialized analytical method tailored to distinguish LNAPE from isomeric PEs. This method enabled more definitive detection and structural characterization of LNAPE, validating the tentative findings of our previous analysis while offering new clarity on the presence of these unique lipids.

EIC for both LNAPE and their PE isomers are shown in **Figures 5A and 5B**. The

chromatograms exhibited two distinct, well-separated peaks for each lipid class. These peaks were labeled as 1a/1b and 2a/2b, corresponding to different RT. Due to the modified phosphoethanolamine headgroup in LNAPE, which lowers their polarity relative to standard PE, the LNAPE eluted earlier. Based on this retention behavior, peaks 1a and 2a were assigned to LNAPE, while peaks 1b and 2b were confirmed as their corresponding PE isomers.

Further validation was achieved via high-resolution mass spectrometry. The precursor ions observed at *m/z* 714.5076 and 738.5099 (**Figures 5C** and **5D)** matched the expected mass values for the LNAPE under investigation. These compounds were ionized in negative mode, producing $[M-H]^-$ ions, and their MS/MS fragmentation patterns were consistent with previously reported data for similar structures.

Detailed analysis of the MS/MS spectra (**Figures 5E** and **5F**) supported the assignments. The spectrum of peak 1b showed characteristic fragment ions at *m/z* 255 and 279, corresponding to the carboxylate anions of FA 16:0 and FA 18:2, respectively. Additional ions resulting from the neutral loss of acyl chains as ketenes ($[M-H\text{-ketene}]^-$) appeared at *m/z* 476 and 452, while neutral losses of intact fatty acids ($[M-H-FA]^-$) were detected at *m/z* 458 and 434. The predominance of ketene loss peaks relative to free fatty acid losses is typical of PEs, confirming that peak 1b represented PE 16:0/18:2.

Conversely, the MS/MS spectrum of peak 1a displayed a different fragmentation pattern, characterized by intense signals corresponding to the loss of N-palmitoylphosphoethanolamine (*m/z* 378) and N-octadecadienoylphosphoethanolamine (*m/z* 402). These signals confirmed that peak 1a contained regioisomeric LNAPE, where the fatty acid chains were differently distributed between the glycerol backbone and the amino group. A similar analytical approach was applied to peaks 2a and 2b (**Figure 5F**),

which both contained two FA 18:2 acyl chains. In these cases, the MS/MS spectra displayed a carboxylate anion at *m/z* 279. However, the relative intensity of the product ions *m/z* 476 ([M-H-ketene-18:2]$^-$) and *m/z* 458 ([M-H-FA-18:2]$^-$), along with the presence of the *m/z* 402 ion, confirmed that peak 2a corresponded to LNAPE 18:2/18:2, with one acyl chain linked to the glycerol backbone and the other attached to the amine group. The remaining three LNAPE were identified using the same fragmentation criteria, based on their characteristic MS/MS fragmentation behavior that clearly differentiated them from isomeric PE. Complete EICs and MS/MS spectra for these LNAPEs are provided in the **Appendix Figure 3**.

This study demonstrates that through the use of advanced chromatographic and high-resolution mass spectrometry techniques, alongside targeted fragmentation analysis, it is possible to accurately identify and distinguish LNAPE from structurally similar lipid species in complex plant matrices.

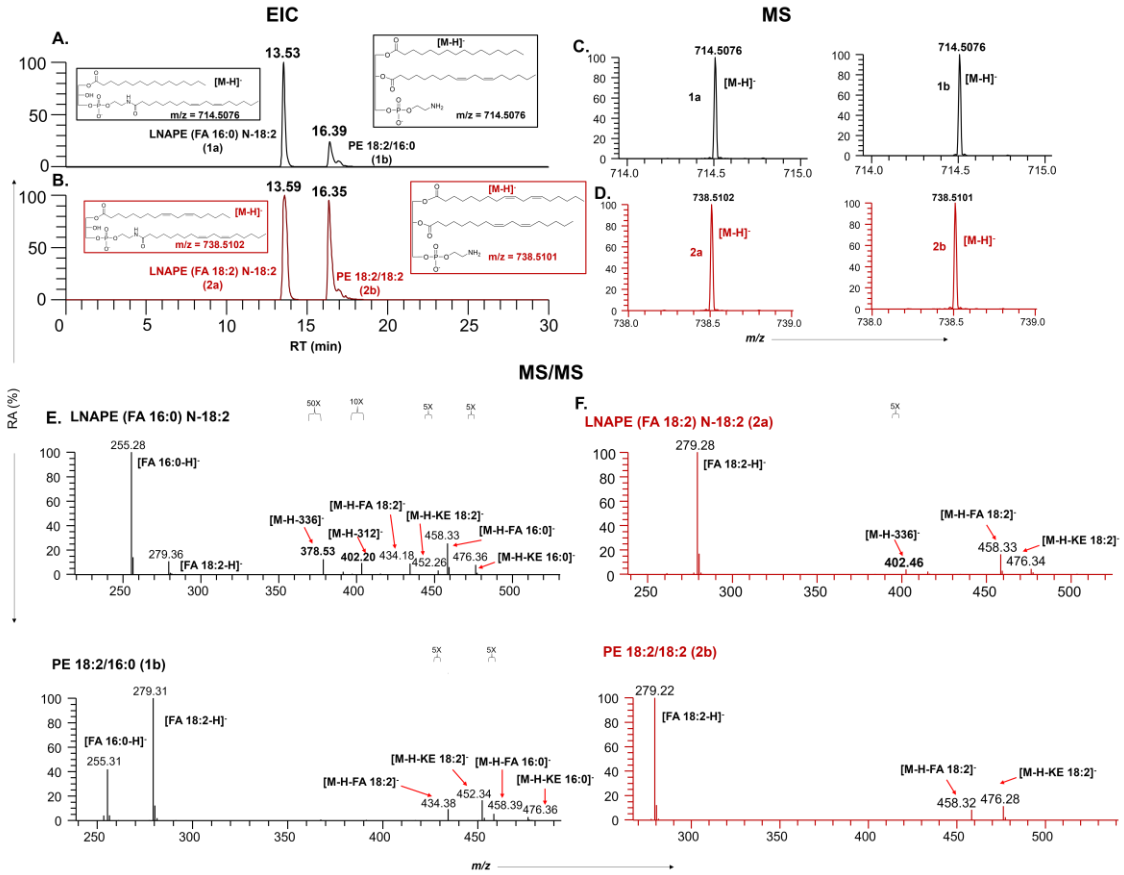

Figure 5: (A) Extracted ion chromatograms (EICs) of LNAPEs and their corresponding PEs at *m/z* 714.5076. (B) Extracted ion chromatograms (EICs) at *m/z* 738.5012. (C) High-resolution mass spectra (MS) of the detected lipid species at *m/z* 714.5076, identifying both LNAPE and PE molecular species. (D) High-resolution mass spectra (MS) at *m/z* 738.5012, confirming the presence of both LNAPE and PE isomers. (E) MS/MS fragmentation spectra differentiating LNAPE (FA 16:0 N-18:2) from its isomer PE 18:2/16:0, based on characteristic fragment ions. (F) MS/MS fragmentation spectra of LNAPE (FA 18:2 N-18:2) and its isomer PE 18:2/18:2, illustrating distinctive fragmentation patterns supporting structural assignment.

4.3.5 MS characterization: Identification of the novel FAHFA 2-OAHNA in rice

FAHFAs are a novel class of bioactive lipokines produced by esterification of the carboxyl group of fatty acids with the hydroxyl group of hydroxy fatty acids[59,60]. These compounds have gained attention due to their anti-diabetic and anti-inflammatory properties, with studies also revealing an inverse correlation between specific FAHFA levels and certain cancers[60-62]. Initially discovered in white adipocytes, FAHFAs have since been identified in various food sources, including vegetables, fruits, and meat[60,63-65]. A previous study also identified FAHFAs in fermented brown rice and rice bran[45]. Along with this, a study also detected FAHFAs in rice and *Arabidopsis*, identifying 49 FAHFA families (262 regioisomers) using chemical isotope labeling-assisted liquid chromatography-mass spectrometry[45]. Furthermore, a recent study documented 1,207 FAHFA isomers across different foods, including 30 FAHFA families (85 regioisomers) in rice grains[66].

Despite these findings, the characterization of FAHFAs in pigmented rice cultivars remains largely unexplored. In this study, we identified nine distinct FAHFAs in pigmented *japonica* rice cultivars, including a unique FAHFA species: oleic acid esters of 2-hydroxy caprylic acid and nonanoic acid (2-OAHCA and 2-OAHNA). This novel FAHFA features a medium-chain hydroxy fatty acid (2-HCA and HNA) esterified with OA. To confirm the structure, we synthesized a standard for 2-OAHNA in the laboratory using a previously established method[27]. Detailed structural characterization was performed using HR-ESI-MS, ^{1}H NMR, and ^{13}C NMR, with results provided in **Appendix Figure 3**.

The EIC and mass spectra (MS and MS/MS) of 2-OAHNA and their corresponding fragmentation patterns are depicted in **Figures 6A** and **B,** respectively. The

black and red color spectra represent the standard and sample 2-OAHNA respectively. The standard 2-OAHNA, ionized in negative mode, produced a precursor ion at *m/z* 437.3618 ($[M-H]^-$). The MS/MS spectra revealed characteristic fragmentation, including *m/z* 281 and 173, corresponding to the loss of OA and HNA, respectively. Further fragmentation at *m/z* 173 produced *m/z* 155 with a neutral loss of H_2O, confirming that the compound was HNA. Further, the *m/z* 127 from *m/z* 173, causing loss of HCOOH (46 Da) confirms the position of the -OH group to be in the second position. The exact similar fragmentation observed in green rice-24 confirms the position of the -OH group in rice OAHNA at the C2 position and is named 2-OAHNA. Similarly, other FAHFAs detected in the rice cultivars are confirmed, and the representative MS^n analysis is depicted in **Appendix Figure 4**. Previous studies on rice grains have identified a range of FAHFAs, including OAHOA, PAHOA, palmitoleic acid esters of hydroxy oleic acid (POHOA), and LAHLA[45,66]. However, these investigations primarily focused on non-pigmented rice varieties, leaving the FAHFAs' composition of pigmented rice cultivars unexplored. In our study, we not only identified FAHFAs already reported in rice grains but also detected unique FAHFAs such as OAHCA, OAHNA, FAHFA (16:1/18:1), and FAHFA (11:0/7:0), which were absent in prior reports. This highlights the diversity of FAHFAs in pigmented *japonica* rice cultivars.

Further, the derivatization of FAHFAs from DMED-labeled lipid extracts of the green rice-24 gives information about the position of the -OH group based on MS^n analysis of the DMED-labeled FAHFA standard. The position-based fragmentation was compared to the fragmentation pattern of standard 12-OAHOA as a reference. The representative EIC and MS^n analysis spectra of standard DMED-labeled 12-OAHOA and sample DMED-labeled OAHOA are shown in **Figure 6C**. MS^n analyses were performed

to confirm the position of -OH in the sample of the FAHFAs, this analysis aligns with **Chapter 3**, **Section 3.3.4**. Every lipid molecular species in the DMED-labeled-FAHFA family underwent positive mode ionization, producing $[M+H]^+$ as the precursor ion. In brief, the standard 12-OAHOA ionizes to give a $[M+H]^+$ ion at *m/z* 633.5918. The MS/MS spectra showed subsequent ionization, resulting in *m/z* 588, indicating the neutral loss of the dimethylamino group (45 Da) $[M+H–C_2H_7N]^+$. The product ion at *m/z* 351 was due to the loss of the oleoyl group. Afterward, *m/z* 306 represented the loss of the oleoyl group with the dimethylamino group. Further fragmentation at *m/z* 306 based on MS^3 analysis produced *m/z* 208 (as loss of $C_{13}H_{22}NO^+$) with *m/z* 98 ($C_7H_{14}O^{\cdot+}$) and *m/z* 222 ($C_{14}H_{24}NO^+$), identifying the -OH position at C12 of HOA, confirming the structure to be 12-OAHOA (**Figure 6C i**). The same fragmentation observed in DMED-labeled OAHOA in rice cultivar confirms the position of the -OH group in rice OAHOA at the C12 position and is named 12-OAHOA (**Figure 6C ii**). A previous report suggests that, as derivatives of unsaturated FAs, OAHOAs have good anti-inflammatory properties[68].

Similar fragmentation has been observed for DMED-labeled-FAHFAs in the sample, except for LAHLA. The EIC and fragmentation pattern for MS^n analysis is represented in **Figure 6D**. In **Figure 6D i**, DMED-labeled PAHOA ionizes to give an $[M+H]^+$ ion at *m/z* 607.5782. The MS/MS spectra showed subsequent ionization, resulting in *m/z* 562, indicating the neutral loss of the dimethylamino group (45 Da) $[M+H–C_2H_7N]^+$. The product ion at *m/z* 351 was due to the loss of the palmitoyl group. Afterward, *m/z* 306 represented the loss of the palmitoyl group with the dimethylamino group. Further fragmentation at *m/z* 306 based on MS^3 analysis produced *m/z* 208 (as loss of $C_{13}H_{22}NO^+$) with *m/z* 98 ($C_7H_{14}O^{\cdot+}$) and *m/z* 222 ($C_{14}H_{24}NO^+$), identifying the -OH position at C12 of HOA, confirming the structure to be 12-PAHOA similar to the standard

12-OAHOA. The same fragmentation pattern is followed by other DMED-labeled FAHFAs OAHLA, where the position of the -OH group is identified at C12 (**Figure 6D ii**), however LAHLA with HLA as its hydroxy fatty acid follows a different fragmentation pattern, and the position of the -OH group is identified at C14 (**Figure 6D iii**). In brief, the DMED-labeled LAHLA produced $[M+H]^+$ as the precursor ion at *m/z* 629.5613. The MS/MS spectra showed subsequent ionization, resulting in *m/z* 584, indicating the neutral loss of the dimethylamino group (45 Da) $[M+H–C_2H_7N]^+$. The product ion at *m/z* 351 was due to the loss of the linoleoyl. Along with this, *m/z* 349 indicates the loss of $C_{23}H_{41}O_2^+$, which confirms the position of -OH to be at C14 in MS/MS spectral analysis. Afterward, *m/z* 306 represented the loss of the linoleoyl group with the dimethylamino group. Further fragmentation at *m/z* 306 based on MS^3 analysis produced *m/z* 208 ($C_{13}H_{22}NO^+$) with *m/z* 98 ($C_7H_{14}O^{\cdot+}$), *m/z* 222 ($C_{14}H_{24}NO^+$), *m/z* 236 ($C_{15}H_{26}NO^+$), and *m/z* 250 ($C_{16}H_{28}NO^+$), which also identify the -OH position at C14 of HLA, confirming the structure to be 14-LAHLA.

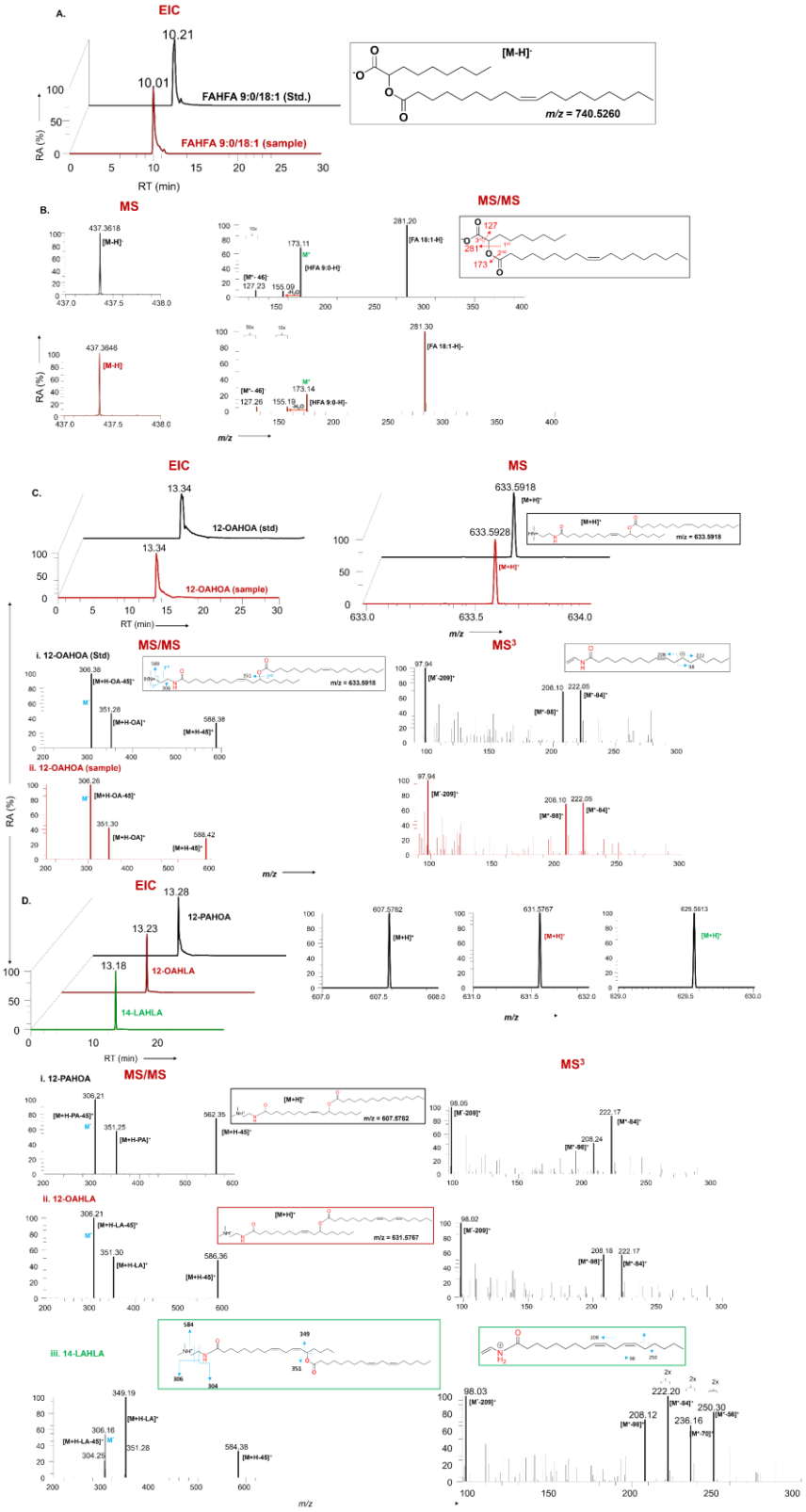

Figure 6: Detection of oleic acid esters of 2-hydroxy nonanoic acid (2-OAHNA) and

DMED-derivatized FAHFAs pigmented *japonica* rice cultivar. (A) EIC of standard 2-OAHNA and sample 2-OAHNA. The standard spectra and sample spectra are represented in black and red colors, respectively. (B) The MS and MS/MS spectra of standard and sample. The fragmentation pattern of 2-OAHNA is shown in the rectangular box. (C) The EIC and MS^n spectra DMED-labeled (i) standard oleic acid esters of 12-hydroxy oleic acid (12-OAHOA) and (ii) DMED-labeled sample 12-OAHOA. (D) The EIC and MS^n analyses of DMED-labeled sample FAHFAs, such as (i) palmitic acid esters of hydroxy-oleic acid (12-PAHOA), (ii) oleic acid esters of hydroxy-linoleic acid (12-OAHLA), and (iii) linoleic acid esters of hydroxy-linoleic acid (14-LAHLA) are shown. The fragmentation pattern of DMED-labeled FAHFAs are shown in the rectangular box.

4.3.6 *In-vitro* starch digestion: Insights into total Starch, glycemic index, and starch fractions (SDS, RDS, RS) in rice

The *in-vitro* starch digestibility assay utilized gastrointestinal enzymes (pepsin, α-amylase, and AMG) to simulate the digestion process and estimate the eGI of rice cultivars[68]. The protocol for performing the *in-vitro* starch digestibility assay is illustrated in **Figure 7A**. The total starch content of the rice cultivars was determined using a standard TS assay presented in **Figure 7B**. The total starch content ranged from 55% to 70% across all tested cultivars, encompassing both *japonica* and *indica* rice varieties. Among *japonica* cultivars, green rice-24 exhibited the highest total starch content, while red rice-19 had the lowest. In *indica* cultivars, parboiled rice showed a significantly higher starch content compared to white rice. This observation aligns with a previous study on *indica* cultivars, which demonstrated that non-pigmented rice generally contains higher starch percentages than pigmented varieties[68]. Additionally, a separate study examining eight non-pigmented and 19 pigmented *indica* genotypes reported variations in total

starch content across cultivars, further corroborating these findings[70]. Interestingly, our study also highlights that a pigmented *japonica* cultivar, green rice-24, possesses a significantly higher starch content than polished *indica* rice. This deviation from the expected trend may be attributed to external factors such as genetic, environmental, and agronomic influences. Previous research supports the notion that a combination of genetic traits, growing conditions, and cultivation practices modulates starch concentration in grains[71].

The hydrolysis of starch was monitored over time, with glucose release quantified as the percentage of starch hydrolyzed (SH) at 30-minute intervals from 0 to 180 minutes. The AUC derived from these SH values represents the digestibility of the test food. The HI is then calculated as the ratio of the AUC of the test food to that of a reference food, expressed as a percentage[25]. The starch hydrolysis curve, illustrated in **Figure 7C**, shows that corn starch exhibited the highest percentage of starch hydrolysis among the samples. The eGI values of the rice cultivars ranged from 61.24 (black rice-42) to 76.37 (*indica* white rice), as presented in **Table 2**. Pigmented rice varieties generally exhibited a slower starch hydrolysis rate, resulting in moderate eGI values that often fall within the low GI (≤55) or medium GI (56–69) categories. These characteristics are associated with a reduced postprandial blood glucose response, supporting their nutritional benefits[72]. In this study, black rice-42 exhibited the lowest eGI (61.24), consistent with previous studies on Thai black and purple rice, which reported eGI values ranging from 60 to 65[18,73]. For *japonica* red rice, eGI values were 68.61 (red rice-40) and 71.36 (red rice-19). While red rice-40 falls within the medium GI range, red rice-19 is classified as high GI. These findings align with previous studies on Sri Lankan red rice cultivars, which reported eGI values between 71 and 76, and Thai red rice cultivars, with

an eGI of 65.5[18,74]. This consistency supports the observation that red rice typically exhibits eGI values within a moderate-to-high range. The eGI of *japonica* brown rice-48 and 55 were 69.24 and 71.78, respectively, while polished brown rice-55 had a higher eGI of 75.04. These results align with earlier findings that brown rice generally has a lower eGI than white milled rice[25]. However, the eGI value for polished brown rice-55 (75.04) in this study differs from a previous report, which recorded an eGI of 63.11. This discrepancy may be attributed to variations in cooking methods, water-to-rice ratios, and cooking times between studies[25]. Notably, the eGI values of brown rice observed in this study (66–76) are consistent with findings from *in-vitro* digestion studies on cooked Philippine brown rice[25]. For green rice cultivars, eGI values were in the medium range, with 68.61 for cultivar-24 and 66.52 for cultivar-41. Comparisons with *indica* cultivars showed that *indica* brown rice had a lower eGI (67.36) than *japonica* brown and white rice. Among *indica* cultivars, parboiled rice exhibited a higher eGI than brown rice but a lower GI than milled white rice, corroborating prior research indicating that parboiling reduces the eGI of rice grains[75].

The composition of RDS, SDS, and RS significantly influences the rate of starch hydrolysis and subsequent glucose release, ultimately impacting the glycemic response. RDS contributes to a rapid glycemic response, SDS provides a sustained release of glucose, and RS minimizes glucose release, leading to a lower glycemic response[76]. Among the *japonica* cultivars, black rice-42 exhibited the lowest percentage of RDS (28.78%) and SDS (32.46%) while demonstrating the highest RS content (0.72%). These results align with a previous study indicating that elevated RS levels are associated with reduced starch digestibility and a moderated glycemic response[76]. In contrast, black rice-15, despite having low RDS and SDS percentages, showed a comparatively lower RS

content, potentially due to differences in starch granule size and structure, which are known to significantly influence starch digestion rates in pigmented rice[72,77]. For *indica* cultivars, brown rice exhibited a higher RS percentage (0.86%) compared to white rice (0.56%), a trend similarly observed in *japonica* brown-55 and polished brown-55 cultivars. This supports findings from earlier studies on the effects of milling, which demonstrate that brown rice generally retains higher RS levels than white rice due to the preservation of the bran layer and associated structural integrity[78].

To further investigate the factors contributing to the observed variations in eGI, we explored the interactions between starch and lipids during cooking. Our *in-vitro* starch digestibility analysis demonstrated significant differences among rice cultivars, with black rice showing the lowest eGI among the tested samples. This finding aligns with the lipidomics analysis, which revealed a moderate percentage of FA distribution and a notable FFA content, predominantly composed of SFAs (**Figure 3A** and **3C**). During cooking, interactions between rice starch and lipids lead to the formation of starch-lipid complexes, which stabilize the starch matrix and reduce its susceptibility to enzymatic hydrolysis[72]. In particular, SFAs are more effective at forming stable V-type starch-lipid complexes compared to unsaturated fatty acids, resulting in a lower rate of starch digestibility[79]. Conversely, the higher eGI observed in brown *japonica* rice may be attributed to its lower FA content and the predominance of unsaturated FAHFAs, which form less stable complexes, thereby facilitating enzymatic breakdown (**Figure 3A** and **3C**).

Table 2: The % distribution of RDS, SDS, RS, and value of eGI in the selected cultivars.

Rice cultivar	RDS (%)	SDS (%)	RS (%)	eGI
Red-19	43.67 ± 2.15	44.16 ± 0.18	0.48± 0.02	71.36
Red-40	34.04 ± 0.18	38.56 ± 0.11	0.56 ± 0.03	68.61
Green-24	39.06 ± 0.30	39.84 ± 0.45	0.59 ± 0.03	66.52
Green-41	36.43 ± 0.29	39.15 ± 0.46	0.56 ± 0.01	67.64
Black-15	28.79 ± 0.93	34.29 ± 1.14	0.49 ± 0.03	64.41
Black-42	28.78 ± 0.71	32.46 ± 0.41	0.72 ± 0.03	61.24
Brown-48	46.02 ± 1.78	45.32 ± 0.38	0.48 ± 0.03	71.78
Brown-55	42.08 ± 0.26	39.63 ± 0.79	0.64± 0.03	69.24
Polished brown-55	46.03 ± 2.23	52.30 ± 4.45	0.55 ± 0.09	75.04
Indica-brown	40.19 ± 1.66	40.80 ± 0.80	0.86 ± 0.05	67.36
Indica-white	45.87 ± 3.21	48.95 ± 2.62	0.56 ± 0.01	76.37
Par-boiled	31.00 ± 0.16	41.07 ± 2.78	0.52 ± 0.07	69.08

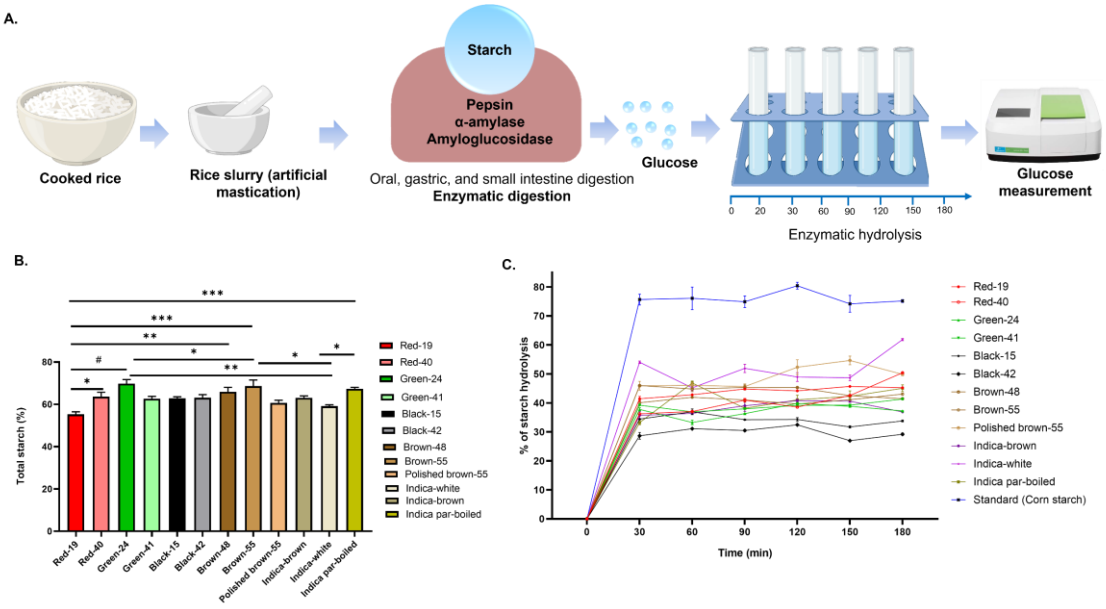

Figure 7: Total starch content and starch hydrolysis kinetics of pigmented Japonica and Indica rice cultivars. (A) The schematic diagram represents the *in-vitro* starch assay. (B) Bar graph showing the percentage of total starch in 8 pigmented Japonica rice cultivars, polished brown rice, and Indica rice varieties (parboiled, basmati brown, and polished basmati brown). Data are presented as mean ± SEM (n = 4). Statistical significance was determined using two-way ANOVA followed by Tukey's multiple comparisons test, with different letters indicating significant differences at $p < 0.05$.(C) Starch hydrolysis kinetics of rice cultivars were measured over 0–180 minutes, with corn starch used as the standard for the assay.

4.4 Limitations

This study integrates lipidomics profiling with *in-vitro* starch digestibility analysis to investigate the nutritional and functional properties of pigmented *japonica* rice cultivars. However, several limitations must be considered. Firstly, the rice samples were sourced from online stores, and factors such as agronomic conditions, ripening stages, and

postharvest handling were not controlled, which could influence the lipid composition and eGI. Due to the large sample size, the heatmap presents average concentrations of lipid major classes. *In-vitro* starch digestibility assays were performed on a limited sample size (n=2) for each pigmented rice type. Additionally, the data are semiquantitative, and internal standards were added post-homogenization to minimize lipid loss. Variations in grinding methods could also affect results. The absence of commercial standards required MS spectrum analysis for identifying new lipids, such as LNAPE, and FAHFAs, and the low concentration of certain FAHFAs (16:1/18:1 and 16:0/18:2) hindered confirmation of their -OH position. Future studies should address these limitations to provide a more comprehensive understanding of lipid profiles in pigmented *japonica* rice.

4.5 Conclusion

In conclusion, this study provides insights into the lipid profiles and glycemic response of pigmented *japonica* rice cultivars through lipidomics analysis and *in-vitro* starch digestibility assessment. The findings highlight distinct lipidomic differences among rice cultivars based on pigmentation, geographic origin, and farming methods. The nutritional indices reveal that green and black rice exhibit superior nutritional profiles, with high levels of P:S, ω-6 to ω-3 ratios, suggesting potential cardiovascular health benefits, positioning these cultivars as promising options for promoting overall health. Furthermore, the abundance of bioactive lipids such as FAHFAs in green rice and LNAPEs in black rice underscores their potential for metabolic health benefits. The lower eGI observed in black and green rice cultivars supports their role in moderating glycemic responses, making them potential candidates for reducing the risk of T2D. Notably, indica brown rice, with its relatively low eGI, presents a valuable alternative to japonica rice,

highlighting its suitability for individuals seeking nutritional benefits with a reduced glycemic response. Overall, pigmented *japonica* rice cultivars offer promising health benefits, making them strong candidates for functional foods targeting metabolic and cardiovascular health.

While previous chapters focused on profiling bioactive lipids and their health-related significance in food crops, **Chapter 5** extends the scope by exploring novel bio-derived nanomaterials and their biological effects on rice seed germination. Together, these studies contribute to a holistic understanding of how natural and engineered bioactive compounds can enhance both the nutritional quality and biological performance of crop plants, supporting future strategies for functional food production and sustainable agriculture.

4.6 References

1. Linares, O. F. (2002). African rice (Oryza glaberrima): history and future potential. Proceedings of the National Academy of Sciences, 99(25), 16360-16365.
2. Liu, L., Waters, D. L., Rose, T. J., Bao, J., & King, G. J. (2013). Phospholipids in rice: Significance in grain quality and health benefits: A review. *Food chemistry*, *139*(1-4), 1133-1145.
3. Mir, S. A., Shah, M. A., Bosco, S. J. D., Sunooj, K. V., & Farooq, S. (2020). A review on nutritional properties, shelf life, health aspects, and consumption of brown rice in comparison with white rice. *Cereal Chemistry*, *97*(5), 895-903.
4. Rathna Priya, T. S., Eliazer Nelson, A. R. L., Ravichandran, K., & Antony, U. (2019). Nutritional and functional properties of coloured rice varieties of South India: a review. *Journal of Ethnic Foods*, *6*(1), 1-11.
5. Xiong, Q., Zhang, J., Shi, Q., Zhang, Y., Sun, C., Li, A., Lu, W., Hu, Jinlong, Zhou, N., Wei, H., Wang, S., Zhang, H., & Zhu, J. (2022). The key metabolites associated with nutritional components in purple glutinous rice. *Food Research International*, *160*, 111686.
6. Chang, L., Liu, Z., Ying, X., Kalandarov, B., Ergashev, M., Tong, X., Zhang, J., jin, J., & Ying, J. (2024). Molecular Basis of Lipid Metabolism in Oryza sativa L. Plants, 13(23), 3263.
7. Zhao, L., Duan, X., & Liu, H. (2023). Novel grade classification tool with lipidomics for Indica rice eating quality evaluation. Foods, 12(5), 944.
8. Yoon, M. R., Lee, S. C., & Kang, M. Y. (2012). The lipid composition of rice cultivars with different eating qualities. *Journal of the Korean Society for Applied Biological Chemistry*, *55*, 291-295.

9. Zhang, D., Zhao, L., Wang, W., Wang, Q., Liu, J., Wang, Y., Liu, H., Shnag, B., Duan, X., & Sun, H. (2022). Lipidomics reveals the changes in non-starch and starch lipids of rice (Oryza sativa L.) during storage. Journal of Food Composition and Analysis, 105, 104205.
10. Naveed, A., Zubair, M., Baig, A., Farid, M., Ahmed, W., Rehman, R., Ayub, M. A., Hassoun, A., & Cropotova, J. (2023). Effect of storage on the nutritional and antioxidant properties of brown Basmati rice. Food Science & Nutrition, 11(5), 2086-2098.
11. Zhang, X., Shen, Y., Zhang, N., Bao, J., Wu, D., & Shu, X. (2019). The effects of internal endosperm lipids on starch properties: Evidence from rice mutant starches. *Journal of Cereal Science*, *89*, 102804.
12. Kaur, B., Ranawana, V., & Henry, J. (2016). The glycemic index of rice and rice products: a review, and table of GI values. *Critical reviews in food science and nutrition*, *56*(2), 215-236.
13. Atkinson, F. S., Foster-Powell, K., & Brand-Miller, J. C. (2008). International tables of glycemic index and glycemic load values: 2008. *Diabetes care*, *31*(12), 2281-2283.
14. Wolever, T. M. S., Vorster, H. H. Inger Bj€ orck, J. Brand-Miller, F. Brighenti, J. I. Mann, and D. D. Ramdath. (2003). Determination of the glycaemic index of foods: interlaboratory study. European Journal of Clinical Nutrition 57 (3).
15. Zhao, S., Shi, J., Cai, S., Xiong, T., Cai, F., Li, S., Chen, X., Fan, C., Mei, X., & Sui, Y. (2024). Impact of rice variety, cooking equipment and pretreatment method on the quality of lightly milled rice. Food Chemistry, 451, 139271.
16. de Souza Batista, C., Dittgen, C. L., da Silva Lindemann, I., Wang, Y. J., Elias, M. C., Vanier, N. L., & Colussi, R. (2024). Effects of cooking temperature on technological

properties and in vitro digestibility of quick-cooking black and brown rice. *Cereal Chemistry*, *101*(3), 654-667.

17. Wang, L., Hu, F., Bainto-Ancheta, L., Aumasa, T., Wonglek, S., Prempree, P., & Ogawa, Y. (2024). Structural characteristics and in vitro starch digestibility of oil-modified cooked rice with varied addition manipulations. Food Research International, 186, 114381.
18. Thuengtung, S., Niwat, C., Tamura, M., & Ogawa, Y. (2018). In vitro examination of starch digestibility and changes in antioxidant activities of selected cooked pigmented rice. *Food bioscience*, *23*, 129-136.
19. Sivakamasundari, S. K., Priyanga, S., Moses, J. A., & Anandharamakrishnan, C. (2022). Impact of processing techniques on the glycemic index of rice. *Critical Reviews in Food Science and Nutrition*, *62*(12), 3323-3344.
20. Putseys, J. A., Lamberts, L., & Delcour, A. J. (2010). Amylose-inclusion complexes: Formation, identity and physico-chemical properties. *Journal of Cereal Science*, *51*(3), 238-247.
21. Krishnan, V., Mondal, D., Bollinedi, H., Srivastava, S., Ramesh, S. V., Madhavan, L., Thomas, B., R, A. T., Singh, A., Singh, A. K., & Praveen, S. (2020). Cooking fat types alter the inherent glycaemic response of niche rice varieties through resistant starch (RS) formation. International Journal of Biological Macromolecules, 162, 1668-1681.
22. Qu, L., Zhao, Y., Li, Y., & Lv, H. (2024). Effect of storage temperature on the quality of brown rice revealed by integrated GC–MS and lipidomics analysis. *Food Chemistry*, 142107.
23. Yamashita, K., Kato, N., Sakakibara, K., Seguchi, A., Kobayashi, A., Miyagawa, S., & Uchimura, T. (2023). Characterization of Cooked Nonglutinous Rice Cultivars

Based on Flavor Volatiles and Their Change during Storage. *ACS omega*, *8*(16), 14823-14829.

24. Zhang, D., Duan, X., Shang, B., Hong, Y., & Sun, H. (2021). Analysis of lipidomics profile of rice and changes during storage by UPLC-Q-extractive orbitrap mass spectrometry. Food Research International, 142, 110214.
25. Tuaño, A. P. P., Barcellano, E. C. G., & Rodriguez, M. S. (2021). Resistant starch levels and in vitro starch digestibility of selected cooked Philippine brown and milled rices varying in apparent amylose content and glycemic index. Food Chemistry: Molecular Sciences, 2, 100010.
26. Gowda, S. G. B., Fuda, H., Tsukui, T., Chiba, H., & Hui, S. P. (2020). Discovery of eicosapentaenoic acid esters of hydroxy fatty acids as potent Nrf2 activators. Antioxidants, 9 (5), 397.
27. Gowda, S. G. B., Hou, F., Gowda, D., Chiba, H., Kawakami, K., Fukiya, S., Yokota, A., & Hui, S. P. (2024). Synthesis and quantification of short-chain fatty acid esters of hydroxy fatty acids in rat intestinal contents and fecal samples by LC-MS/MS. Analytica Chimica Acta, 1288, 342145.
28. Goñi, I., Garcia-Alonso, A., & Saura-Calixto, F. (1997). A starch hydrolysis procedure to estimate glycemic index. Nutrition research, 17(3), 427-437.
29. Xiong, Q., Sun, C., Shi, H., Cai, S., Xie, H., Liu, F., & Zhu, J. (2022). Analysis of related metabolites affecting taste values in rice under different nitrogen fertilizer amounts and planting densities. Foods, 11(10), 1508.
30. Xu, Y., Weng, X., Tang, S., Zhang, W., Zhu, K., Zhu, G., Zhang, H., Wang, Z., & Yang, J. (2024). Untargeted lipidomic analysis of milled rice under different alternate wetting and soil drying irrigation regimes. Journal of Integrative Agriculture.

31. Yoshida, H., Tomiyama, Y., Mizushina, Y., & Yoshida, N. (2012). Profiles of fatty acid distribution of different acyl lipids from red and black rices. Journal of Food Research, 1(3), 46.
32. Kaur, P., Singh, N., Pal, P., & Kaur, A. (2018). Variation in composition, protein and pasting characteristics of different pigmented and non pigmented rice (Oryza sativa L.) grown in Indian Himalayan region. Journal of food science and technology, 55, 3809-3820.
33. Waewkum, P., & Singthong, J. (2021). Functional properties and bioactive compounds of pigmented brown rice flour. Bioactive Carbohydrates and Dietary Fibre, 26, 100289.
34. Chen, J., & Liu, H. (2020). Nutritional indices for assessing fatty acids: A mini-review. International journal of molecular sciences, 21(16), 5695.
35. Mapiye, C., Chimonyo, M., Dzama, K., Hugo, A., Strydom, P. E., & Muchenje, V. (2011). Fatty acid composition of beef from Nguni steers supplemented with Acacia karroo leaf-meal. Journal of Food Composition and Analysis, 24(4-5), 523-528.
36. Gowda, S. G. B., Minami, Y., Gowda, D., Chiba, H., & Hui, S. P. (2022). Detection and characterization of lipids in eleven species of fish by non-targeted liquid chromatography/mass spectrometry. Food Chemistry, 393, 133402.
37. Samaranayake, M. D. W., Abeysekera, W. K. S. M., Hewajulige, I. G. N., Somasiri, H. P. P. S., Mahanama, K. R. R., Senanayake, D. M. J. B., & Premakumara, G. A. S. (2024). Saturated, monounsaturated and polyunsaturated fatty acid profiles of commercially important traditional and new improved red and white rice varieties of Sri Lanka. Journal of Food Composition and Analysis, 130, 106154.
38. Simopoulos, A. P. (2002). The importance of the ratio of omega-6/omega-3 essential

fatty acids. Biomedicine & pharmacotherapy, 56(8), 365-379.

39. Garaffo, M. A., Vassallo-Agius, R., Nengas, Y., Lembo, E., Rando, R., Maisano, R., ... & Giuffrida, D. (2011). Fatty acids profile, atherogenic (IA) and thrombogenic (IT) health lipid indices, of raw roe of blue fin tuna (Thunnus thynnus L.) and their salted product “Bottarga”. Food and Nutrition Sciences, 2(7), 736-743.
40. Khalili Tilami, S., & Kouřimská, L. (2022). Assessment of the nutritional quality of plant lipids using atherogenicity and thrombogenicity indices. Nutrients, 14(18), 3795.
41. Zawistowski, J., Kopec, A., & Kitts, D. D. (2009). Effects of a black rice extract (Oryza sativa L. indica) on cholesterol levels and plasma lipid parameters in Wistar Kyoto rats. Journal of Functional Foods, 1(1), 50-56.
42. Yu, L., Li, G., Li, M., Xu, F., Beta, T., & Bao, J. (2016). Genotypic variation in phenolic acids, vitamin E and fatty acids in whole grain rice. Food Chemistry, 197, 776-782.
43. Samaranayake, M. D. W., Abeysekera, W. K. S. M., Hewajulige, I. G. N., Somasiri, H. P. P. S., Mahanama, K. R. R., Senanayake, D. M. J. B., & Premakumara, G. A. S. (2022). Fatty acid profiles of selected traditional and new improved rice varieties of Sri Lanka. Journal of Food Composition and Analysis, 112, 104686.
44. Watanabe, A., Balas, L., Saigusa, D., Ogura, J., Durand, T., Mano, N., & Yamaguchi, H. (2022). Analytical evaluation of fatty acid esters of hydroxy fatty acid quantity in fermented brown rice and rice bran (FRBA). Food Chemistry Advances, 1, 100040.
45. Zhu, Q. F., Yan, J. W., Zhang, T. Y., Xiao, H. M., & Feng, Y. Q. (2018). Comprehensive screening and identification of fatty acid esters of hydroxy fatty acids in plant tissues by chemical isotope labeling-assisted liquid chromatography–mass spectrometry. Analytical chemistry, 90(16), 10056-10063.

46. Yoshida, H., Tanigawa, T., Kuriyama, I., Yoshida, N., Tomiyama, Y., & Mizushina, Y. (2011). Variation in fatty acid distribution of different acyl lipids in rice (Oryza sativa L.) brans. Nutrients, 3(4), 505-514.
47. Margutti, M. P., Reyna, M., Vilchez, A. C., & Villasuso, A. L. (2019). Lipid profiling shows tissue-specific differences in barley for glycerolipid composition in response to chilling. Environmental and Experimental Botany, 158, 150-160.
48. Küllenberg, D., Taylor, L. A., Schneider, M., & Massing, U. (2012). Health effects of dietary phospholipids. Lipids in health and disease, 11, 1-16.
49. Sniezek, O. L., Anzmann, A. F., Claypool, S. M., & Vernon, H. J. (2020). Cardiolipin's Remodeling Rules Revealed: The Role of the Cellular Lipidome. Cell Reports, 30(12), 3949-3950.
50. Subramanian, V., Dhandayuthapani, U. N., Kandasamy, S., Sivaprakasam, J. V., Balasubramaniam, P., Shanmugam, M. K., Nagappan, S., Elangovan, S., Subramani, U. K., Palaniyappan, K., Vellingiri, G., & Muthurajan, R. (2024). Unravelling the metabolomic diversity of pigmented and non-pigmented traditional rice from Tamil Nadu, India. BMC Plant Biology, 24(1), 402.
51. Kim, J. K., Lee, S. Y., Chu, S. M., Lim, S. H., Suh, S. C., Lee, Y. T., Cho, H. S., & Ha, S. H. (2010). Variation and correlation analysis of flavonoids and carotenoids in Korean pigmented rice (Oryza sativa L.) cultivars. Journal of agricultural and food chemistry, 58(24), 12804-12809.
52. Pant, D. C., Aguilera-Albesa, S., & Pujol, A. (2020). Ceramide signalling in inherited and multifactorial brain metabolic diseases. Neurobiology of disease, 143, 105014.
53. Arias-Gaguancela, O., & Chapman, K. D. (2022). The biosynthesis and roles of N-acylethanolamines in plants. In *Advances in Botanical Research* (Vol. 101, pp. 345-

373). Academic Press.

54. Petersen, G., Moesgaard, B., Schmid, P. C., Schmid, H. H., Broholm, H., Kosteljanetz, M., & Hansen, H. S. (2005). Endocannabinoid metabolism in human glioblastomas and meningiomas compared to human non-tumour brain tissue. *Journal of neurochemistry*, *93*(2), 299-309.
55. Rudt, E., Schneider, S., & Hayen, H. (2024). Hyphenation of Liquid Chromatography and Trapped Ion Mobility–Mass Spectrometry for Characterization of Isomeric Phosphatidylethanolamines with Focus on N-Acylated Species. *Journal of the American Society for Mass Spectrometry*, *35*(7), 1584-1593.
56. Holmback, J., Karlsson, A., & Arnoldsson, K. C. (2001). Characterization of N-acylphosphatidylethanolamine and acylphosphatidylglycerol in oats. Lipids, 36(2), 153-165.
57. Schneider, S., Hammann, S., & Hayen, H. (2023). Determination of polar lipids in wheat and oat by a complementary approach of hydrophilic interaction liquid chromatography and reversed-phase high-performance liquid chromatography hyphenated with high-resolution mass spectrometry. *Journal of agricultural and food chemistry*, *71*(29), 11263-11275.
58. Choi, S. K., Takahashi, E., Inatsu, O., MANO, Y., & OHNISHI, M. (2005). Component fatty acids of acidic glycerophospholipids in rice grains: universal order of unsaturation index in each lipid among varieties. *Journal of Oleo Science*, *54*(7), 369-373.
59. Brejchova, K., Balas, L., Paluchova, V., Brezinova, M., Durand, T., & Kuda, O. (2020). Understanding FAHFAs: From structure to metabolic regulation. Progress in lipid research, 79, 101053.

60. Yore, M. M., Syed, I., Moraes-Vieira, P. M., Zhang, T., Herman, M. A., Homan, E. A., Patel, R. T., Lee, J., Chen, S., Peroni, O. D., Dhaneshwar, A. S., Hammarstedt, A., Smith, U., McGraw, T. E., Saghatelian, A., & Kahn, B. B. (2014). Discovery of a class of endogenous mammalian lipids with anti-diabetic and anti-inflammatory effects. Cell, 159(2), 318-332.
61. Liu, T., Tan, Z., Yu, J., Peng, F., Guo, J., Meng, W., Chen, Y., Rao, T., Liu, Z., & Peng, J. (2020). A conjunctive lipidomic approach reveals plasma ethanolamine plasmalogens and fatty acids as early diagnostic biomarkers for colorectal cancer patients. Expert review of proteomics, 17(3), 233-242.
62. Zhu, Q. F., Yan, J. W., Gao, Y., Zhang, J. W., Yuan, B. F., & Feng, Y. Q. (2017). Highly sensitive determination of fatty acid esters of hydroxyl fatty acids by liquid chromatography-mass spectrometry. Journal of Chromatography B, 1061, 34-40.
63. Benlebna, M., Balas, L., Gaillet, S., Durand, T., Coudray, C., Casas, F., & Feillet-Coudray, C. (2021). Potential physio-pathological effects of branched fatty acid esters of hydroxy fatty acids. Biochimie, 182, 13-22.
64. Liberati-Čizmek, A. M., Biluš, M., Brkić, A. L., Barić, I. C., Bakula, M., Hozić, A., & Cindrić, M. (2019). Analysis of fatty acid esters of hydroxyl fatty acid in selected plant food. Plant foods for human nutrition, 74, 235-240.
65. Pham, T. H., Vidal, N. P., Manful, C. F., Fillier, T. A., Pumphrey, R. P., Doody, K. M., & Thomas, R. H. (2019). Moose and caribou as novel sources of functional lipids: fatty acid esters of hydroxy fatty acids, diglycerides and monoacetyldiglycerides. Molecules, 24(2), 232.
66. An, N., Wang, Y., He, D. X., Mei, P. C., Zhu, Q. F., & Feng, Y. Q. (2023). A dataset of branched fatty acid esters of hydroxy fatty acids diversity in foods. *Scientific*

Data, *10*(1), 790.

67. Dong, X. J., Chen, J. Y., Chen, S. F., Li, Y., & Zhao, X. J. (2021). The composition and anti-inflammatory properties of pumpkin seeds. Journal of Food Measurement and Characterization, 15, 1834-1842.
68. Pautong, P. A., Añonuevo, J. J., de Guzman, M. K., Sumayao Jr, R., Henry, C. J., & Sreenivasulu, N. (2022). Evaluation of in vitro digestion methods and starch structure components as determinants for predicting the glycemic index of rice. LWT, 168, 113929.
69. Deepa, G., Singh, V., & Naidu, K. A. (2010). A comparative study on starch digestibility, glycemic index and resistant starch of pigmented ('Njavara'and 'Jyothi') and a non-pigmented ('IR 64') rice varieties. Journal of food science and technology, 47, 644-649.
70. Veni, B. K., Raja, D. S., Sridevi, P., & Tushara, M. (2024). Impact of starch profile on glycemic index of coloured and non-pigmented genotypes of rice (Oryza sativa L.). Electronic Journal of Plant Breeding, 15(3), 700-707.
71. da Silva, L. R., de Carvalho, C. W. P., Velasco, J. I., & Fakhouri, F. M. (2020). Extraction and characterization of starches from pigmented rice. International journal of biological macromolecules, 156, 485-493.
72. Kraithong, S., Theppawong, A., Bunyameen, N., Zhang, X., & Huang, R. (2024). Advancements in understanding low starch hydrolysis in pigmented rice: A comprehensive overview of mechanisms. Food Chemistry, 439, 138079.
73. Thiranusornkij, L., Thamnarathip, P., Chandrachai, A., Kuakpetoon, D., & Adisakwattana, S. (2019). Comparative studies on physicochemical properties, starch hydrolysis, predicted glycemic index of Hom Mali rice and Riceberry rice flour and

their applications in bread. *Food chemistry*, *283*, 224-231.

74. Rebeira, S. P., Prasantha, B. D. R., Jayatilake, D. V., Dunuwila, G. R., Piyasiri, C. H., & Herath, H. M. K. W. P. (2022). A comparative study of dietary fiber content, In vitro starch digestibility and cooking quality characteristics of pigmented and non–pigmented traditional and improved rice (Oryza sativa L.). Food Research International, 157, 111389.
75. Rondanelli, M., Ferrario, R. A., Barrile, G. C., Guido, D., Gasparri, C., Ferraris, C., Cavioni, A., Mansueto, F., Mazzola, G., Patelli, Z., Peroni, G., Pirola, M., Razza, C., Tartara, A., & Perna, S. (2023). The Glycemic Index of Indica and Japonica Subspecies Parboiled Rice Grown in Italy and the Effect on Glycemic Index of Different Parboiling Processes. Journal of Medicinal Food, 26(6), 422-427.
76. Sahoo, B., Mohan, A., & Anupam, R. (2023). The combined effect of oil-in-water emulsion soaking and modified pressure parboiling on starch digestibility of whole rice grains. LWT, 184, 114953.
77. Bhat, F. M., & Riar, C. S. (2019). Effect of chemical composition, granule structure and crystalline form of pigmented rice starches on their functional characteristics. Food chemistry, 297, 124984.
78. Tuncel, N. Y., Andac, A. E., Kaya, H. P., & Tuncel, N. B. (2025). The impact of milling degree on physicochemical, nutritional, rheological, textural properties, and in vitro digestibility of rice: From brown rice to white rice. Food Chemistry, 464, 141795.
79. Copeland, L., Blazek, J., Salman, H., & Tang, M. C. (2009). Form and functionality of starch. Food hydrocolloids, 23(6), 1527-1534.

Chapter 5

Uptake of Hijiki-Derived Carbon Nanodots Across the Rice Seed Coat and Their Role in Enhancing Seed Germination

5.1 Introduction

Nanotechnology has emerged as one of the most promising interdisciplinary fields, offering novel solutions across agriculture, biology, materials science, and chemistry[1]. Among the various nanomaterials explored, carbon nanodots (CDs) have attracted significant attention for their unique physicochemical properties, including high water solubility, biocompatibility, low toxicity, excellent photostability, and strong fluorescence[2-4]. CDs are carbon-based nanoparticles with quasi-spherical structures less than 10 nm in size, possessing abundant surface functional groups such as hydroxyl (–OH), carboxyl (–COOH), and amino ($–NH_2$) groups[5,6]. These functional groups not only confer solubility but also enable interaction with biological molecules and plant tissues. Unlike conventional nanomaterials such as cadmium-based quantum dots or metal oxides, CDs derived from natural sources such as plants and marine materials are environmentally benign and safe for biological systems[7]. Their biocompatibility and rich surface chemistry make them especially attractive for agricultural applications, including nutrient delivery, stress resistance improvement, and growth promotion[8].

Given the accelerating global population — projected to exceed 9.7 billion by 2064 — the demand for food security and sustainable crop production strategies has never been more urgent[9]. Rice (*Oryza sativa*) remains one of the most essential staple crops worldwide, serving as a primary calorie source for billions of people. Improving rice production in both quality and quantity is critical to meeting future food demands[10]. Seed germination and early seedling vigor are foundational to crop establishment, yield, and resilience, making this stage particularly important for intervention[11]. Recent studies have demonstrated the potential of nanomaterials in agriculture, not only as carriers of nutrients but also as plant growth stimulators[13]. Among these, CDs have shown unique advantages:

their small particle size, hydrophilic nature, and photoluminescent properties allow them to traverse biological barriers, enhance water and nutrient uptake, and even participate in light-mediated processes within plant tissues[13]. Unlike other carbon nanomaterials like graphene, nanotubes, or fullerenes, CDs possess intrinsic fluorescence, enabling real-time tracking of their uptake and distribution in plant systems[14]. Additionally, their ability to mimic enzymatic functions further enhances their biological compatibility and utility in promoting plant vitality[15]. In agriculture, CDs have been shown to improve nutrient utilization efficiency by enhancing plant absorption mechanisms rather than directly supplying macronutrients like nitrogen, phosphorus, and potassium[16]. By facilitating water and ion uptake and activating physiological processes related to photosynthesis and metabolism, CDs have demonstrated their potential as nanofertilizers and bio-stimulants. Functionalized CDs, particularly those doped with nitrogen, have shown improved interactions with plant tissues and nutrient systems, supporting plant growth under diverse conditions[17].

Despite growing interest in the use of nanomaterials in agriculture, most research has focused on synthetic or chemically derived nanoparticles, while studies utilizing naturally sourced carbon nanodots (CNDs) remain limited. Furthermore, while CDs have demonstrated potential in enhancing plant growth and stress resistance, few studies have systematically examined their uptake pathways, biological effects, and metabolic consequences in rice grains, a globally important staple crop[18-21]. In particular, the influence of CNDs on lipid metabolism during seed germination has not been explored. This represents a critical knowledge gap, especially given the nutritional and functional importance of lipids in rice grains. Addressing this gap could open new avenues for improving rice quality and yield through safe, sustainable, and multifunctional

nanomaterials.

In this context, this study investigates the biological effects of Hijiki-derived carbon nanodots (CND-H), synthesized from edible brown seaweed (*Sargassum fusiforme*), on the germination and early growth of rice seeds. The CND-H was synthesized using the standard hydrothermal method of CD synthesis[22]. Using a combination of confocal microscopy and physiological assays, we evaluated the ability of these naturally sourced, ~5 nm sized CNDs to penetrate the rice seed coat and enhance germination rates, root elongation, and seedling development. Furthermore, we explored how the internalization of CNDs may influence physiological processes, including lipid metabolism-related gene expression, potentially improving seed lipid content, a factor relevant to rice bran oil production and nutritional quality. By integrating this work into the broader context of bioactive lipidomics and plant functional food research, this chapter provides new insight into the synergistic applications of nanomaterials and crop science. This exploration not only supports the sustainable development of rice as a health-promoting functional food but also contributes to the growing field of nanobiotechnology-driven agriculture.

5.2 Materials and methods

5.2.1 Seedling cultivation and CND treatment

Brown rice grains of the Koshihikari cultivar (sourced from Chiba, Japan) were selected for seedling cultivation. The grains were first surface sterilized by immersing them in 75% ethanol for two minutes, followed by thorough rinsing with deionized water five times to ensure complete removal of residual ethanol. The sterilized grains were then placed in Petri dishes containing ultrapure Milli-Q water and incubated in the dark at

room temperature to promote germination[23]. The seedlings were cultivated under these controlled conditions for a total of ten days. For treatment, hijiki-derived CNDs (CND-H) were added to the Milli-Q water at a final concentration of 1 mg/mL. Milli-Q water without CND-H was used as the control. After ten days of growth, the rice seedlings from both the control and CND-H-treated groups were collected for phenotypic evaluation (**Figure 1**). Root length and shoot length were measured to assess the influence of CND-H treatment on early seedling development.

5.2.2 Phenotype and imaging studies of rice seedlings

After ten days of germination, the phenotypic characteristics of both control and CND-H-treated brown rice grains were evaluated. The physical growth of the seedlings was assessed by manually measuring the root and shoot lengths using a standard measuring scale. This allowed for the comparison of growth responses between the treated and untreated groups, providing preliminary insight into the influence of CND-H on seedling development.

To investigate the uptake and internal localization of CND-H within the rice grains, a detailed fluorescence bioimaging study was performed. Following germination, selected brown rice grains were carefully sectioned using a microtome to obtain thin, uniform slices suitable for imaging. These sections were then examined using a Zeiss LSM 880 confocal laser scanning microscope to detect the inherent fluorescence signals emitted by the CNDs. The imaging confirmed the successful penetration of the CND-H through the seed coat and its presence within the internal tissues of the germinated grains.

5.2.3 Transcriptomic analysis of rice seedlings

Total RNA was extracted from the rice seedlings using the RNeasy Plant Mini Kit (Cat. No. 69106; Qiagen, Germany), following the manufacturer's recommended protocol[24]. Approximately 50 mg of finely powdered seedling tissue was used for each extraction to ensure high-quality RNA yield suitable for downstream analysis. Thereafter, 100 μg of the synthesised RNA was used to form Complementary DNA (cDNA) using ReverTra Ace qPCR RT Master Mix with gDNA Remover (Cat. No. FSQ-301) according to the manufacturer's instructions. To investigate the molecular effects of CND treatment, the expression levels of two lipid metabolism-related genes, diacylglycerol acyltransferase (DGAT) and acyl-CoA-binding protein 4 (ACBP4), were quantified. This was performed using Real-Time quantitative PCR (qPCR) with the TaqMan Gene Expression Assay system, enabling precise measurement of gene expression changes in response to CND-H exposure in the rice seedlings (**Figure 1**).

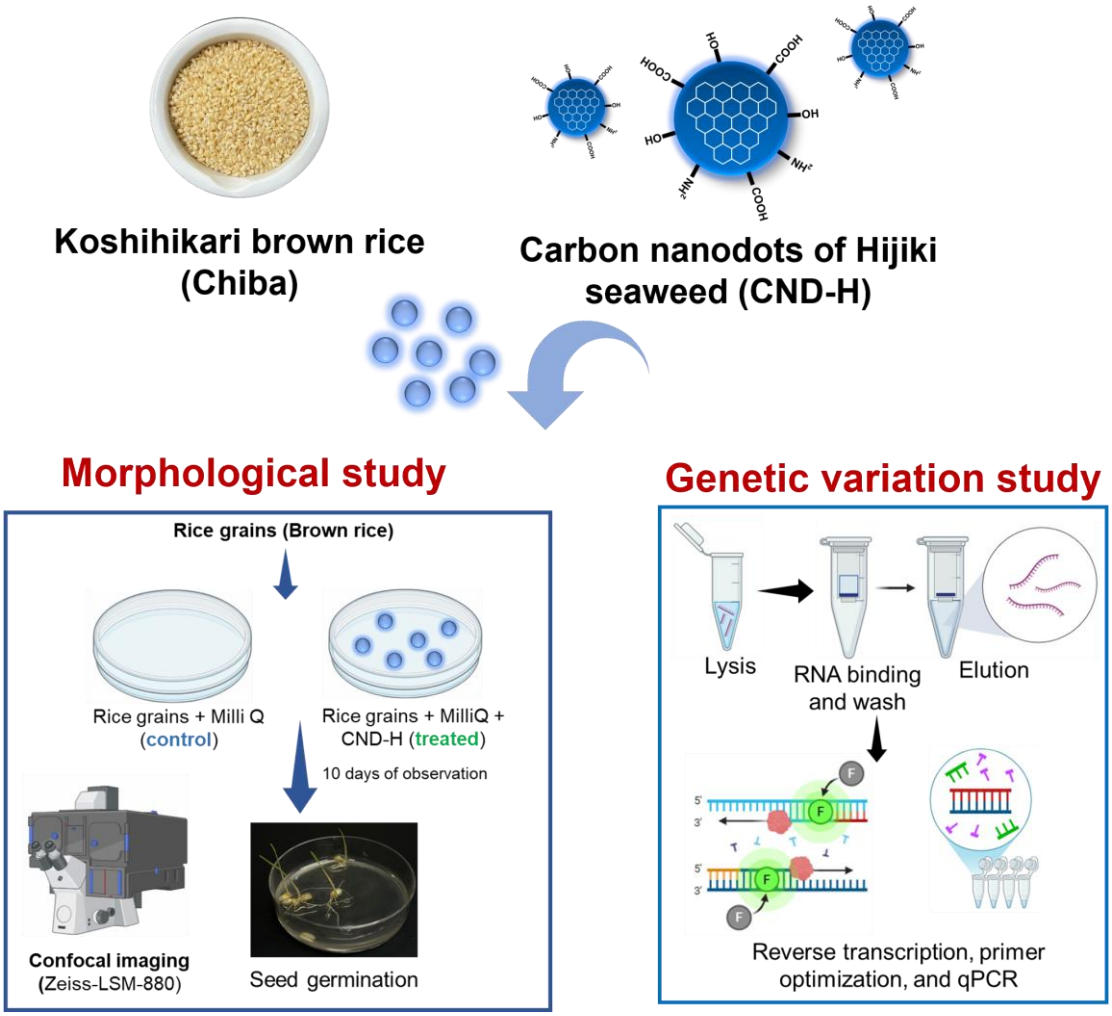

Figure 1: Overview of the workflow of the CND-H application study.

5.2.4 Statistical analysis

Data visualization was performed using Microsoft Excel 2021, with results presented as mean ± standard error of the mean (SEM). For statistical analysis, one-way analysis of variance (ANOVA) was conducted using GraphPad Prism 8, and compared using Tukey's multiple comparisons test at $p < 0.05$ levels.

5.3 Results and discussion

5.3.1 Effect of CND-H on rice seed germination and seedling growth

The impact of CND-H on rice seed germination was evaluated by monitoring the growth of the radicle and plumule from the initial emergence stage up to 10 days. Compared to the control group, the CND-H-treated grains exhibited visibly enhanced root and shoot elongation from the early stages of germination (**Figure 1A**). In addition to visual observation, the germination percentage was calculated using the formula (number of germinated seeds / total number of seeds) × 100 [25]. The results revealed that the germination rate was notably higher in the CND-H-treted group than in the control group, indicating that CND-H facilitates faster and more efficient germination (**Figure 1B**).

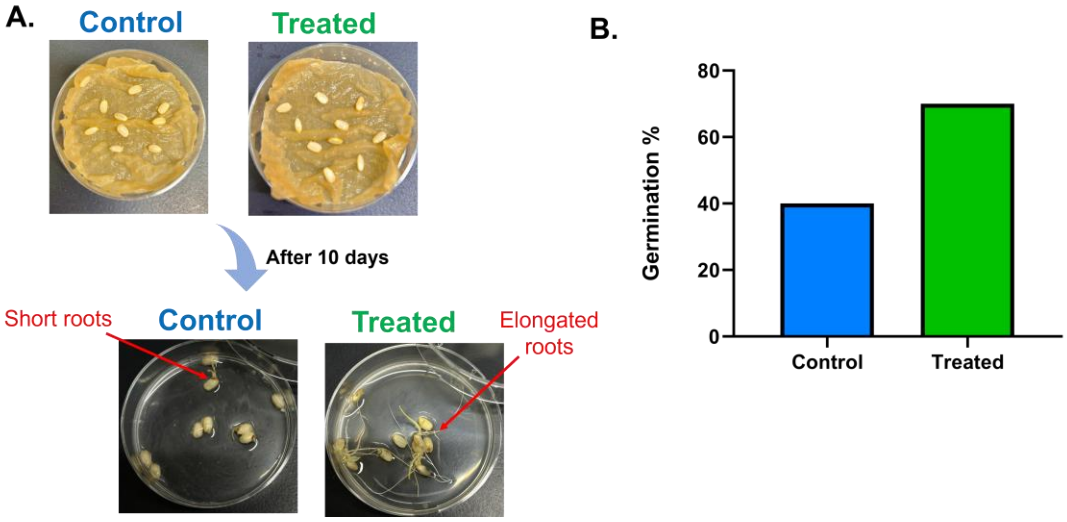

Figure 2: (A) Representative images of control and CND-H-treated rice grains showing radicle and plumule elongation. (B) Bar graph representing the germination percentage of rice grains in the control and CND-H-treated.

Quantitative measurements of root length, shoot length, and the number of adventitious roots formed were recorded after the ten-day growth period and are

summarized in **Table 1**. These parameters were consistently higher in the CND-H-treated seedlings compared to the untreated controls. The treated seedlings developed longer roots, taller shoots, and a greater number of adventitious roots, suggesting an overall enhancement in early seedling vigor due to CND-H exposure. These findings are consistent with previous studies reporting that carbon dots can significantly improve water content, seedling length, and root elongation in rice seeds compared to untreated controls[18,26,27]. Such enhancements have also been shown to be concentration-dependent, further supporting the biological activity of carbon-based nanomaterials in plant systems. The beneficial effects of CND-H on seed germination may be attributed to their unique hydrophilic surface structure and their ability to influence water uptake mechanisms[28]. It has been suggested that carbon nanodots can modulate the function of water channel proteins (aquaporins), thereby improving the water absorption efficiency of seeds[29]. Enhanced water uptake is a crucial factor during the early stages of germination, as it activates metabolic processes necessary for radicle and plumule emergence, ultimately promoting more vigorous seedling growth[30].

Collectively, these results demonstrate that CND-H has a positive influence on rice seed germination and early seedling development, providing a potential strategy to improve crop establishment and productivity through nanomaterial-based seed treatments.

Table 1: Effect of CND-H treatment on root length, shoot length, and number of adventitious roots, in rice seedlings after 10 days

	Root length in mm	**Shoot length in mm**	**Number of adventitious roots**
Water	8	7.5	1
	4	3	1
	3	2	1
CND-H	33	22	4
	33	24	4
	34	25	4

5.3.2 Uptake and localization of CND-H in germinated brown rice grains

After determining the seed germination and seed growth, the cellular uptake and bioimaging of CND-H in germinating brown rice grains were visualized using confocal laser scanning microscopy (Zeiss LSM 880). Confocal microscopy suggests bright fluorescence uptake of CND-H at an emission wavelength of 470 nm, as compared to the bright-field image, showing the general structure of the rice bran layer (**Figure 3A**). Under fluorescence imaging, a distinct blue fluorescence signal corresponding to CND-H uptake was observed in the bran and aleurone layer regions of the rice grain **(Figure 3B**). To validate the presence of CND-H within the grains, the emission spectra of the CND-H solution were first measured, exhibiting a peak emission at approximately 470 nm, indicating characteristic blue fluorescence (**Figure 3C**). Subsequently, the emission spectra were acquired from selected regions of the fluorescence images of CND-H-treated grains, specifically from the aleurone layer and the bran. These spectra closely matched

the emission profile of the CND-H solution (**Figure 3D**), confirming the successful uptake and localization of CND-H within the rice grain tissues. This finding aligns with previous studies reporting the ability of carbon-based nanomaterials to penetrate plant tissues, particularly due to their hydrophilic nature and small size[31]. Such efficient uptake highlights the potential of CND-H as a non-toxic bio-compatible material for seed treatment applications, which may influence early germination processes by enhancing water absorption or modulating biochemical pathways.

Figure 3: (A) Bright-field image showing the general structure of the rice bran layer and fluorescence image of CND-H-treated grains showing blue fluorescence in the bran and aleurone layers. (B) Emission spectrum of the CND-H solution, with a peak at 470 nm. (C) Emission spectra from fluorescence images of CND-H-treated grains, collected from the aleurone layer (red) and bran (green) regions, closely match the CND-H solution spectrum, confirming successful uptake. Objective: 10X.

5.3.3 Analysis of lipid metabolism-related gene expression in rice seedlings

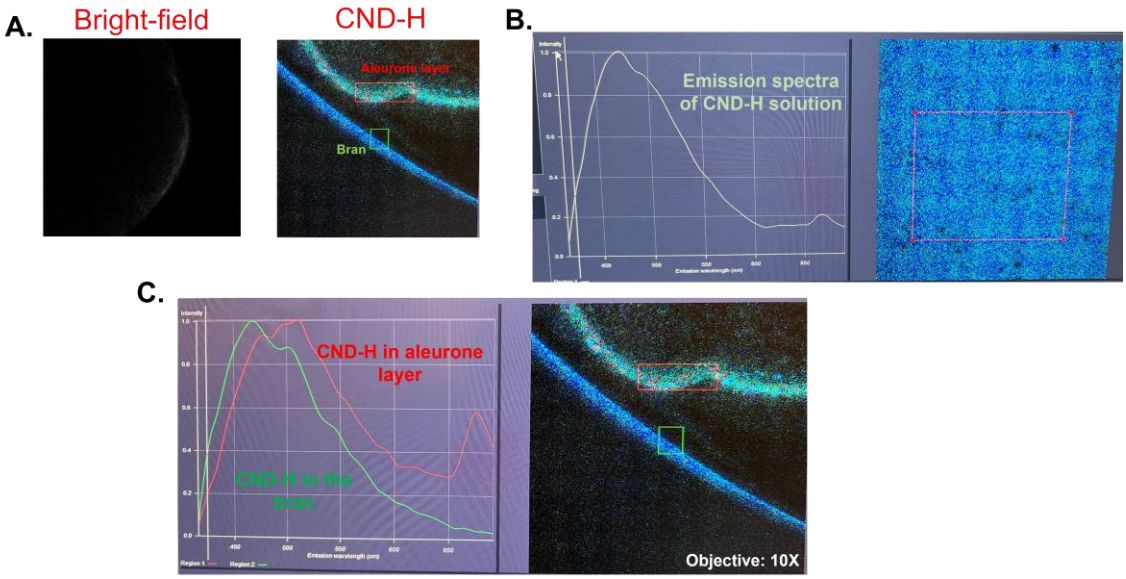

To explore the influence of CND-H treatment on lipid metabolism in rice seedlings, the expression levels of two key lipid metabolism-related genes, *OsDGAT1* and *OsACBP4*,

were evaluated using qRT-PCR. The results showed that *OsDGAT1* (Diacylglycerol acyltransferase 1), a key enzyme responsible for catalyzing the final step in triacylglycerol (TAG) biosynthesis, was significantly upregulated in the CND-H-treated seedlings compared to the control[32]. This is particularly relevant since the upregulation of this gene has been previously associated with increased oil accumulation in several plant species, including soybean, Arabidopsis, canola, rapeseed, garden nasturtium, and maize[32-36]. The enhanced expression of *OsDGAT1* suggests that CND-H treatment may promote lipid accumulation in rice seedlings by increasing triacylglycerol synthesis, potentially improving their nutritional and metabolic qualities.

In contrast, the expression of *OsACBP4* (Acyl-CoA-binding protein 4), which is involved in intracellular fatty acid transport and lipid metabolism regulation, did not show a significant change following CND-H treatment (**Figure 4**)[37]. While ACBP proteins play important roles in plant lipid metabolism and stress response, the lack of significant alteration in *OsACBP4* expression suggests that CND-H primarily affects lipid biosynthesis pathways, such as triacylglycerol formation, rather than fatty acid transport mechanisms at the seedling stage[37,38]. These findings indicate that CND-H exposure specifically enhances the expression of triacylglycerol biosynthesis-related genes without markedly influencing lipid transport pathways, providing insight into the potential of carbon nanodots to selectively modulate plant lipid metabolism.

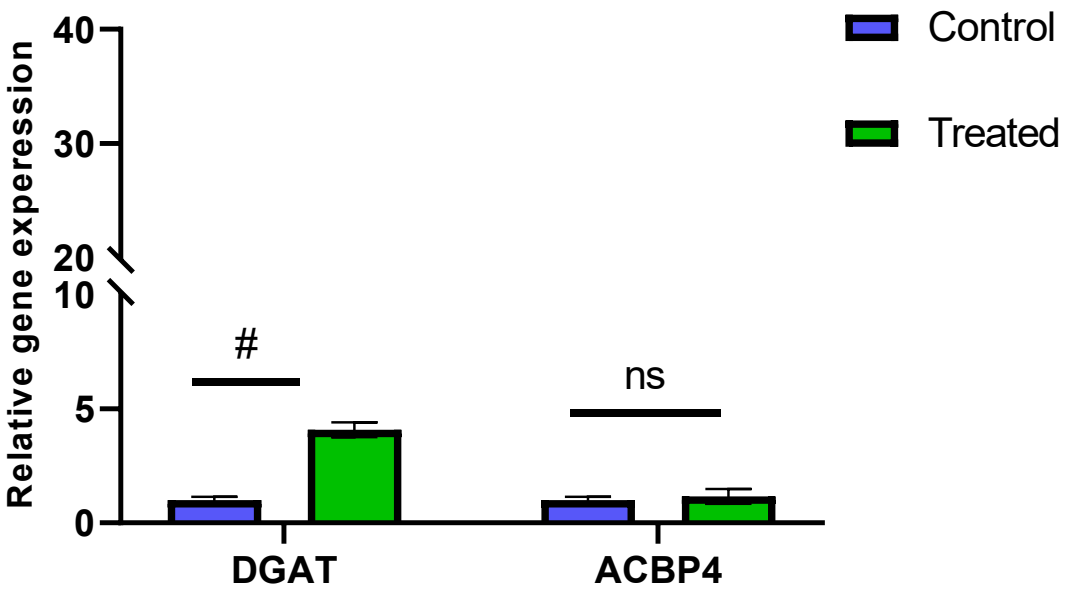

Figure 4: Relative expression levels of OsDGAT1 and OsACBP4 in rice seedlings treated with CND-H compared to the control. Data are presented as mean ± SEM (n = 4). Statistical significance was determined using two-way ANOVA followed by Tukey's multiple comparisons test, with different letters indicating significant differences at $p < 0.05$.

5.4 Limitations

While the present study provides valuable preliminary insights into the effects of CND-H application on rice seedling growth and lipid metabolism-related gene expression, it is important to acknowledge several limitations. Firstly, this investigation was conducted on a small experimental scale using a petri dish-based germination system, which may not fully represent the complex environmental conditions experienced in soil-based or field cultivation systems. Additionally, the number of biological replicates was limited, which could affect the statistical robustness of the results. Increasing the number of replicates in

future experiments will help to enhance the reliability and reproducibility of the findings. Furthermore, this study serves as a pilot investigation, and several aspects of the CND-H effects on rice physiology and metabolism remain to be explored. In particular, more comprehensive analyses are needed to confirm the observed trends in gene expression and to assess their downstream effects on lipid composition, seed quality, and plant development under different environmental conditions.

Ongoing and future studies will focus on scaling up the experiments, increasing replication, and incorporating additional physiological, biochemical, and transcriptomic analyses. These efforts will provide a more detailed understanding of the mechanisms underlying the interaction between carbon nanodots and plant metabolic processes, to evaluate the practical applications of nanomaterials in crop improvement strategies.

5.5 Conclusion

In this study, we explored the effects of hijiki-derived carbon nanodots (CND-H) on the early growth and lipid metabolism of rice seedlings. The application of CND-H significantly promoted seed germination, as evidenced by enhanced root and shoot elongation and a higher germination percentage compared to untreated controls. Confocal imaging confirmed the successful uptake and localization of CND-H within the bran and subaleurone layers of the rice grains, supported by consistent fluorescence emission spectra between the CND-H solution and the treated grains. At the molecular level, CND-H treatment led to a significant upregulation of OsDGAT1, a key gene involved in triacylglycerol biosynthesis, suggesting that CND-H may influence lipid accumulation processes during seedling development. However, no significant change was observed in the expression of *OsACBP4*, indicating a more selective effect of CND-H on lipid

metabolism-related pathways. These findings collectively suggest that hijiki-derived CND-H can enhance rice seedling growth and selectively stimulate lipid metabolic processes, particularly by promoting triacylglycerol synthesis. This highlights the potential of carbon nanodots as novel, biocompatible nanomaterials for agricultural applications, including seed priming and crop biofortification strategies. As a pilot study, these promising results provide a foundation for future, larger-scale investigations to validate and expand upon these findings under soil-based and field conditions, and to further elucidate the broader physiological and molecular impacts of nanomaterials in crop plants.

5.6 References

1. El-Ramady, H.; Abdalla, N.; Sári, D.; Ferroudj, A.; Muthu, A.; Prokisch, J.; Fawzy, Z. F.; Brevik, E. C.; Solberg, S. Ø. Nanofarming: Promising Solutions for the Future of the Global Agricultural Industry. Agronomy 2023, 13 (6), 1600.
2. Zheng, X. T., Ananthanarayanan, A., Luo, K. Q., & Chen, P. (2015). Glowing graphene quantum dots and carbon dots: properties, syntheses, and biological applications. *small*, *11*(14), 1620-1636.
3. Li, H., Kong, W., Liu, J., Liu, N., Huang, H., Liu, Y., & Kang, Z. (2015). Fluorescent N-doped carbon dots for both cellular imaging and highly-sensitive catechol detection. *Carbon*, *91*, 66-75.
4. Shi, W., Guo, F., Han, M., Yuan, S., Guan, W., Li, H., ... & Kang, Z. (2017). N, S co-doped carbon dots as a stable bio-imaging probe for detection of intracellular temperature and tetracycline. *Journal of Materials Chemistry B*, *5*(18), 3293-3299.
5. Maholiya, A., Ranjan, P., Khan, R., Murali, S., Nainwal, R. C., Chauhan, P. S., ... & Srivastava, A. K. (2023). An insight into the role of carbon dots in the agriculture system: a review. *Environmental Science: Nano*, *10*(4), 959-995.
6. Singh, P., Rani, N., Kumar, S., Kumar, P., Mohan, B., Bhankar, V., ... & Kumar, K. (2023). Assessing the biomass-based carbon dots and their composites for photocatalytic treatment of wastewater. *Journal of Cleaner Production*, *413*, 137474.
7. Shen, J., Zhu, Y., Yang, X., & Li, C. (2012). Graphene quantum dots: emergent nanolights for bioimaging, sensors, catalysis and photovoltaic devices. *Chemical communications*, *48*(31), 3686-3699.
8. Li, G., Xu, J., & Xu, K. (2023). Physiological functions of carbon dots and their applications in agriculture: A review. *Nanomaterials*, *13*(19), 2684.

9. Vollset, S. E., Goren, E., Yuan, C. W., Cao, J., Smith, A. E., Hsiao, T., ... & Murray, C. J. (2020). Fertility, mortality, migration, and population scenarios for 195 countries and territories from 2017 to 2100: a forecasting analysis for the Global Burden of Disease Study. *The Lancet*, *396*(10258), 1285-1306.
10. Kuhlman, T., & Farrington, J. (2010). What is sustainability?. *Sustainability*, *2*(11), 3436-3448.
11. Tan, T. L., Nulit, R., Jusoh, M., & Rashid, S. A. (2023). Recent developments, applications and challenges for carbon quantum dots as a photosynthesis enhancer in agriculture. *RSC advances*, *13*(36), 25093-25117.
12. Khodakovskaya, M., Dervishi, E., Mahmood, M., Xu, Y., Li, Z., Watanabe, F., & Biris, A. S. (2009). Carbon nanotubes are able to penetrate plant seed coat and dramatically affect seed germination and plant growth. *ACS nano*, *3*(10), 3221-3227.
13. Avellan, A., Yun, J., Zhang, Y., Spielman-Sun, E., Unrine, J. M., Thieme, J., ... & Lowry, G. V. (2019). Nanoparticle size and coating chemistry control foliar uptake pathways, translocation, and leaf-to-rhizosphere transport in wheat. *ACS nano*, *13*(5), 5291-5305.
14. Singh, P., Kumar, S., Kumar, P., Kataria, N., Bhankar, V., Kumar, K., ... & Khoo, K. S. (2023). Assessment of biomass-derived carbon dots as highly sensitive and selective templates for the sensing of hazardous ions. *Nanoscale*, *15*(40), 16241-16267.
15. Xu, G., Liu, K., Jia, B., Dong, Z., Zhang, C., Liu, X., ... & Li, Y. Q. (2024). Electron lock manipulates the catalytic selectivity of nanozyme. *ACS nano*, *18*(4), 3814-3825.
16. Wang, A., Kang, F., Wang, Z., Shao, Q., Li, Z., Zhu, G., ... & Li, Y. Y. (2019). Facile Synthesis of Nitrogen-Rich Carbon Dots as Fertilizers for Mung Bean

Sprouts. *Advanced Sustainable Systems*, *3*(3), 1800132.

17. Abu Salha, B., Saravanan, A., Maruthapandi, M., Perelshtein, I., & Gedanken, A. (2023). Plant-derived nitrogen-doped carbon dots as an effective fertilizer for enhanced strawberry growth and yield. *ACS ES&T Engineering*, *3*(8), 1165-1175.
18. Li, H., Huang, J., Lu, F., Liu, Y., Song, Y., Sun, Y., ... & Kang, Z. (2018). Impacts of carbon dots on rice plants: boosting the growth and improving the disease resistance. *ACS Applied Bio Materials*, *1*(3), 663-672.
19. Li, Y., Pan, X., Xu, X., Wu, Y., Zhuang, J., Zhang, X., ... & Liu, Y. (2021). Carbon dots as light converter for plant photosynthesis: Augmenting light coverage and quantum yield effect. *Journal of Hazardous Materials*, *410*, 124534.
20. Tan, T. L., Zulkifli, N. A., Zaman, A. S. K., binti Jusoh, M., Yaapar, M. N., & Rashid, S. A. (2021). Impact of photoluminescent carbon quantum dots on photosynthesis efficiency of rice and corn crops. *Plant Physiology and Biochemistry*, *162*, 737-751.
21. Li, Y., Xu, X., Lei, B., Zhuang, J., Zhang, X., Hu, C., ... & Liu, Y. (2021). Magnesium-nitrogen co-doped carbon dots enhance plant growth through multifunctional regulation in photosynthesis. *Chemical Engineering Journal*, *422*, 130114.
22. Zhang, J., Zheng, G., Tian, Y., Zhang, C., Wang, Y., Liu, M., ... & Yu, W. (2022). Green synthesis of carbon dots from elm seeds via hydrothermal method for Fe3+ detection and cell imaging. *Inorganic Chemistry Communications*, *144*, 109837.
23. Yao, Q., Zheng, X., Zhou, G., & Zhang, J. (2024). SGR-YOLO: a method for detecting seed germination rate in wild rice. *Frontiers in Plant Science*, *14*, 1305081.
24. Lai, S. H., & Chye, M. L. (2021). Plant acyl-CoA-binding proteins—their lipid and protein interactors in abiotic and biotic stresses. *Cells*, *10*(5), 1064.
25. Onofri, A., Benincasa, P., Mesgaran, M. B., & Ritz, C. (2018). Hydrothermal-time-

to-event models for seed germination. *European Journal of Agronomy*, *101*, 129-139.

26. Tripathi, S., Sonkar, S. K., & Sarkar, S. (2011). Growth stimulation of gram (Cicer arietinum) plant by water soluble carbon nanotubes. *Nanoscale*, *3*(3), 1176-1181.
27. He, Y., Hu, R., Zhong, Y., Zhao, X., Chen, Q., & Zhu, H. (2018). Graphene oxide as a water transporter promoting germination of plants in soil. *Nano Research*, *11*, 1928-1937.
28. Zhang, Z., Wu, C., Hu, J., Li, C., Liu, Y., Lei, B., & Zheng, M. (2025). Recent Advances of Carbon Dots: Synthesis, Plants Applications, Prospects, and Challenges. *ACS Applied Bio Materials*.
29. Sun, X., Chen, J., Fan, W., Liu, S., & Kamruzzaman, M. (2022). Production of reactive oxygen species via nanobubble water improves radish seed water absorption and the expression of aquaporin genes. *Langmuir*, *38*(38), 11724-11731.
30. Tripathi, S., & Sarkar, S. (2015). Influence of water soluble carbon dots on the growth of wheat plant. *Applied Nanoscience*, *5*, 609-616.
31. López-Vargas, E. R., González-García, Y., Pérez-Álvarez, M., Cadenas-Pliego, G., González-Morales, S., Benavides-Mendoza, A., ... & Juárez-Maldonado, A. (2020). Seed priming with carbon nanomaterials to modify the germination, growth, and antioxidant status of tomato seedlings. *Agronomy*, *10*(5), 639.
32. Torabi, S., Sukumaran, A., Dhaubhadel, S., Johnson, S. E., LaFayette, P., Parrott, W. A., ... & Eskandari, M. (2021). Effects of type I Diacylglycerol O-acyltransferase (DGAT1) genes on soybean (Glycine max L.) seed composition. *Scientific reports*, *11*(1), 2556.
33. Wang, Z., Yang, M., Sun, Y., Yang, Q., Wei, L., Shao, Y., ... & Li, W. (2019). Overexpressing Sesamum indicum L.'s DGAT1 increases the seed oil content of

transgenic soybean. *Molecular Breeding*, *39*, 1-9.

34. Taylor, D. C., Zhang, Y., Kumar, A., Francis, T., Giblin, E. M., Barton, D. L., ... & Weselake, R. J. (2009). Molecular modification of triacylglycerol accumulation by over-expression of DGAT1 to produce canola with increased seed oil content under field conditions. *Botany*, *87*(6), 533-543.
35. Xu, J., Francis, T., Mietkiewska, E., Giblin, E. M., Barton, D. L., Zhang, Y., ... & Taylor, D. C. (2008). Cloning and characterization of an acyl-CoA-dependent diacylglycerol acyltransferase 1 (DGAT1) gene from Tropaeolum majus, and a study of the functional motifs of the DGAT protein using site-directed mutagenesis to modify enzyme activity and oil content. *Plant biotechnology journal*, *6*(8), 799-818.
36. Oakes, J., Brackenridge, D., Colletti, R., Daley, M., Hawkins, D. J., Xiong, H., ... & Deikman, J. (2011). Expression of fungal diacylglycerol acyltransferase2 genes to increase kernel oil in maize. *Plant physiology*, *155*(3), 1146-1157.
37. Rasmussen, J. T., Færgeman, N. J., Kristiansen, K., & Knudsen, J. (1994). Acyl-CoA-binding protein (ACBP) can mediate intermembrane acyl-CoA transport and donate acyl-CoA for β-oxidation and glycerolipid synthesis. *Biochemical Journal*, *299*(1), 165-170.
38. Lai, S. H., & Chye, M. L. (2021). Plant acyl-CoA-binding proteins—their lipid and protein interactors in abiotic and biotic stresses. *Cells*, *10*(5), 1064.

Conclusion remarks

This doctoral research was conducted to explore the diversity of lipid molecular species in plant-based food systems and to evaluate their nutritional, functional, and biological significance using advanced untargeted lipidomics combined with complementary analyses. The thesis is organized into five chapters, each addressing a specific research objective within this broader scope. The chapter-wise concluding remarks are summarized below.

Chapter one provided a comprehensive introduction to the importance of dietary lipids, their bioactivities, and the growing relevance of food lipidomics. It outlined the gaps in existing food lipid research and established the scope and significance of this thesis. It emphasized how integrating modern analytical platforms like LC-MS-based lipidomics can uncover previously uncharacterized lipids in plant-derived foods, offering insights into their potential roles in human health and nutrition.

Chapter two focused on the untargeted lipidomics profiling of four traditional herbal teas widely consumed in Japan. This chapter successfully identified over 300 lipid molecular species, including several novel SFAHFAs for the first time in herbal teas. Multivariate and hierarchical clustering analyses revealed distinct lipidomic patterns among the tea species, highlighting their diversity and potential functional properties. The identification of PUFA-rich lipid species and novel bioactive compounds suggested these teas' possible contributions to antioxidant and anti-inflammatory benefits.

Chapter three extended this approach to sorghum, a nutritionally important and drought-resilient cereal. The lipidome of six commercial sorghum cultivars from Australia was comprehensively profiled, revealing significant inter-cultivar variability, particularly in fatty acids, glycerophospholipids, and bioactive FAHFAs. The study also

employed DMED derivatization to confirm the structures and hydroxyl positions of FAHFAs. This work demonstrated sorghum's lipidomic richness and highlighted cultivars like MR43 and Buster as having distinct and health-promoting lipid profiles, supporting their value in dietary and functional food applications.

Chapter four investigated the lipid profiles of 56 cultivars of *japonica* rice from different prefectures of Japan and the glycemic index of eight pigmented *japonica* rice cultivars. The study correlated lipid composition with nutritional traits using untargeted lipidomics and *in vitro* digestion-based glycemic index estimation. The discovery of LNAPEs alongside bioactive lipids like FAHFAs in pigmented rice provided new insights into the health-promoting potential of these grains. The findings reinforced the idea that pigmented rice cultivars offer enhanced nutritional properties and lipidomic complexity compared to non-pigmented varieties. The lower GI of black rice cultivars makes it suitable for the type II diabetic population.

Chapter five introduced a novel exploration into applying nanomaterials in agriculture by evaluating the effects of Hijiki-derived carbon nanodots (CND-H) on rice seed germination and lipid metabolism. The study demonstrated that CND-H enhanced seedling growth and significantly upregulated OsDGAT1 expression, a key gene in lipid biosynthesis. Confocal imaging confirmed the uptake of CND-H by rice grains, marking an innovative step in understanding nanomaterial–plant interactions. While this chapter represented a pilot-scale study, it provides a promising foundation for future research into nanotechnology's role in crop improvement and lipid regulation.

In summary, this thesis systematically revealed the diversity and biological relevance of lipids in plant-based food systems, while also demonstrating how modern lipidomics and bioanalytical techniques can uncover new bioactive compounds. The

findings enhance our understanding of food lipid composition, its nutritional implications, and potential applications in functional foods and agricultural biotechnology. Future work should expand on these findings using larger, multi-season, and field-based studies to further validate and translate these discoveries into practical applications for food and health science.

Appendix

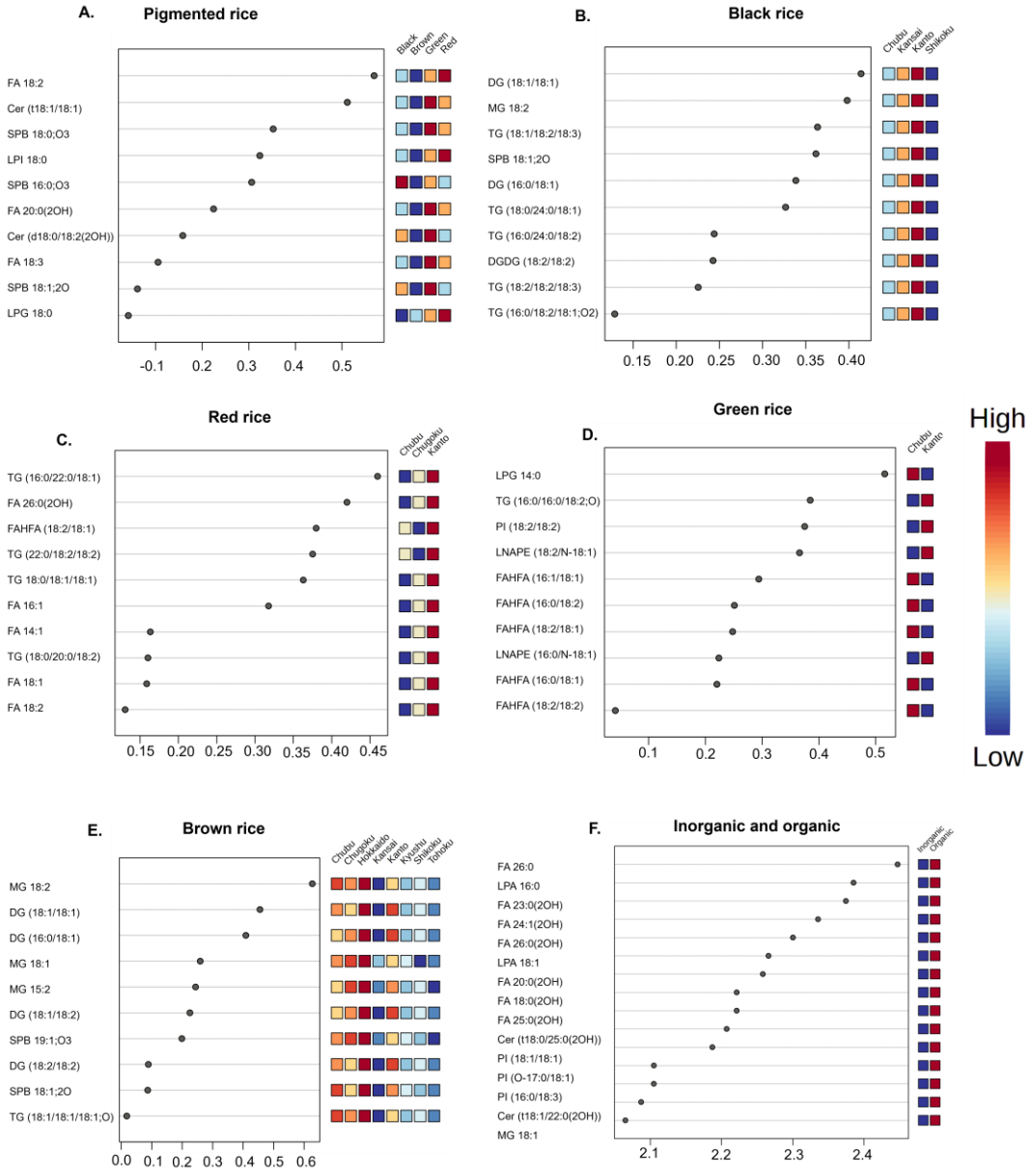

Figure 1: Sparse partial least squares discriminant analysis loading plot of (A) all pigmented *japonica* rice cultivars, (B) black rice, (C) red rice, (D) green rice, and (E) brown rice. The orthogonal partial least squares discriminant analysis variable importance in projection (VIP) score plot of the *japonica* cultivar based on the farming method i.e. organic and inorganic.

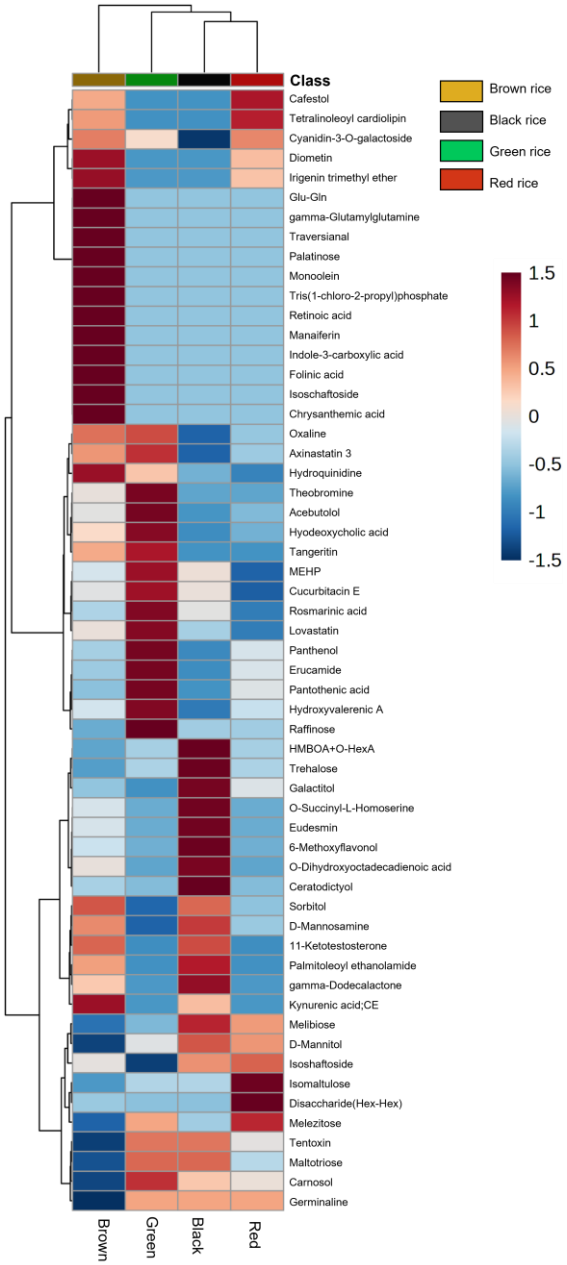

Figure 2: Heatmaps illustrate the Z-score normalized area of metabolites detected in 56 *japonica* rice cultivars based on pigmentation.

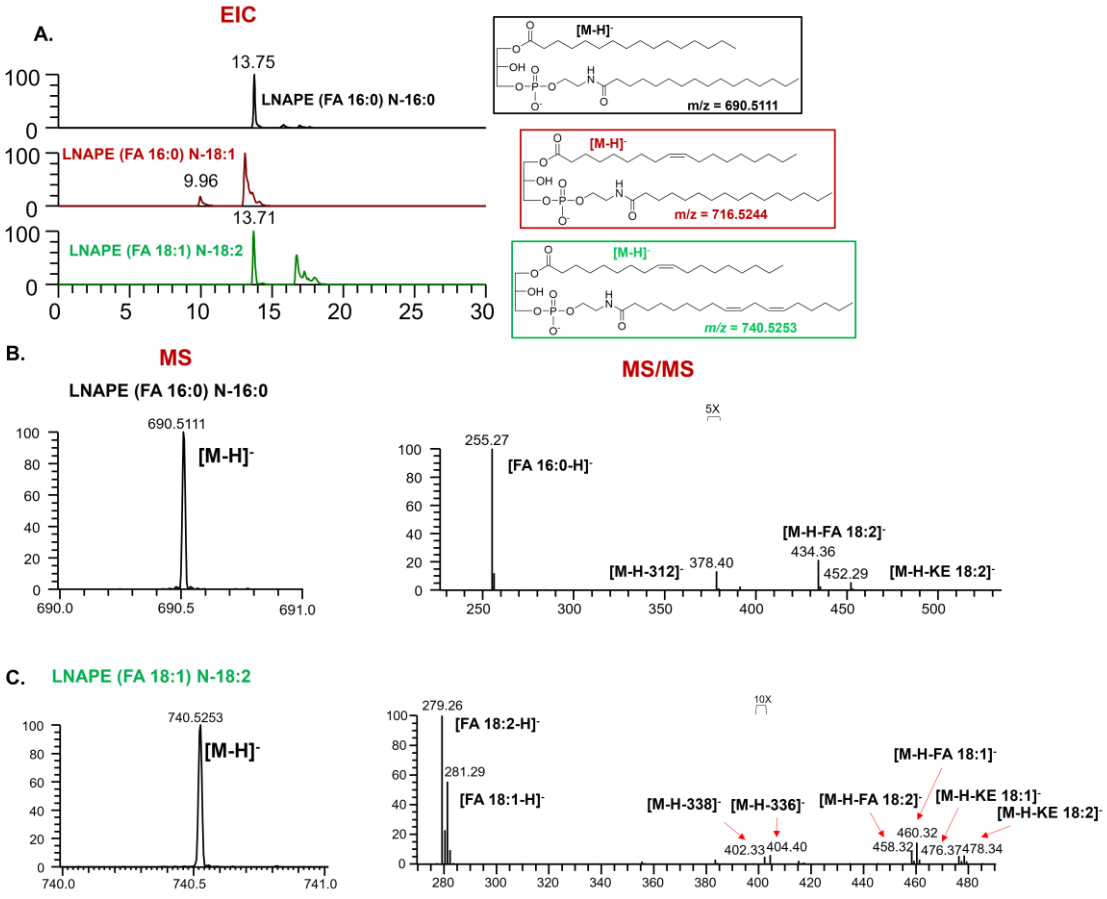

Figure 3: (A) The extracted ion chromatograms (EIC) of N-acyl-lysophosphatidylethanolamines (LNAPEs). (B) The mass spectra (MS) and MS/MS spectra of LNAPE (FA 16:0) N-16:0. (C) LNAPE (FA 18:1) N-18:2.

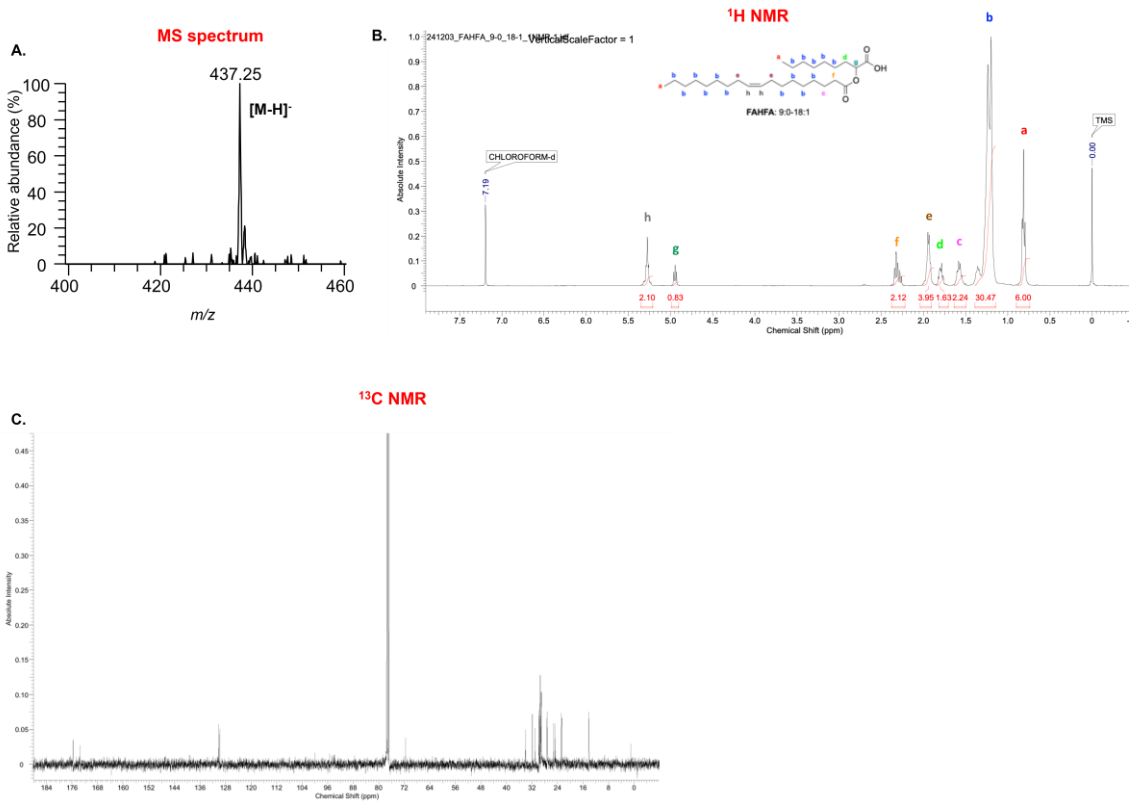

Figure 4: (A) High-resolution electrospray ionization mass spectrometry of 2-2-hydroxy nonanoic acid (2-OAHNA). (B) proton nuclear magnetic resonance (^{1}H NMR). (C) carbon-13 nuclear magnetic resonance (^{13}C NMR) of 2 OAHNA.

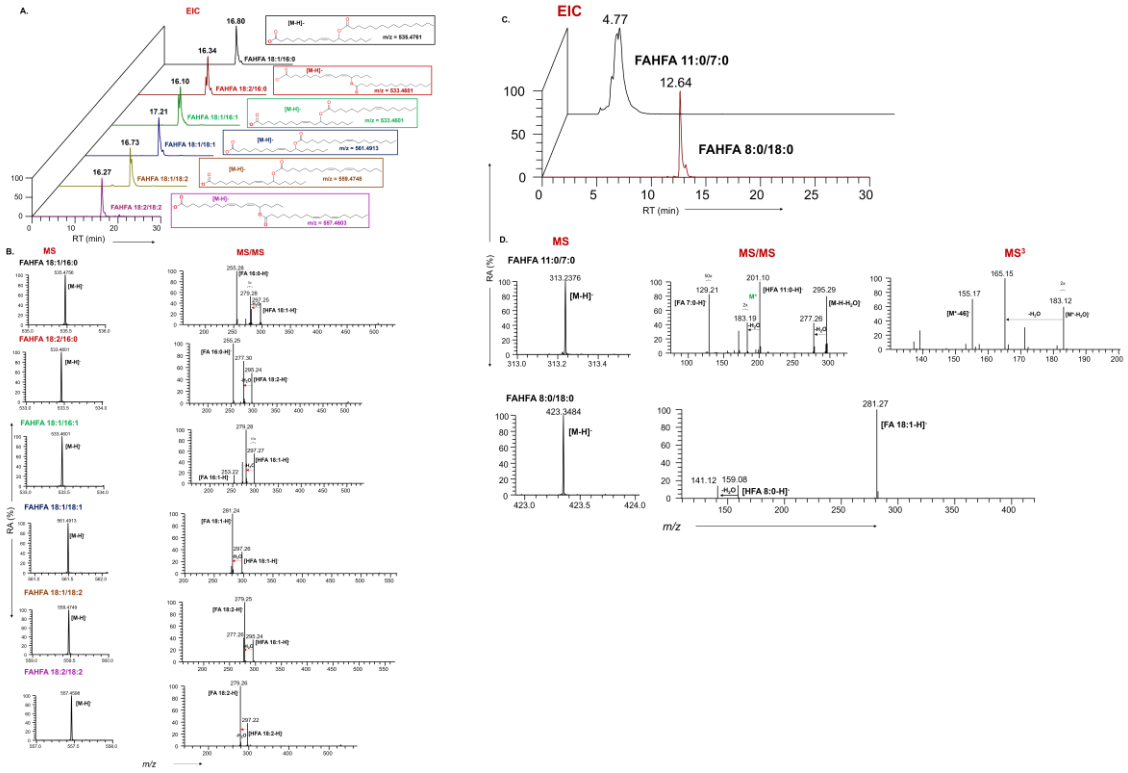

Figure 5: (A) The extracted ion chromatogram (EIC) of long-chain fatty acid esters of hydroxy fatty acids (FAHFAs). (B) MS and MS/MS spectra of detected long-chain FAHFAs in rice. (C) The EIC of medium-chain FAHFAs, (D) MS^n spectra of detected medium-chain FAHFAs.